2013-10-28

hox Gene Regulation and Function During Zebrafish Embryogenesis: A Dissertation

Steven E. Weicksel
University of Massachusetts Medical School

hox GENE REGULATION AND FUNCTION DURING ZEBRAFISH EMBRYOGENESIS

A Dissertation Presented

BY

Steven E. Weicksel

Submitted to the Faculty of the

University of Massachusetts Graduate School of Biomedical Sciences, Worcester

in partial fulfillment of the requirements for the degree of

DOCTOR OF PHILOSOPHY

OCTOBER, 28TH 2013

hox GENE REGULATION AND FUNCTION DURING ZEBRAFISH EMBRYOGENESIS

A Dissertation Presented
By
Steven Edward Weicksel

The signatures of the Dissertation Defense Committee signify completion and approval as to style and content of the Dissertation

Charles Sagerström, Ph.d., Thesis Advisor

Oliver Rando, M.D., Ph.d., Member of Committee

Zhiping Weng, Ph.D., Member of Committee

Jesse Mager, Ph.d., Member of Committee

The signature of the Chair of the Committee signifies that the written dissertation meets the requirements of the Dissertation Committee

Craig Peterson, Ph.d., Chair of Committee

The signature of the Dean of the Graduate School of Biomedical Sciences signifies that the student has met all graduation requirements of the school

Anthony Carruthers, Ph.D.,
Dean of the Graduate School of Biomedical Sciences

Program
Biochemistry and Molecular Pharmacology

Date
October, Twenty-eighth, Two-thousand and thirteen

Dedication

This dissertation is dedicated to my family. To my Mom and Dad who taught me to work hard and to never give up. To my siblings for always cheering me on. Finally, to my loving wife who supported me every step of the way.

For all of your support, I am thankful and blessed.

Acknowledgements

I would like to acknowledge members of the Sagerström lab for thoughtful discussions and insight into the work presented within. Fluorescent confocal images were graciously taken by Dr. Denise Zannino. I would also like to acknowledge Dr. Scot Wolfe and Dr. Ankit Gupta for contributing their expertise in zinc-finger and TALE nuclease construction and design to this project. Finally, I would like to acknowledge the mentorship of Dr. Charles Sagerström who guided this ship straight.

Abstract

Hox genes encode a conserved family of homeodomain containing transcription factors essential for metazoan development. The establishment of overlapping *Hox* expression domains specifies tissue identities along the anterior-posterior axis during early embryogenesis and is regulated by chromatin architecture and retinoic acid (RA). Here we present the role nucleosome positioning plays in *hox* activation during embryogenesis. Using four stages of early embryo development, we map nucleosome positions at 37 zebrafish *hox* promoters. We find nucleosome arrangement to be progressive, taking place over several stages independent of RA. This progressive change in nucleosome arrangement on invariant sequence suggests that trans-factors play an important role in organizing nucleosomes. To further test the role of trans-factors, we created *hoxb1b* and *hoxb1a* mutants to determine if the loss of either protein effected nucleosome positions at the promoter of a known target, *hoxb1a*. Characterization of these mutations identified hindbrain segmentation defects similar to targeted deletions of mouse orthologs *Hoxa1* and *Hoxb1* and zebrafish *hoxb1b* and *hoxb1a* morpholino (MO) loss-of-function experiments. However, we also identified differences in hindbrain segmentation as well as phenotypes in facial motor neuron migration and reticulospinal neuron formation not previously observed in the MO experiments. Finally, we find that nucleosomes at the *hoxb1a* promoter are positioned differently in *hoxb1b*$^{-/-}$ embryos compared to

wild-type. Together, our data provides new insight into the roles of *hoxb1b* and *hoxb1a* in zebrafish hindbrain segmentation and reticulospinal neuron formation and indicates that nucleosome positioning at *hox* promoters is dynamic, depending on sequence specific factors such as Hox proteins.

Table of Contents

List of Tables:

List of Figures:

List of Third Party Copyrighted Material:

Figure Number	Publisher	License Number
Figure 1-2	Elsevier	3262250893779

CHAPTER I: Introduction

The central dilemma of a developing multicellular organism is how to control the differentiation and arrangement of a single cell into different structures and functions in a reproducible, stereotypic way. One method that has evolved throughout biology is to partition or segment cells into seemingly autonomous units. Within these units the cells respond uniquely to developmental cues based on their positioning within the organism and timing of environmental cues, thus creating diverse segments of differential gene expression. It is these differential units of gene expression that create the first diversity within the organism. Cells begin to differentiate and distinguish themselves from the other segments by their function. Positional signals further subdivide these segments creating greater specialization of these early segments. This method of segmentation and differentiation has given rise to the multitude of diversity amongst the animal kingdom. In 1894 Dr. William Bateson, while studying mutations found within populations of animals, observed unexpected changes in body segments that were replaced by other body segments (Bateson, 1894). These transformations included antennae of honey bees being transformed into legs and flies that had four wings instead of two. These observations extended to humans as well with some individuals possessing extra ribs or even extra fingers. Bateson described these transformations as “homeotic”. His were the first recorded observations of the function of a conserved family of transcription factors what would become known as the homeobox genes, or as they are referred to now, *Hox* genes.

Hox discovery and conservation throughout the animal kingdom

First characterized in *Drosophila melanogaster*, *Hox* genes were identified on the third *Drosophila* chromosome in two loci, the *Antennapedia*- and *bithorax* complexes (ANT-C and BX-C respectively) which makes up the *Drosophila Homeodomain* complex (HOM-C). Based on initial studies of mutations within these two clusters, it became clear that the ANT-C and BX-C clusters each controlled the development of a particular region of the fly. For example, mutations within the ANT-C genes resulted in transformation in the anterior segments, such as antennae into legs (Hazelrigg and Kaufman, 1983; Kaufman et al., 1980). On the other hand, mutations in the BX-C cause homeotic transformations within the posterior regions, such as transforming haltere into wings in the second thoracic segment (Lewis, 1978). Mapping of the genes, through analysis of polytene chromatin banding, of the ANT-C and BX-C revealed that the genes had colinear expression: The linear arrangement of the genes on DNA correlated with area of function along the anterior-posterior (AP) axis of the animal (Lewis, 1978).

Soon after the discovery that the ANT-C and BX-C clusters were associated with segmental identity in the fly, Southern hybridization revealed that portions of the HOM-C genes shared a highly conserved sequence (McGinnis et al., 1984b; Scott and Weiner, 1984). The sequence homology was determined to be an ~180bp sequence, that came to be known as the homeobox, encoded a 60 amino acid peptide termed the homeodomain (McGinnis et al., 1984a). The high

degree of sequence homology of the homeobox between the HOM-C genes suggested a potential for conservation among other segmented species. Indeed, since these initial observation in *Drosophila*, *Hox* genes have been found to be highly conserved and essential for bilateral metazoa development (Amores et al., 1998; Burglin and Ruvkun, 1993; Carrasco et al., 1984; McGinnis et al., 1984a; McGinnis and Krumlauf, 1992; Simeone et al., 1987).

Genome mapping of many metazoan species has revealed that most invertebrates have 8-13 *Hox* genes that are either arranged in one continuous linear cluster, as in sea urchins and lancelets, or in two discontinuous linear clusters, as in *Drosophila* and nematodes (Lemons and McGinnis, 2006). However, vertebrates have multiple *Hox* clusters with genes arranged in continuous linear clusters. A majority of vertebrates have four clusters with 39 genes with the exception of some teleost that have seven clusters with 48 genes (Hurley et al., 2005). Vertebrate *Hox* genes also retain the colinear expression (Duboule and Dolle, 1989; Kmita and Duboule, 2003) observed in some invertebrates. This suggests that despite the differences in gene arrangements observed between species, *Hox* clusters potentially arose from a single ancestor (Fig. 1-1). In line with this view, full length sequence homology is greater between genes found in the 3' end of frog, mouse, and *Drosophila* clusters than between 3' and 5' genes of the same species (Carrasco et al., 1984; McGinnis et al., 1984a). Most likely this ancestral cluster would be similar to the invertebrate lancelet cluster that is comprised of 14 genes in one continuously linear cluster.

Figure 1-1

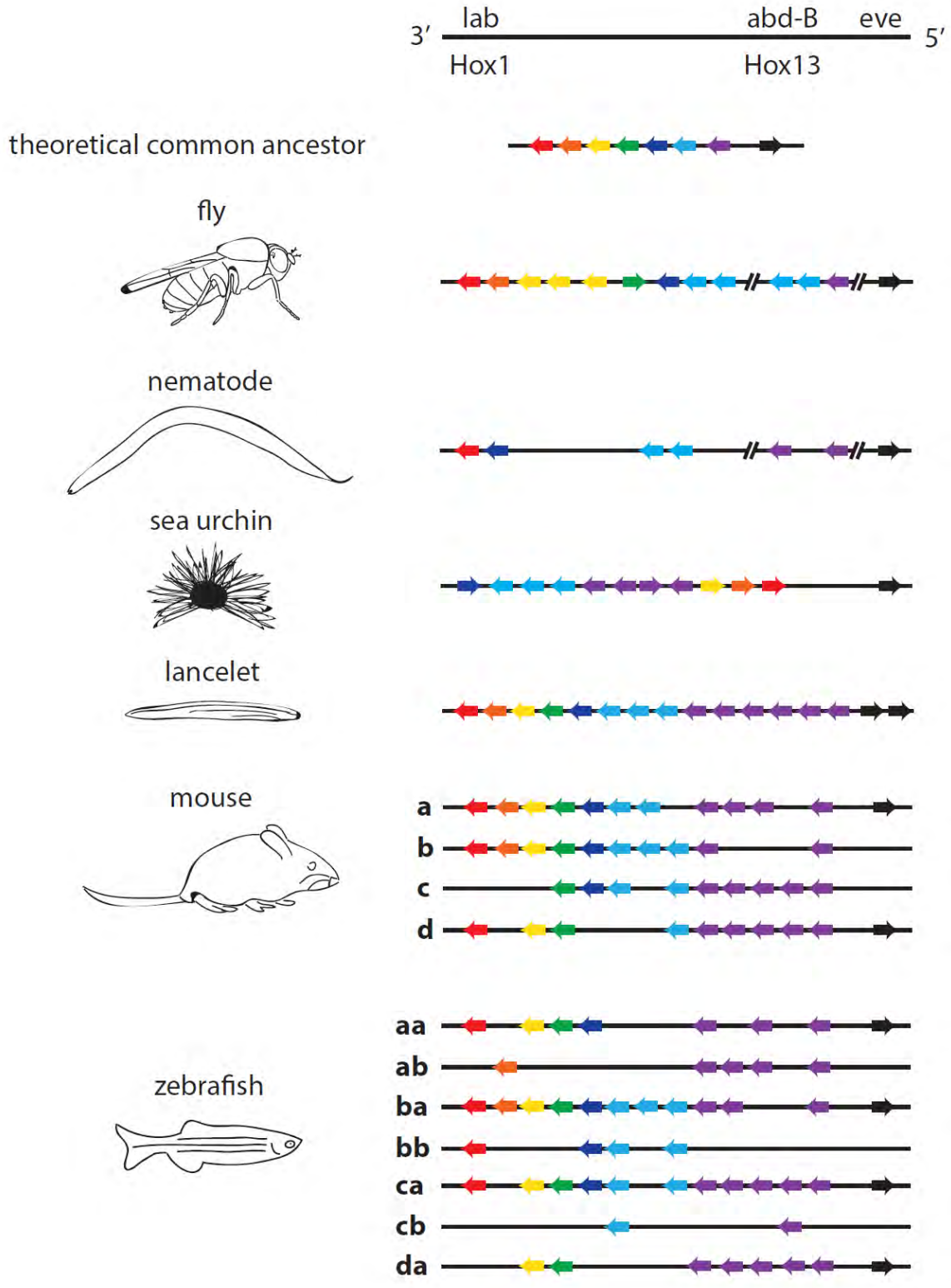
3′
lab
abd-B
eve
5′
Hox1
Hox13
theoretical common ancestor
fly
nematode
sea urchin
lancelet
mouse
a
b
c
d
zebrafish
aa
ab
ba
bb
ca
cb
da

Figure 1-1. Representation of Hox gene clusters in metazoan genomes. Schematic view of *Hox* clusters in several metazoan species including the hypothetical founder. Arrow indicates direction of transcription, colors indicate *Hox* genes with similar homeodomains, and hatched lines indicate chromosomal breaks within *Hox* clusters of *Drosophila* and *Nematode*. Lancelot is the closest ancestral cluster to vertebrates with all *Hox* genes in a single linear cluster relative to transcription. Tetrapods, i.e. the mouse, have four clusters while most teleost, i.e. zebrafish have seven clusters.

However, it is not well understood why vertebrates have duplicated clusters. Duplication has often been considered a quicker, more efficient mechanism to increase complexity of biological structures, diversity between species, and is a popular theory given the increase in relative complexity of vertebrate systems (Taylor and Raes, 2004). In the case of the vertebrate *Hox* clusters, this may explain why so many genes have been retained after the initial duplication events from invertebrate species. The duplication events that created the vertebrate *Hox* clusters created paralogous genes that initially had similar function, and expression domains. Through evolution some common functional redundancies have been retained, like the function of *Hox10* and *Hox11* paralogs in mouse that control the patterning of posterior axial skeleton (Wellik and Capecchi, 2003). Functional redundancy has also been lost, either as single genes of a paralog, like *Hoxc2*, *Hoxd5*, or *hoxb10* in mouse, or as a cluster, like the *hoxdb* cluster in zebrafish. While other paralogs have diverged to gain function like zebrafish *hoxb1b* and *hoxb1a*, orthologs of mouse *Hoxb1*, that have gained separate functions during zebrafish hindbrain development (McClintock et al., 2002) . Despite these examples, it remains unclear if the old school of thought that more genes equate to more function is really a valid argument for the duplication of *Hox* genes. However, these gene duplications may play another role such as acting as a safe guard to ensure correct function. As stated previously, many of these redundant genes appear to still have similar functions

meaning there must be some selective pressure to keep these duplications or else these genes would be lost.

Hox protein structure, DNA binding, and complex formation

As stated above, the Hox genes encode transcription factors that contain a DNA binding element termed the homeodomain. The homeodomain is comprised of 60 amino acids that, based on nuclear magnetic resonance and x-ray crystal structures, form a three alpha helical structure that closely resembles the helix-turn-helix motif found in prokaryotic repressor proteins (Kissinger et al., 1990; Klemm et al., 1994; Otting et al., 1990; Qian et al., 1989; Wolberger et al., 1991). From these structures it became clear that the homeodomain bound to DNA through two domains: (1) The third helix, often referred to as the recognition helix, that contacts DNA in the major groove and (2) an unstructured arm N-terminal to the homeodomain that contacts the minor groove. The N-terminal arm also contains 4-6 conserved residues at the end termed the YPMW-domain. Mutational analysis determined that the homeodomain/DNA interaction is mediated by 9 residues equally dispersed between the N-Terminal arm and the recognition helix (Ades and Sauer, 1995; Damante et al., 1996; Ekker et al., 1994; Fraenkel et al., 1998; Phelan et al., 1994). Recent in vitro binding studies indicate that Hox proteins bind a 5'-T(A/T)AT(T/G)(A/G)-3' motif (Noyes et al., 2008). The degeneracy of the motif is supported by in vitro binding studies that indicate that Hox proteins recognize relatively similar sequences

(Hoey and Levine, 1988). However, binding in vivo appears to be much more directed, such that a general binding site cannot explain the diversity of functions Hox proteins control, suggesting that homeodomain and N-terminal arms must have specificity determinants. To test this theory, the function of chimeric Hox proteins comprised of swapped homeodomains and N-terminal arms from Hox proteins with divergent function were tested in vivo. In mouse, the HoxA11 homeodomain was swapped for either the HoxA4, HoxA10, or HoxA13 homeodomain (Zhao and Potter, 2001, 2002). All three chimeric HoxA11 proteins had specific defects in the female reproductive system, consistent with a homeotic transformation to posterior structures, as in the case of the HoxA11-A13 chimeras, and anterior structures of HoxA11-A10 chimeras. In Drosophila, swapping of the N-terminal arm of Ultrabithorax (Ubx) with that of Abdominal-A (AbdA) led to activation of Abd-A in a Ubx-AbdA chimera dependent manner (Chauvet et al., 2000). These results indicate that in the context of the cell, that the homeodomain and N-terminal arm recognize specific DNA sequences.

PBC and MEINOX proteins complex with HOX in vivo

In vivo specificity is, in part, due to cofactors that complex with Hox proteins that enhance target binding (LaRonde-LeBlanc and Wolberger, 2003). The two major groups of these cofactors are the TALE homeodomain proteins PBC and MEINOX (Moens and Selleri, 2006). PBC and MEINOX proteins have an atypical homeodomain that is characterized by an additional three amino acids between the first and second loops of the homeodomain, from which the TALE

(Three Amino acid Loop Extension) homeodomain gets its name. The PBC gene family consists of *Pbx1-4* in vertebrates as well as *Drosophila Extradentical* (*Exd*) and worm *ceh-20*, while the MEINOX gene family includes vertebrate *Prep 1-2, Meis1-3*, zebrafish *Meis4*, *Drosophila Homothorax* (*Hth*), and worm *unc-62* (Moens and Selleri, 2006). Unlike the discrete domains of *Hox* expression, *PBC* and *MEINOX* family members are expressed in broad domains that coincide with *Hox* expression (Vlachakis et al., 2000) and are also maternally supplied, such as Prep proteins that are found ubiquitously early in the developing embryo (Deflorian et al., 2004; Vaccari et al., 2010).

Consistent with their role as Hox cofactors, Pbx and Meis proteins have been shown to require DNA to form complexes with Hox proteins in *Drosophila* (Ebner et al., 2005; Ryoo et al., 1999), mouse (Jacobs et al., 1999), and zebrafish (Choe et al., 2002). In the absence of either DNA or specific binding sites, Hox/Pbx/Meis complexes are not observed. Correlating with these binding studies, PBC, MEINOX, and Hox binding sites have been found together at several Hox promoters in both vertebrates and *Drosophila* (Ferretti et al., 2000; Popperl et al., 1995; Ryoo et al., 1999).

Loss-of-function studies indicate that PBC and MEINOX play a role in embryonic segmentation. In *Drosophila*, *Exd* loss-of-function leads to a posteriorization of anterior abdominal segments, creating a uniform thoracic domain (Peifer and Wieschaus, 1990). In vertebrates, Pbx and Meis/Prep loss-of-function leads to hindbrain segmentation defects. In particular, loss of

either Pbx4 (Popperl et al., 2000) or Pbx2 (Waskiewicz et al., 2002) in zebrafish leads to a loss in the 2-6 hindbrain segments, termed rhombomeres (r). Loss of Meis3 appears to have a similar phenotype, with hindbrain segmentation completely lost (Dibner et al., 2001). These phenotypes are similar to previously reported Hox loss-of-function phenotypes in Xenopus. Here, *Hox* paralog-group 1 (*Hox-pg1*) genes, *hoxa1, hoxb1, and hoxd1*, were knocked down using morpholino anti-sense oligos and resulted in the loss of hindbrain segments r2-6 (McNulty et al., 2005). These similar phenotypes indicate that PBC, MEINOX, and Hox function within the same pathways.

The interaction of PBC proteins with Hox proteins is mediated by the interactions between the TALE homeodomain of PBC proteins and the YPMW- domain of Hox proteins. It is important to note that the YPMW domain is a special feature to some Hox proteins for which it plays an important role in Hox/PBC interactions. This interaction has been visualized by X-ray crystallography on DNA with the homeodomains of Pbx1 and HoxA1 (Piper et al., 1999)(Fig. 1-2). Based on this study, the TALE domain creates a pocket for the YPMW-domain to bind. Functional analysis of this domain indicates that removal of the YPMW- domain from Hox proteins, such as mouse HoxA1 and HoxB4, disrupts dimerization of Hox and Pbx on DNA (Chang et al., 1995; Remacle et al., 2004). In vivo the disruption of the HoxA1/Pbx interaction leads to defects in

Figure 1-2

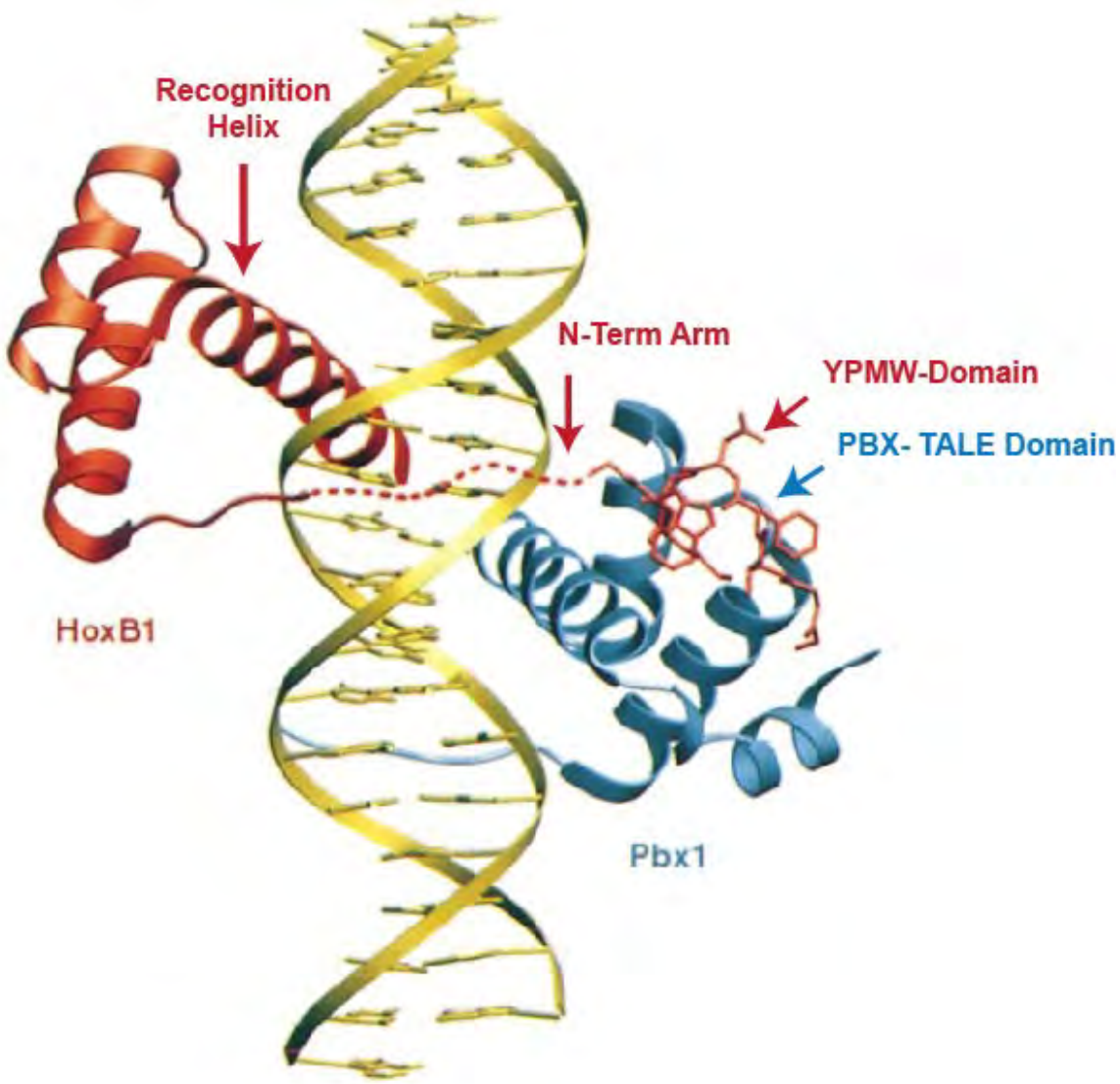
Recognition
Helix
N-Term Arm
YPMW-Domain
PBX- TALE Domain
HoxB1
Pbx1

Figure 1-2. Hox-PBX complex on DNA.

Ribbon diagram of the solved crystal structure depicting complex formation between mouse Hoxb1 homeodomain and mouse Pbx1 TALE domain on DNA. Structure indicates that the recognition of Hoxa1 binds DNA in the major groove, while the N-terminal arm fills the minor groove. The interaction of the YPMW-Domain with the TALE domain of Pbx1 can also be observed. Indicated by associated colors: the recognition helix, the flexible N-terminal arm, and the YPMW-domain of Hoxb1, as well as the TALE domain of Pbx1. Adapted from:(Piper et al., 1999)

hindbrain segmentation and development consistent with HoxA1 loss-of-function (Remacle et al., 2004). Conversely, the addition of the YPMW-domain to Hox proteins that lack the domain appears to greatly increase Pbx-Hox interactions. For instance, the addition of the YPMW-domain to HoxA10 greatly increased the interaction between Pbx and HoxA10 as well as the HoxA10/Pbx complex with DNA in vitro (Chang et al., 1995). Taken together, these data indicate that PBC and MEINOX family members are important cofactors in function of Hox complexes, in part, by increasing the specificity of Hox complexes for DNA, as well as increasing affinity.

Hox gene functions during embryogenesis

The main function of *Hox* genes during development is to determine tissue identities along the AP axis during early development. An intricate system of *Hox* gene activation and repression results in an overlapping pattern of *Hox* expression domains often referred to as the "*Hox* code" (Krumlauf, 1994) (Fig. 1-3). *Hox* genes function within these domains to segment, specify, and differentiate the tissues within. Hox proteins play this role in many structures along the AP axis and for the sake of relevancy to the work within, this introduction will focus on the role *Hox* genes play in vertebrate hindbrain segmentation.

Figure 1-3

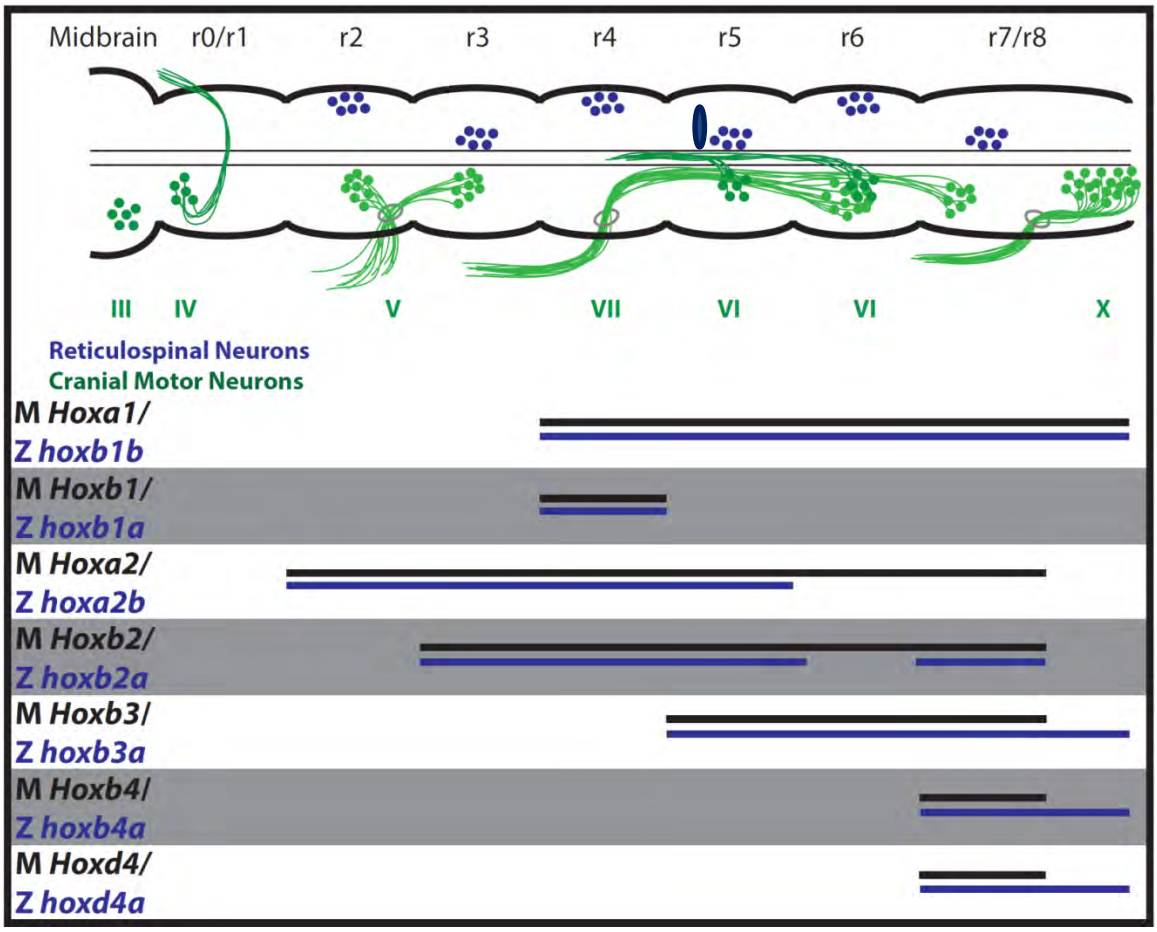
Midbrain
r0/r1
r2
r3
r4
r5
r6
r7/r8
III
IV
V
VII
VI
VI
X
Reticulospinal Neurons
Cranial Motor Neurons
M Hoxa1/
Z hoxb1b
M Hoxb1/
Z hoxb1a
M Hoxa2/
Z hoxa2b
M Hoxb2/
Z hoxb2a
M Hoxb3/
Z hoxb3a
M Hoxb4/
Z hoxb4a
M Hoxd4/
Z hoxd4a

Figure 1-3. Vertebrate hindbrain structures and neurons are patterned by *Hox* expression.

Diagram of vertebrate hindbrain structure accompanied with *Hox* expression domains illustrated in black for mouse and blue for zebrafish. Rhombomere specific motor neuron and reticulospinal neuron populations are labeled in the hindbrain structure in green and blue, respectively. *Hox* function forms the abducens in r2 and r3, facial motor neurons that are born in r4 and migrate to r6 and r7, the trigeminal neurons in r5 and r6, and the vagal neurons in r7/r8. For clarity, only one of the two Mauthner neurons (blue oval) formed in r4 is depicted without an axon.

Hox genes segment the vertebrate hindbrain during embryogenesis

The hindbrain lies anterior to the spinal cord and is the most anterior structure segmented by the *Hox* genes. Shortly after gastrulation, as the first *Hox* gene is transcribed the first hindbrain segment is formed, starting the process that forms seven to eight segments. These segments, termed rhombomeres, form transiently but have been visualized as physical "bulges" in the developing hindbrain of mouse, chick, and zebrafish (Gavalas et al., 1997; Hanneman et al., 1988; Moens et al., 1998; Vaage, 1969). From this structure various motor neuron populations as well as interneuron populations form. Segmentation of the hindbrain is not linear and starts with the formation of rhombomere-four (r4) followed by formation of the r1/r2 boundary, the r2/r3 boundary, the r6/r7 boundary, and then the r5/r6 boundary. The formation of rhombomeres 2-8 (r1 is "*hox*-less") are dependent upon the initiation of temporal colinear expression of *Hox* genes by developmental signals, such as retinoic acid (RA), the activity of specific *Hox* genes, such as *Hoxa1/hoxb1b*, and the activity of downstream *Hox* targets, such as *Kreisler/valentino*. Indeed, disruption of any of these factors leads to improper segmentation of the hindbrain. In mouse, targeted deletion of *Aldh1a2* results in reduction of hindbrain RA concentration and the loss of r5-7, causing a severe reduction in the hindbrain (Niederreither et al., 2000). In addition, the loss of *Hoxa1* or its ortholog *hoxb1b* in zebrafish leads to a reduction in r4 and r6 as well as an increase in r3 (Carpenter et al., 1993; Chisaka et al., 1992; Lufkin et al., 1991; McClintock et al., 2002; Rossel and

Capecchi, 1999). While *valentino*$^{-/-}$, ortholog of mouse *Kreisler*, zebrafish embryos lose the formation of rhombomere boundaries posterior to the r4/r5 boundary (Moens et al., 1996). However, though mutations in *Hox* genes and their targets lead to segmentation defects, the Hox and similar factors do not directly segment the hindbrain.

Hox initiate cell sorting mechanisms that actively segment hindbrain.

As stated above, Hox function does not directly segment the hindbrain. Instead, hindbrain cells separate into rhombomeres due to differential expression of two cell surface molecule families, the erythropoietin-producing hepatocellular (Eph) receptor tyrosine kinases and their membrane-bound ligands ephrins. Shortly after gastrulation and before *Hox* gene activation the presumptive hindbrain is made up of undifferentiated cells that are freely diffusible within the neuroectoderm. Lineage tracing of cells within the presumptive hindbrain reveals that shortly after *Hox* expression is initiated these movements become restricted. In chicken embryos, cells labeled with DiI or fluorescent dextran prior to *Hox* activation, can diffuse through the hindbrain and can be found in separate rhombomere domains (Birgbauer and Fraser, 1994; Fraser et al., 1990). However, when these cells are labeled after *Hox* expression, movements of the labeled cells appear restricted, coinciding with rhombomere domains (Fraser et al., 1990). The rhombomere boundaries are not physical barriers however, as removal of boundary cells do not induce subsequent cell mixing from adjacent rhombomeres (Guthrie and Lumsden, 1991). Instead, these cells separate into

rhombomeres due to differential expression of Eph receptors and ephrin ligands. When Eph receptors are bound by ephrin ligands signals are transduced into both cells creating a bidirectional signaling pathway of either repulsion or attraction (Xu et al., 1999).

Ephs are divided broadly into two classes, EphA receptors that generally bind ephrin-A ligand and EphB receptors that bind ephrin-B ligands. During hindbrain development, Eph and ephrins have alternating rhombomere expression with Eph receptors, EphA4, EphB2, and EphB3, expressed in r3 and r5, while ephrin ligands, ephrin-B1, ephrin-B2, and ephrin-B3, expressed in r2, r4, and r6. The alternating pattern of Ephs and ephrins is driven by Hox and Hox targets, in particular, *Krox20* that drives *EphA4* transcription in r3 and r5 (Theil et al., 1998) and *Kreisler/valentino* that also drives *EphB2* in r5 (Cooke et al., 2001). These alternating domains of Ephs in odd rhombomeres and ephrins in even presents an apparent mechanism by which cells expressing Eph are repulsed by cells expressing ephrins and vice versa and is supported by several findings. First, when two even or two odd numbered rhombomeres, from chicken hindbrain, where grafted together, new boundaries did not form and cells mixed (Guthrie and Lumsden, 1991); indicating that cells within the even and the odd domains were similar. Second, using a dominant-negative approach, injected *EphA4* RNA lacking the kinase domain (dnEphA4) disrupted the formation of tight rhombomere boundaries in zebrafish and X*enopus* embryos (Xu et al., 1995). In these experiments dnEphA4 created a loss of the normal segmental

rhombomere formation, with EphA4 cells not restricted to r3/r5 but also found in even rhombomeres r2, r4, and r6. Third, ectopic expression of ephrin-B2 in Eph expressing cells still caused the dual expressing cells to segregate to their own populations at rhombomere boundaries (Xu et al., 1999). In these experiments mRNA encoding ephrin-B2 was injected into one cell of an 8 cell zebrafish blastocysts; creating mosaic expression of ectopic ephrin-B2 cells within the embryo, some of which become part of the presumptive hindbrain. At the 3-somite stage, r3 and r5 begin to form and cells expressing ectopic ephrin-B2 can be seen within r3, r4, and r5. After r3 and r5 domains have fully segmented by the 10-somite stage, ectopic ephrin-B2 cells are found at the boundaries of r2/r3, r3/r4, and r4/r5 but found scattered within r2, r4, and r6. Interestingly, the ectopic cells that formed in r3 and r5 formed their own clusters at the r2/r3, r3/r4, and r4/r5 borders indicating endogenous Ephs kept these cells from mixing with r2, r4, and r6. Together, these data indicate that *Hox* expression patterns activate Eph/ephrins and that these Eph/ephrin interactions are essential for segregation of the cells within the hindbrain into rhombomeres.

Hox genes specify neuronal identity and function within rhombomeres.

Just as *Hox* expression is important for rhombomere formation, *Hox* expression is also important for hindbrain neuroanatomy. Rhombomere formation provides cells with anterior-posterior positioning information as well as cell to cell interactions that lead to compartmental specificity and function. Within each rhombomere a particular combination of *Hox* genes and Hox targets are

expressed that will give rise to a rhombomere specific sets of neurons, specifically discussed here, motor neurons and interneurons.

Motor neurons within the hindbrain form the V-X cranial nerves that innervate the head and neck of the embryo controlling muscles in the face involved with jaw and eye movements (Fig. 1-3). In zebrafish this includes the trigeminal neurons in r2 and r3 that form the Vth nerve, the facial motor neurons (FMN) that form in r4 and migrate to r6 and r7 and form the VIIth nerve, the abducens in r5 and r6 that form the VIth, and the vagal neurons in r7 and r8 that form the Xth nerve (Higashijima et al., 2000). Each of these domains is dependent on *Hox* genes and their targets for proper function. Loss-of-function experiments in mouse have shown that *Hoxa3*$^{-/-}$ mouse embryos fail to form abducens neurons in r5 (Watari et al., 2001), while in *Hoxb1*$^{-/-}$ mouse embryos FMN fail to migrate out of r4 (Studer et al., 1996), both phenotypes correlating with the endogenous rhombomere expression domain. Neuronal fates have also been altered in gain-of-function experiments. In zebrafish, injection of *hoxb1b* drives the expression of *hoxb1a* into r2 and as a consequence r2 and r3 trigeminal neurons take on the appearance of r4 FMN (McClintock et al., 2001). In general, neuronal patterning has been found to be conserved among mice, chickens, amphibians, and zebrafish, suggesting that there is conservation in the function of *Hox* genes in neuronal specification. Such conservation can be seen in the roles of *Hoxb1* and the zebrafish ortholog *hoxb1a*. Loss-of-function experiments for *Hoxb1* and *hoxb1a* have similar phenotypes with FMNs stuck in

r4 (McClintock et al., 2002; Studer et al., 1996). However, some differences do exist between species and the neuronal patterns formed (Fritzsch, 1998; Glover, 2001). For example, in mouse trigeminal neurons form in r1, r2, and r3, however in zebrafish and chicken trigeminal neurons form in just r2 and r3. FMNs in mouse and chicken form in r4 with a portion migrating to r5, opposed to zebrafish where FMNs form in r4 and migrate to r6 and r7. Abducens neurons form in r5 in mouse but form in r5 and r6 in zebrafish and chicken. However, these differences may be related to the slightly different patterns of *Hox* expression between species. For instance, the r5 location of the abducens neurons coincides with the r5 expression domain of *Hoxa3*, while the location of zebrafish abducens neurons coincides with r5 and r6 expression of zebrafish *hoxb3a*, the ortholog to mouse *Hoxa3* (Prince et al., 1998a; Watari et al., 2001).

As well as specifying motor neurons, reticulospinal neurons are also formed in a rhombomere specific fashion. A class of interneuron, reticulospinal neurons fills a diverse roll within the vertebrate hindbrain, transmitting various signals from the brain to the spinal cord, including those for breathing, beating of the heart, and locomotion from the brain into the spinal cord. Unlike the motor neurons, there appears to be little conservation in the anatomy of reticulospinal neurons between different species within the hindbrain. Potentially most of these differences are due to the increase in reticular spinal neurons found between species. For example, zebrafish have ~65, frog have ~150, chicken have ~500, and rat/mouse have 2500 interneurons (Glover, 2001). In zebrafish larvae the

fewer reticulospinal neurons equate to fewer connections that created a simple ladder like appearance of the neurons within the hindbrain. On the other hand the large numbers of reticulospinal neurons in rat/mouse creates a large web of interactions that also include small specialized domains of important functions. However, unlike mouse and chicken, zebrafish reticulospinal neurons continue to form and increase in number as the animal becomes bigger (Glover, 2001) indicating that this simplistic structure may be transient.

In zebrafish reticulospinal neurons alternate between medial and lateral positions within rhombomere in the hindbrain. However, reticulospinal neurons are studied in the zebrafish because of two easily identifiable reticulospinal neurons, the Mauthners. The Mauthner neurons (MN) are comprised of two large bilateral cells within r4 that each extended a single wide diameter axon posteriorly contralateral to the neural tube. MNs function as part of the C-start swimming mechanism used in the evasion of predators. Both structure and function of MNs appears conserved as they are found in other teleost fish and some amphibians. Like motor neurons, *Hox* genes also play a role in the formation of the MNs in zebrafish. In a loss-of-function approach, anti-sense MO to zebrafish *hoxb1b* and *hoxb1a* were co-injected into developing zebrafish embryos resulting in a random loss of one or both MNs (McClintock et al., 2002). Gain-of-function experiments have also yielded similar observations. Treatment of zebrafish and frog embryos with retinoic acid forms ectopic MNs in what appears to be r2 (Alexandre et al., 1996; Manns and Fritzsch, 1992). An

observation that is also supported by the injection of *hoxb1b* mRNA, that forms similar ectopic MNs in r2 (McClintock et al., 2001). These results indicate that segmentation and specification of r4 is also important for MNs formation.

***Hox* gene regulation**

Hox genes are regulated at several levels, including developmental signaling molecules, chromatin structure, and *Hox* expression. There is no one factor that regulates all aspects of *Hox* expression. Instead it is the interplay of an overlapping set of mechanisms that gives rise to the colinear *Hox* expression pattern along the AP axis.

The role of retinoic acid in Hox gene regulation

The initiation of colinear *Hox* transcription comes shortly after gastrulation in vertebrates with the activation of *Hoxa1* in mammals and its ortholog *hoxb1b* in teleost. This activation is directed by the RA signaling pathway. RA is a lipid soluble molecule that, in addition to *Hox* activation, is essential in a wide array of other developmental pathways in the embryo. RA is a teratogen and changes in the endogenous levels either through chemical, genetic, or dietary mean leads to improper formation of the AP axis. This includes hindbrain segmentation defects, posteriorization of the fore- and midbrain, as well as developmental defects in the eyes and ears all of which are consistent with improper *Hox* activation (Begemann et al., 2001; Dupe et al., 1997; Dupe et al., 1999; Gavalas et al., 1998; Niederreither et al., 2000; Serpente et al., 2005; Studer et al., 1998).

RA is synthesized in two oxidative steps from maternal stores of vitamin A (or retinol), into retinaldehyde (or retinal) followed by further oxidation into RA during early embryogenesis. The first step of retinol to retinal by alcohol- and retinol- dehydrogenases (Adh and Rdh respectively) appears to be a ubiquitous process in the embryo, with *Adh* and *Rdh* expression throughout most of the embryo in overlapping domains (Ang et al., 1996; Sandell et al., 2007; Zhang et al., 2007). The next oxidation step is done by aldehyde dehydrogenases (Aldh) and converts retinal to RA. Unlike the conversion of retinol to retinal, the conversion of retinal to RA appears to be restricted by the expression pattern of *Alhd1a* genes. During embryogenesis RA is generated by the *Aldh1a2* within the developing mesoderm posterior to the presumptive hindbrain (Shimozono et al., 2013). While in the cytoplasm, RA is bound by cellular RA-binding protein (CRABP). CRABP acts as an anchor, to keep RA from diffusing out of the cell, as well as an intercellular-transport, shuttling RA into the nucleus for signal transduction. Once in the nucleus RA binds a heterodimeric complex of retinoic acid- and retinoid-X receptors (RAR and RXRs respectively). In tetrapods there are 3 RARs and 3 RXRs that make up alpha, beta, and gamma gene classes. In zebrafish the RAR and RXR genes have been duplicated resulting in four RAR genes (alpha/gamma a and b) and six RXR genes (alpha/beta/gamma a and b). These duplications of RAR and RXR in both mouse and fish result in overlapping expression patterns that function redundantly (Dupe et al., 1999; Oliveira et al., 2013). The RA-RAR/RXR complex binds DNA at specific recognition sites,

termed RA response elements (RAREs), in the enhancers of genes and activates target gene transcription (Apfel et al., 1995; Perissi et al., 1999; Roy et al., 1995). RA-RAR/RXR complexes also target suppressors of RA signaling, thus creating an inhibitory feedback loop (Feng et al., 2010; Hernandez et al., 2007). These suppressors included members of the cytochrome p450 family of enzymes, such as *cyp26a1*, *cyp26b1*, and *cyp26c1* that function to further oxidize RA into inactive forms (Fujii et al., 1997; Niederreither et al., 2002; White et al., 1996).

Temporal colinear activation of *Hox* genes appears to be initiated by an RA gradient that is conserved among vertebrates. This is apparent due to the timing of expression along with the sensitivity of *Hox* genes to RA. For example, *Hox-pg1* genes found in the 3' end of clusters appear to be more sensitive to RA and activated earlier with less RA than *Hox-pg4* genes found in the 5' end of clusters that are activated later and with more RA. Also, in the human embryonic carcinoma cell line NT2/D1, 3' genes of the *HOXB* cluster, *HOXB1* and *HOXB2* were activated at low doses of RA relative to 5' genes, *HOXB8* and *HOXB9* (Simeone et al., 1990). This study also showed that the ordered expression of 3' genes, *HOXB1* and *HOXB2,* was induced at a greater rate than 5' genes, *HOXB8* and *HOXB9,* and that these rates could be modified, becoming faster with increased RA and slower with less. Similar sensitivities have also been observed in studies that knockdown or block RA signaling in the embryo. In developing chicken embryos an inhibitor of RA signaling, BMS493 an RAR agonist, binds RARs and inhibits signal transduction (Germain et al., 2009).

Varying concentrations of BMS493 effected hindbrain formation in different manner. Highest doses of BMS493 created an expanded r3 as well as a loss of r5 (Dupe and Lumsden, 2001). While conversely, low doses had little effect, with only increasing the size of r4-7 slightly. The drug also had different effect depending on the time it was added, with r4-7 the most effected early in development, becoming less so later. Taken together these studies indicated that the concentration of RA detected within the cell plays a role in the profile of *Hox* expression. This broad *Hox* expression profile would be later fine-tuned by other developmental signaling proteins such as fibroblast growth factor (FGF) and Wnt through the repression of *Hox* gene expression. An example of such is the r4/r5 boundary of zebrafish *hoxb1a* (ortholog to mouse *Hoxb1*) expression that is defined indirectly by FGF through the activation of *valentino* (*val*, ortholog of mouse *mafB/Kreisler*) that represses r4 fates in r5 (Hernandez et al., 2004).

Until recently however, the existence of an RA gradient was a point of debate within the field. This centered around two points that contradicted the requirement for an RA gradient. (1) An RA gradient had not been observed. Unlike other peptide signaling molecules, like fibroblast growth factor (FGF) or Wnt that could be tagged and endogenous levels could be viewed in vivo, the chemical nature of RA makes visualization by these methods impossible. Without means of tagging RA, initial attempts to visualize RA within embryos focused on identifying areas of RA activity. This was accomplished by use of an RA reporter transgene containing three RAREs in the promoter driving *LacZ*

(*RARE-LacZ*) (Rossant et al., 1991). Exogenous RA activates the reporter in all cells of the developing embryo, while in *Aldh1a2*$^{-/-}$ embryos the reporter remained silent (Mic et al., 2002; Niederreither et al., 1999). Characterization of the reporter during embryogenesis indicated that RA did not form a gradient within the embryo. Instead, RA was contained in sharp well defined domains that shifted posteriorly during embryogenesis (Rossant et al., 1991; Sirbu et al., 2005). (2) Embryos that had been depleted of RA could be rescued by the addition of ectopic RA at a single concentration. In particular, AP segmentation defects observed in *Aldh1a2*$^{-/-}$ mouse embryos and zebrafish embryos treated with 4-diethylaminobenzaldehyde (DEAB), a reversible chemical inhibitor that competes with retinal for Aldh (Russo et al., 1988), were both rescued by the administration ectopic RA (Begemann et al., 2001; Niederreither et al., 2000). Since RA was not administered in the form of a gradient, these observations indicated that an RA gradient was unneeded for correct AP patterning, putting a strain on the model of colinearity through an RA gradient.

However, analysis of Cyp26 expression in the developing embryo helped clarify these results. In loss-of-function experiments detailing the role of three Cyp26 genes, *cyp26a1*, *cyp26b1*, and *cyp26c1*, in zebrafish embryos indicated that these proteins were expressed in a dynamic pattern that made them important modulators of RA signaling. As stated previously, Cyp26 family members mediate RA levels within the cell by oxidizing RA to other inactive molecules (White and Schilling, 2008). In addition, loss-of-function experiments

demonstrated that *cyp29a1* was necessary for hindbrain segmentation in mouse (Abu-Abed et al., 2001) and zebrafish (Emoto et al., 2005). These observations were further supported by MO loss-of-function of all three Cyp26 genes, *cyp26a1*, *cyp26b1*, and *cyp26c1*, in zebrafish (Hernandez et al., 2007). The defects in AP patterning, particularly the posteriorization of the hindbrain and the ectopic *Hox* transcription were consistent with the teratogenic effects of increased RA. *Cyp26* genes are also expressed in opposing domains that flank the *aldh1a2* domain in the anterior-trunk mesoderm of the embryo (Hernandez et al., 2007; Shimozono et al., 2013). These observations taken together with those of the colinear expression of *Hox* genes built a model in which a RA gradient forms from an original area of high RA concentration in the posterior hindbrain that diffuses in rostral and caudal directions within the embryo where it is degraded to form a gradient by Cyp26 protein. This model was recently realized by the visualization of the RA gradient by fluorescent resonance energy transfer (FRET) between free RA and modified RARs (Shimozono et al., 2013). Together these data indicate that establishment of a RA gradient is important for temporal colinear expression of the *Hox* genes.

The role of chromatin in *Hox* gene regulation

In addition to being regulated through RA signaling, *Hox* genes are also regulated through changes in global chromatin structure as well as local chromatin marks around the promoters of *Hox* genes. Using fluorescent in situ

hybridization, the global chromatin changes occurring at the *HoxB* and *HoxD* clusters were tracked prior to and during *Hox* activation (Chambeyron et al., 2005; Morey et al., 2007). Tissues harvested at time points when *Hox* genes were not transcribed had probes that remained close together, in what was observed to be condensed chromatin. At time points prior to, or during, gene expression from the *Hoxb* or *Hoxd* clusters, the probes diverged from one another, indicating chromatin decondensation and opening. This mechanism of slow unwinding of the compacted chromatin to a more open state appeared to be important for colinearity, in particular, since after decondensation commenced, *Hox* transcripts could be identified in a colinear order. This process was also mimicked in mouse embryonic-stem cells by adding exogenous RA (Chambeyron and Bickmore, 2004) indicating that RA signaling played a role in *Hox* chromatin architecture.

Hox genes are also regulated locally at promoters and gene bodies through a host of histone modifying enzymes. First characterized in *Drosophila*, Polycomb-Group (PcG) and Trithorax-Group (trxG) proteins were found to have a role in *Hox* regulation. PcG and trxG genes were identified by a series of mutations outside of *HOM-C* genes that resulted in the similar homeotic transformations linked to *Hox* gene expression. For example, mutations in the *Polycomb* gene led to *BX-C* gain-of-function phenotypes, posteriorizing the embryo (Lewis, 1978). These observations indicated that *Polycomb* conferred repressive information upon the *BX-C* cluster, keeping these genes silent in the

anterior portions of the embryo. Opposed to the gain-of-function observed with *Polycomb* mutations, mutations to *trithorax* led to the loss-of-function phenotypes, such as genitalia to legs and/or antenna into leg (Ingham, 1985). Interestingly, unlike the phenotypes of *Hox* mutations, PcG and trxG mutations effected a larger portion of the developing embryo, not just a specific *Hox* domain. The global effect of PcG and trxG mutations are reminiscent of the PBC and MEINOX mutations, as they do not directly effect expression of *Hox* genes, indicating that these genes function in parallel to maintain *Hox* expression in some cells, while continuing to repress expression in others.

PcG and trxG proteins are general chromatin modifiers that function in several multiprotein complexes. In metazoa there are two major PcG complexes, Polycomb repressive complex 1 and 2 (PRC1 and PRC2). PRC1 and PRC2 are made up of different components that work in parallel to repress gene activation. PRC2 is responsible for di- and tri-methylation of lysine 27 of histone H3 (H3K27-me3 and me3), a repressive histone mark that is catalyzed by the set domain of Enhancer of zeste [E(z)], a conserved function in the vertebrate ortholog EZH1/2 (Cao et al., 2002; Margueron et al., 2008; Muller et al., 2002). The H3K27me3 itself does little to silence gene targets, instead H3K27me3 acts as a signal, labeling chromatin for PRC1. PRC1 recognizes the H3K27me3 marks through the chromodomain of Polycomb (Pc) and the vertebrate ortholog Cbx, targeting these complexes to chromatin in a sequence independent manner (Fischle et al., 2003). Once at chromatin, PRC1 marks lysine 119 of histone H2A (H2AK119ub)

with ubiquitin through the E3 ubiquitin ligases Ring/Ring1A/B (Wang et al., 2004). The repressive function of the PRC1 complex appears to be mediated by Posterior sex combs (Psc). Truncations of Psc identified a domain in the N-terminus that confers the repressive features of PRC1, in vitro, in cell free transcription assays, and in vivo, in wing imaginal disc that ectopically expressed Abd-B in the presence of the truncated Psc (King et al., 2005). The mechanism for transcriptional repression by Psc appears to be compaction of chromatin. The truncated form of Psc, that lacks transcriptional silencing, was shown to be unable to compact reconstituted nucleosomes in vitro like WT Psc (Francis et al., 2004).

trxG proteins make up five groups in metazoa, SWI/SNF and NURF that are conserved between *Drosophila* and vertebrates, MLL 1-3 found in vertebrates, and TAC1 and Ash1 found in *Drosophila*. Like the PcG complexes, the trxG complexes can be subdivided into two main groups based on function. In one group is TAC1, ASH1, and MLL. All three of these trxG complexes have histone methyltransferases, Trx in TAC1, Ash1 in ASH1, and MLL in MLL complexes. These enzymes all show a preference for methylating H3K4 (Byrd and Shearn, 2003; Milne et al., 2002) a mark that is associated with active gene transcription. Similar to the PRC2 complex of PcG proteins, the TAC1, ASH1, and MLL complexes do not directly control chromatin structure, instead they act through methyltransferase activity to mark chromatin. The second group, made up of the SWI/SNF and NURF complexes, contain ATP-dependent chromatin

modifiers that position nucleosomes favorably for transcription. The SWI/SNF complex contains the ATP-dependent modifier Brahma (Brm) in *Drosophila* and BRM and Brm-related gene one (Brg1) in vertebrates. NURF complex function is dependent on Inhibitor of switch (ISWI) and the vertebrate ortholog SNF2L.

Histone marks have been mapped across the *Hox* cluster to gain insight in to how chromatin states are maintained as *Hox* genes are activated. Interestingly, mapping of H3K27me3 and H3K4me3 marks in mouse and human embryonic stem (ES) cells indicated that at *Hox* loci prior to differentiation both marks were present on the same nucleosome (Bernstein et al., 2006; Shahhoseini et al., 2013). H3K27me3 and H3K4me3 bivalency has also been found at *Hox* clusters during zebrafish embryogenesis (Vastenhouw et al., 2010). The purpose of bivalency has yet to be resolved, for *Hox* clusters however, it is hypothesized to provide quick activation of *Hox* genes once the repressive H3K27me3 mark is removed. In agreement with this hypothesis, in differentiating mouse ES cells treated with RA, levels of H3K27me3 decrease as levels of H3K4me3 increase correlating with *Hox* transcription (Shahhoseini et al., 2013).

My contribution to the field

What remains unanswered in the field is how regulatory mechanisms of *Hox* transcription interact with *hox* promoters in the context of chromatin during development. As stated above, in previous *Hox* studies that assessed chromatin structure, observations were made on the global scale, such as the chromatin

decondensation experiments at the *HoxB* and *HoxD* clusters (Chambeyron et al., 2005; Morey et al., 2007). These experiments indicated that RA plays a role in the temporal-colinear activation of the *Hox* genes in these clusters through global chromatin rearrangements however, how decondensation of the cluster relates to the chromatin architecture at *hox* promoters is still in question. In particular, how nucleosomes are positioned at the *Hox* promoters is of great interest due to the intrinsic regulatory nature of nucleosomes as sequences bound within the nucleosome structure is precluded from the soluble factors within the nucleus, such as transcription factors and other regulatory molecules that bind DNA. Genome-wide nucleosome mapping studies have been completed in yeast (Albert et al., 2007; Kaplan et al., 2009; Lee et al., 2007; Mavrich et al., 2008a; Yuan et al., 2005), flies (Gilchrist et al., 2010; Mavrich et al., 2008b; Mito et al., 2005), worms (Ercan et al., 2011; Valouev et al., 2008), fish (Sasaki et al., 2009), and humans (Ozsolak et al., 2007; Schones et al., 2008), finding that at poised promoters nucleosomes flank the transcription start site (TSS) with a nucleosome depleted region (NDR) in between. The formation of the NDR presumably leaves important regulatory sequences free at the promoter. Indeed, the removal of nucleosomes around promoters has been observed in inducible systems, correlating with gene transcription (Almer et al., 1986; Fedor and Kornberg, 1989; Lee et al., 2004). Similar nucleosome mapping has been performed at *Hox* promoters using human cell lines (Kharchenko et al., 2008), this study observed similar NDR formation at *Hox* promoters irrespective of *Hox* transcription.

Taken together, nucleosome positions appear to be important for gene regulation in many different organisms, including *Hox* genes. However, much of this data is from cell lines and embryos from mixed stages, leaving much still unknown about how nucleosomes are positioned on the nascent embryonic genome during embryogenesis. This is of particular importance as a genome-wide rechromatinization event occurs upon fusion of sperm and oocyte. To better understand the role that nucleosomes play in regulating *hox* genes during embryogenesis, we present a nucleosome mapping study using the model organism *Danio rerio*, the zebrafish.

Using four stages of early embryo development, we map nucleosome positions at 37 zebrafish *hox* promoters. We find nucleosome arrangement to be progressive, taking place over several stages independent of RA. This progressive change in nucleosome arrangement on invariant sequence suggests that trans-factors play an important role in organizing nucleosomes. To further test the role of trans-factors we created *hoxb1b* and *hoxb1a* mutants to determine if the loss of either protein effected nucleosome positions at the promoter of a known target *hoxb1a*. Characterization of these mutations identified hindbrain segmentation defects similar to targeted deletions of mouse orthologs *Hoxa1* (Carpenter et al., 1993; Chisaka et al., 1992; Lufkin et al., 1991; Rossel and Capecchi, 1999) and *Hoxb1* (Goddard et al., 1996; Studer et al., 1996) and zebrafish *hoxb1b* and *hoxb1a* morpholino (MO) loss-of-function experiments (McClintock et al., 2002). However, we also identified differences in

hindbrain segmentation as well as phenotypes in facial motor neuron migration and reticulospinal neuron formation not previously observed in the MO experiments. Finally, we find that nucleosomes at the *hoxb1a* promoter are positioned differently in *hoxb1b*$^{-/-}$ embryos compared to wild-type. Together our data provides new insight into the roles of *hoxb1b* and *hoxb1a* in zebrafish hindbrain segmentation and reticulospinal neuron formation and indicates that nucleosome positioning at *hox* promoters is dynamic, depending on sequence specific factors such as Hox proteins.

Chapter II: Dynamic nucleosome organization at *hox* promoters during zebrafish embryogenesis

This chapter has previously been published under the title: “Dynamic nucleosome organization at *hox* promoters during zebrafish embryogenesis”

Weicksel, S.E., Xu, J., Sagerstrom, C.G., 2013. Dynamic nucleosome organization at hox promoters during zebrafish embryogenesis. PLoS One 8, e63175.

CONTRIBUTIONS

Steven Weicksel: Conceived and designed experiments, performed experiments, analyzed data, and prepared manuscript.

Jia Xu: Provided bioinformatic support in analyzing nucleosome positioning data.

Charles Sagerström: Conceived and designed experiments, analyzed data, and prepared manuscript.

INTRODUCTION

The nucleosome is comprised of an octamer histone core wrapped nearly 1.7 times by approximately 147bp of DNA that represents the basic unit of eukaryotic chromatin (Kornberg and Lorch, 1999). While packaging of nucleosomes into a higher order structure enables the compaction of chromatin into the nucleus, it also limits access to various DNA binding factors, thereby placing an accessibility constraint on all DNA-dependent processes (e.g. replication, transcription) (Widom, 1998). Nucleosome arrangements on genomic DNA are defined both in terms of positioning (how precisely a nucleosome resides at a particular site in all cells of a population) and occupancy (how frequently a specific position is bound by a nucleosome). In particular, nucleosome positioning and occupancy at transcription start sites (TSSs) is thought to impact gene expression. Accordingly, genome-wide nucleosome mapping studies in yeast have revealed a nucleosome-depleted region (NDR) upstream of most TSSs (Albert et al., 2007; Kaplan et al., 2009; Lee et al., 2007; Mavrich et al., 2008a; Yuan et al., 2005) that likely permits access by the transcription machinery. However, some yeast promoters appear to be occupied by nucleosomes that are actively removed in response to inducing signals (Almer et al., 1986; Fedor and Kornberg, 1989; Lee et al., 2004). Such promoters display higher transcriptional plasticity and are more responsive to signaling pathways, than are promoters with pronounced NDRs, suggesting that nucleosome positioning represents a mechanism to achieve regulated gene expression in yeast (Tirosh and Barkai,

2008). Nucleosome positioning may play an even greater role in the regulation of gene expression in metazoans since regulatory DNA sequences are invariant among all cells of a multi-cellular organism, but only a subset of cells may express a specific gene. Indeed, while many promoters in flies (Gilchrist et al., 2010; Mavrich et al., 2008b; Mito et al., 2005), worms (Ercan et al., 2011; Valouev et al., 2008), fish (Sasaki et al., 2009), and humans (Ozsolak et al., 2007; Schones et al., 2008) display NDRs upstream of TSSs, many other promoters are occupied by nucleosomes (Tillo et al., 2010) and inductive signals cause nucleosome rearrangements at such promoters (e.g. nucleosome occupancy is greatly increased in the region immediately upstream of repressed promoters upon T-lymphocyte stimulation (Schones et al., 2008) and NDRs form at androgen-responsive enhancers in prostate cells (Andreu-Vieyra et al., 2011)). This suggests that nucleosomes need to be rearranged at many metazoan promoters prior to transcription and, accordingly, there is an overall bias towards expressed promoters having a more pronounced NDR (Mito et al., 2005; Ozsolak et al., 2007; Schones et al., 2008).

Nucleosome positioning is partially encoded by the DNA sequence and experimental studies have identified sequences that favor (e.g. dinucleotide repeats (Ioshikhes et al., 1996; Thastrom et al., 1999) and G+C rich regions (Lee et al., 2007; Peckham et al., 2007)) or disfavor (e.g. dA:dT tracts (Iyer and Struhl, 1995; Lee et al., 2007; Ozsolak et al., 2007; Suter et al., 2000; Yuan et al., 2005)) nucleosome binding. More recently, experimentally derived nucleosome

position information has been used to design theoretical models for the purpose of predicting nucleosome positioning *de novo*. These models are reasonably successful at predicting nucleosome positions in yeast (Ioshikhes et al., 2006; Peckham et al., 2007; Segal et al., 2006; Yuan and Liu, 2008), but are less successful in *C. elegans* (Kaplan et al., 2009) or in human cells (Tillo et al., 2010). In particular, the models appear less accurate at predicting nucleosome positioning at metazoan regulatory regions (including promoters (Kaplan et al., 2009; Tillo et al., 2010)). Notably, regulatory regions have higher G+C content in metazoans than in yeast and are therefore more likely to be bound by nucleosomes (Tillo et al., 2010). As discussed above, such nucleosomes are actively removed in cells where the corresponding promoter is expressed, possibly accounting for the observed discrepancies between predicted and actual nucleosome positioning. Nucleosomes may be repositioned from such G+C rich promoter regions by a variety of mechanisms including competition with sequence-specific transcription factors (Badis et al., 2008; Shim et al., 1998) or the RNA Polymerase II complex (Gilchrist et al., 2010; Gilchrist et al., 2008; Mavrich et al., 2008b; Schones et al., 2008; Weiner et al., 2010), as well as by the action of ATP-dependent nucleosome remodelers (reviewed in (Hargreaves and Crabtree, 2011)). It is also worth noting that regions defined as NDRs are not necessarily completely devoid of nucleosomes (Weiner et al., 2010; Xi et al., 2011), but may represent sites with less robust nucleosomes, perhaps because they contain histone variants such as H2.AZ or H3.3 that are less stably bound to

DNA (Jin and Felsenfeld, 2007). Such nucleosomes are more easily displaced and might therefore make promoters more responsive to inductive signals, but would also make them more sensitive to DNase-based methods used to map nucleosome organization. Taken together, work to date suggests that active processes control nucleosome positioning at many promoters and that this is an important regulatory mechanism for inducible and cell-specific gene expression in metazoans.

Nucleosome organization has been analyzed in blastula stage *O. latipes* (medaka fish (Sasaki et al., 2009)) embryos, as well as in samples of mixed stage *D. melanogaster* (Mavrich et al., 2008b) and *C. elegans* (Johnson et al., 2006; Valouev et al., 2008) embryos. In spite of metazoan embryos consisting of multiple cell types, these experiments nevertheless detected well-organized nucleosomes. In particular, many promoters reveal a nucleosome arrangement with pronounced nucleosomes flanking the TSS. One nucleosome is observed downstream of the TSS in the coding sequence (+1 nucleosome) and a second upstream of the TSS (-1 nucleosome) with an intervening NDR observed immediately upstream of the TSS. This represents a canonical arrangement in most embryonic cells regardless of tissue type, stage of development or level of transcription. However, it is not clear that such a pattern is truly fixed throughout embryogenesis since chromatin structure appears to be remodeled during embryonic development. For instance, the *hox* genes, which encode homeodomain-containing transcription factors essential for development of all

metazoans (Krumlauf, 1994; Lewis, 1978) and that are arranged into several genomic clusters, have been observed to decondense coincident with their expression during mouse embryogenesis (Chambeyron et al., 2005; Morey et al., 2007) – a process that can be mimicked by using retinoic acid (RA; an endogenous inducer of *hox* gene expression) to treat murine ES cells (Chambeyron and Bickmore, 2004). Chromatin rearrangements at the *hox* clusters have also been observed during mouse embryogenesis using 4C technology (Noordermeer et al., 2011). Hence, while the canonical arrangement of a +1 nucleosome at the TSS preceded by an upstream NDR has been observed at *hox* promoters in human cell lines (Kharchenko et al., 2008), it is unclear if chromatin remodeling during embryonic development generates nucleosome profiles that differ from the canonical organization. Indeed a time course of nucleosome organization, and its refinement in response to inductive signals, has not been reported for any metazoan embryo.

We have mapped nucleosomes near the TSS (herein referred to as 'promoter') of 37 zebrafish *hox* genes under different conditions. We first examined nucleosome arrangements at the TSS of all 37 genes at various stages of embryogenesis and find relatively poorly positioned and weakly occupied nucleosomes at 2hpf and 4hpf. Notably, no *hox* genes are expressed at these stages of development and we do not observe NDRs at these time points. At the 6hpf and 9hpf time points nucleosomes become better organized. The progressive nature of nucleosome positioning on the invariant sequence of

hox promoters through early development suggests an important role for trans-factors in positioning nucleosomes at *hox* promoters. More detailed analyses revealed that promoters of genes expressed at these stages have better nucleosome organization and occupancy with an NDR immediately upstream of the TSS. Non-expressed promoters have nucleosomes that are less organized and lack an NDR at early stages, suggesting that NDR formation correlates with gene expression. However, blocking *hox* gene transcription by disruption of the RA signaling pathway results in no change in nucleosome positioning or NDR formation, indicating that transcription does not drive nucleosome organization at *hox* promoters. Our data therefore indicate that trans-factors act at *hox* promoters during embryogenesis to dynamically rearrange nucleosomes independently of *hox* gene transcription.

METHODS

This study was performed in strict accordance with the recommendations in the Guide for the Care and Use of Laboratory Animals of the National Institutes of Health. The protocol was approved by the Committee on the Ethics of Animal Experiments of the University of Massachusetts (A-1565).

Fish care

Ekkwill (EK) embryos were collected through natural matings and staged using morphological criteria for two, four, six, and nine hours post fertilization (hpf) as defined by Kimmel et al (Kimmel et al., 1995).

Drug treatments

Retinoic acid (RA): 2 cell embryos (~45 minutes post-fertilization) were treated with 100nM RA diluted in fish-water (5mM NaCl, 0.17mM KCL, 0.33mm $CaCl_2$, 0.33mM $MgSO_4$, and 0.004% methylene blue). Embryos remained in RA-treated water until they were harvested (2hpf RA embryos were treated for ~1hour, 4hpf embryos ~3 hours etc.). Diethylaminobenzaldehyde (DEAB): 4-8 cell embryos (~1-1.25 hours post fertilization) were treated with 10uM DEAB diluted in fish-water. Embryos remained in DEAB-water until the developmental stage harvested. Drug concentrations were chosen based on embryonic survival to limit embryonic death.

Embryo processing and nucleosome cross-linking

Embryos were collected and the chorion was removed using 10mg/ml Pronase. Embryos were then washed with Fish ringers (0.1M NaCl, 3mM KCl, 3mM $CaCl_2$, and 2.4mM $NaHCO_3$) and mechanically dissociated by pipetting. Cells were washed once with PBS, resuspended in 1% formaldehyde in PBS and incubated

for 10 minutes at 27ºC. The reaction was quenched with equal volume of 1M glycine and cells were spun down at 5000g.

Nuclei purification

Protocol was adapted from Dennis et al 2007 (Dennis et al., 2007). Cell pellets were resuspended by pipetting vigorously in sucrose buffer (0.3M sucrose, 2mM $MgAc_2$, 3mM $CaCl_2$, 1% Triton X-100, 500uM DTT, 1x complete protease inhibitor Roche: 11873580001, and 10mM HEPES at pH 7.8) and incubated for 30 minutes on ice. Cells were pipetted vigorously again and diluted 1:1 with GB buffer (25% glycerol, 5mM MgAc2, 0.1 mM EDTA, 500uM DTT, 1x complete protease inhibitor Roche: 11873580001, and 10mM HEPES at pH 7.8). Nuclei were purified by layering on an equal volume of GB and spun at 1000 g for 10 minutes at 4ºC.

MNase digestion and chromatin purification

Protocol was adapted from Yuan et al 2005 (Yuan et al., 2005). Isolated nuclei were resuspended and washed once in Reaction buffer (50mM NaCl, 10mM Tris pH 7.4, 5mM $MgCl_2$, 1mM $CaCl_2$, 1mM β-mercaptoethanol, 500uM spermidine and 500uM DTT) followed by resuspension in reaction buffer with a titrated amount of MNase (5-20 units/ml, Worthington: LS004797) and incubated at 37ºC for 10 minutes. Reactions were terminated with 50mM EDTA and placed on ice. Samples were then diluted in water and treated with 1x RNase cocktail (Ambion:

AM2286) and 200mM NaCl (to remove RNA and reverse crosslinks) and incubated at 55ºC for 2 hours. 2ul proteinase K (20mg/ml) was added and samples were placed at 65ºC overnight. Chromatin was extracted using phenol:chloroform followed by ethanol precipitation. Samples were visualized by gel electrophoresis and samples containing an 80-90% mono-nucleosome DNA (faint tri-nucleosome band visible) were used for tiling array hybridization. Mono-nucleosome sized fragments were gel extracted using the Qiagen Gel Extraction kit (28706).

Array build and hybridization

Zebrafish genome v7 sequence of the seven *hox* clusters was masked for repetitive sequence using the Sanger Institute's Zebrafish RepeatMasker (http://www.sanger.ac.uk/Projects/D_rerio/fishmask.shtml). The resulting sequences were used to construct a 144k feature array of 50bp probes positioned every 20bp designed using Agilent eArray web software (https://earray.chem.agilent.com/earray/ GEO: GPL16536). Isolated mono-nucleosome sized fragments were hybridized to the *hox* array using protocols adapted from Agilent protocols substituting COT DNA for salmon sperm DNA (Mammalian ChIP-on-chip Protocol G4481-90010). Arrays were scanned using either an Axon 4000B or Agilent's High-Resolution C Scanner.

Array analysis and nucleosome positioning

Probe sequences were remapped to Zv9 and the distance from the center of a probe to the TSS of the nearest *hox* gene was calculated. Log_2 ratios were calculated based on normalized r-processed and g-processed signals from the Agilent chip for each probe. Mean signal from two replicates for each sample was assigned to each probe location. Signals were tallied using a 30bp sliding window with a step of 10bp for each window. A Lowess fitting line (f=0.05) was plotted to show the trend of the aggregated signals. Nucleosome spacing was calculated based on the predicted di- and mono-nucleosome sized fragments identified from gel images, represented in Appendix A-2. Our observations indicate that the di-nucleosome band is 320-360bp, the mono-nucleosome band 150-175bp and the linker is 20-60bp, indicating that the peak-to-peak distance between neighboring nucleosomes is 170-210bp. This distance was used in the text when comparing observed peak distances in the aggregate nucleosome plots. Signals for expressed and non-expressed genes were compared using a two-sided non-paired Wilcoxon rank sum test to calculate the significance of the difference between the two gene sets (GEO: GSE43757).

hox expression

*hox g*ene expression was determined using both Agilent and Affymetrix Zebrafish expression arrays. Only genes found to be expressed by both platforms were included in the RA and WT expression groups. Agilent Arrays: RNA was isolated

from retinoic acid treated and untreated WT zebrafish embryos at 2hpf, 4hpf, 6hpf, and 9hpf embryos using Trizol (Invitrogen#15596-026) following standard procedures. RNA was processed and hybridized to Agilent Zebrafish (V3) Gene Expression Microarrays (G2519F-026437) essentially as outlined in Agilent protocols. Since no *hox* genes are reported to be expressed maternally, the 2hpf WT embryonic sample was taken to represent baseline and signal above this baseline was taken to represent expression (GEO: GSE43756). Affymetrix Arrays: RNA was isolated from retinoic acid treated embryos at 4hpf, 6hpf, and 9hpf while RNA from untreated embryos was collected at 9hpf. RNA was processed and hybridized to Zebrafish Genechip Arrays (900487) by the UMass Genomic Core facility using standard Affymetrix protocols. CEL files from Affymetrix were normalized using invariantset probe set and background corrected by mas5 using expresso from the R affy package. Present/absent calls were calculated using mas5call from R affy package with default parameters (GEO: GSE43755).

QPCR and primers

DEAB-treated embryos were collected at 9hpf and RNA was extracted using Trizol. cDNA was synthesized using the Superscript III RT First strand cDNA synthesis kit priming with oligo dT (18080-051). *hox* gene cDNA was quantified by QPCR using the Qiagen QuantiFast SYBR Green PCR kit (204054) on an ABI

7300 thermocycler. *hox* expression was normalized to a beta-actin control. Data represents 3 technical replicates.

Primers:

hoxb1a: FWD-5'-ACC TAC GCT GAC TTA TCG GCC TCT CAA GG

RVS-5'-CTC AAG TGT GGC AGC AAT CTC CAC ACG

hoxb7a: FWD-5'-CCA TCC GAA TCT ACC CAT GGT GAG CGC

RVS-5'-TCT CGA TAC GCC GCC GTC TTG AAA GG

hoxb1b: FWD-5'-GGT TCG TTC AGC AAG TAT CAG GTC TCC CC

RVS-5'-TCT CAA GTT CCG TGA GCT GCT TGG TGG

hoxb5b: FWD-5'-CCT AAC CCA GGA CCA GTG CAA GAC GG

RVS-5'-CGT TCC GTC AAA CAC AGA GCG TGC G

hoxb6b: FWD-5'-AGT GCA AGA CGG ACT GCA CAG AAC AGG

RVS-5'-CGT TCC GTC AAA CAC AGA GCG TGC G

hoxc8a: FWD-5'-AGC AAG AGG CCA CCT TAG CGC AAT ACC

RVS-5'-CTT CAA TAC GGC GCT TGC GTG TGA GG

hoxc9a: FWD-5'-CGG AGA CTG TTT GGG CTC GAA CGG A

RVS-5'-ACC TCA TAT CGC CGG TCT CTT GTG AGG T

Beta-Actin: FWD-5'-ATA CAC AGC CAT GGA TGA GGA AAT CC

RVS-5'-GGT CGT CCA ACA ATG GAG GGG AAA A

Transcription start sites and genes included in study

For this study we used the Embryonic Transcriptome TSSs determined in Pauli et al (Pauli et al., 2012). Genes with multiple TSSs were left out of this study. This resulted in the inclusion of 37 of the 44 known Zebrafish *hox* genes (Table 2-1).

RESULTS

To investigate nucleosome organization at *hox* promoters during embryogenesis, we used zebrafish (*Danio rerio)* embryos from 2, 4, 6, and 9 hours post fertilization (hpf). These time points were chosen since zygotic gene expression is initiated at 3-4hpf in the zebrafish (Schier and Talbot, 2005). Hence, 2hpf and 4hpf embryos consist of a relatively uniform population of largely undifferentiated cells in which *hox* genes are not transcribed, while in 6hpf and 9hpf embryos some cell populations have begun to differentiate and *hox* gene transcription is being initiated. Nucleosome densities were determined by micrococcal nuclease (MNase) digestion of cross-linked chromatin isolated from staged embryos (adapted from (Dennis et al., 2007)). Mononucleosome sized fragments were gel-purified and hybridized to an Agilent custom DNA array tiled with 50bp oligonucleotides positioned every 20bp across the seven zebrafish *hox* clusters. Randomly fragmented mononucleosome sized genomic DNA (gDNA) was co-hybridized as a control. The nucleosomal signal was expressed as a ratio of the MNase digested fragments to the random gDNA fragments. Nucleosome densities were averaged for 37 zebrafish *hox* genes (Table 2-1) from -600bp to +600bp relative to the annotated transcription start site (TSS). Two separate MNase digestions were carried out for each time point and we find that the results are highly reproducible (r^2 values range from 0.70 to 0.93; Appendix A-1).

Table 2-1

9hpf WT non-expressed	9hf WT expressed	6hpf RA treated uninduced	6hpf RA treated induced	RA-only	Genes excluded
hoxa4a	*hoxb1a*	*hoxa9a*	*hoxa4a*	*hoxa4a*	*hoxa1a*
hoxa5a	*hoxb7a*	*hoxa11a*	*hoxa5a*	*hoxa5a*	*hoxa3a*
hoxa9a	*hoxb5b*	*hoxa13a*	*hoxb1a*	*hoxb5a*	*hoxa2b*
hoxa11a	*hoxb6b*	*hoxa9b*	*hoxb5a*	*hoxc1a*	*hoxa10b*
hoxa13a	*hoxc8a*	*hoxa11b*	*hoxb5b*	*hoxc4a*	*hoxb3a*
hoxa9b	*hoxc9a*	*hoxa13b*	*hoxb6b*	*hoxc5a*	*hoxb8a*
hoxa11b		*hoxb2a*	*hoxc1a*		*hoxb10a*
hoxa13b		*hoxb4a*	*hoxc4a*		*hoxb1b*
hoxb2a		*hoxb6a*	*hoxc5a*		*hoxd3a*
hoxb4a		*hoxb7a*			
hoxb5a		*hoxb9a*			
hoxb6a		*hoxb13a*			
hoxb9a		*hoxb8b*			
hoxb13a		*hoxc6a*			
hoxb8b		*hoxc8a*			
hoxc1a		*hoxc9a*			
hoxc4a		*hoxc10a*			
hoxc5a		*hoxc11a*			
hoxc6a		*hoxc12a*			
hoxc10a		*hoxc13a*			
hoxc11a		*hoxc6b*			
hoxc12a		*hoxc12b*			
hoxc13a		*hoxd4a*			
hoxc6b		*hoxd9a*			
hoxc12b		*hoxd10a*			
hoxd4a		*hoxd11a*			
hoxd9a		*hoxd12a*			
hoxd10a		*hoxd13a*			
hoxd11a					
hoxd12a					
hoxd13a					

Table 2-1. *hox* gene expression during zebrafish embryogenesis.

List of non-expressed, expressed and induced *hox* genes at 9hpf and 6hpf as well as the genes only induced by RA (RA only). Expression determined by Affymetrix Zebrafish expression array.

Nucleosome organization at hox promoters is dynamic during embryogenesis

MNase digests revealed that mononucleosome sized fragments are 150-175bp and dinucleosome fragments are 320-360bp (Appendix A-2), indicating that linker regions range from 20-60bp. This is similar to results seen for other fish species (Sasaki et al., 2009). Based on these observations, the expected distance between two nucleosome peaks is 170-210bp.

Our analysis revealed that nucleosomes are poorly occupied and positioned in 2hpf and 4hpf embryos (Fig. 2-1A and B). In particular, we are unable to identify any peaks that correspond to the predicted size of a nucleosome at these stages. Instead peaks have low amplitudes and are broad, indicating low occupancy and a lack of uniform positioning in the promoter region. At 6hpf, nucleosome peaks begin to appear roughly +60, +260 and +480bp from the TSS (+1, +2, and +3 nucleosomes respectively in Fig. 2-1C). The spacing of these peaks (200bp and 220bp respectively) indicates a nucleosomal unit of ~150bp of protected sequence separated by a linker fragment of ~60bp – values that correspond to those expected based on our gel analysis. We note that the amplitudes of the peaks in this region remain modest at 6hpf, suggesting either that nucleosome occupancy is limited in all embryonic cells, or that nucleosomes are becoming more highly occupied in only a subset of cells. As in 2hpf and 4hpf embryos, nucleosomes upstream of the TSS are loosely positioned in 6hpf embryos. At 9hpf, nucleosome peaks are observed at

Figure 2-1

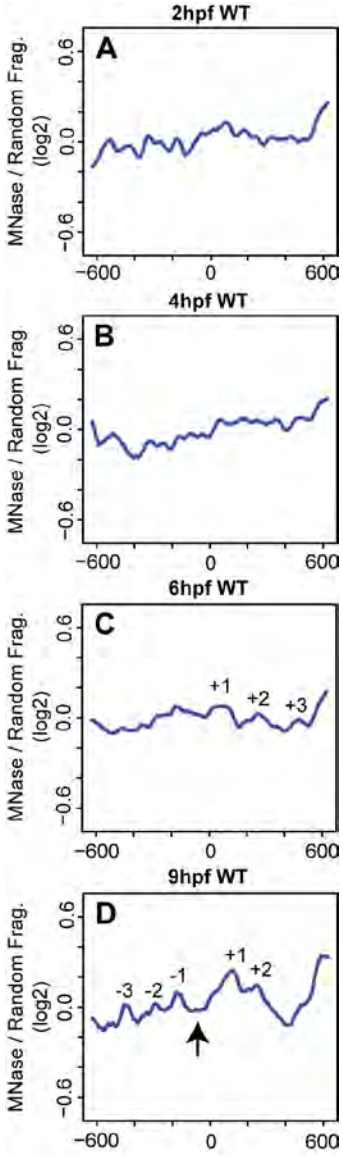
2hpf WT
A
4hpf WT
B
6hpf WT
C
+1
+2
+3
9hpf WT
D
-3
-2
-1
+1
+2
MNase / Random Frag. (log2)
0.6
0.0
-0.6
−600
0
600

Figure 2-1. Nucleosome positioning is progressive during early embryonic development.

(A-D) Average nucleosome density for 37 zebrafish *hox* promoters was calculated as the log2 ratio of MNase digested to randomly fragmented genomic DNA for positions -600 to +600 relative to the TSS (TSS is set as 0 on X-axis) at 2hpf (A), 4hpf (B), 6hpf (C) and 9hpf (D). Detectable nucleosome peaks are numbered in panels C (at positions +60, +260 and +480, separated by 200bp and 220bp respectively) and D (at positions -450, -290, -170, +155, and +250bp, separated by 150bp, 120bp, 290bp, and 130bp respectively). Arrow in panel D indicates a nucleosome depleted region (NDR) formed between the -1 and +1 nucleosomes.

roughly -450, -290, -170, +115, and +250bp (-3, -2, -1, +1, and +2 nucleosomes respectively in Fig. 2-1D). The amplitude of the nucleosome peaks is greater at 9hpf than 6hpf. In particular, the amplitude of the +1 peak increases relative to the other peaks, indicating that nucleosome occupancy increases at this position. We interpret the change in nucleosome occupancy and positioning from 6hpf to 9hpf to mean that nucleosomes are less uniformly positioned at 6hpf and take on more uniform positions by 9hpf. However, the distances between the -3/-2, -2/-1 and +1/+2 peaks (150bp, 120bp, and 130bp respectively) are closer than the expected distance between nucleosomes, possibly due to nucleosomes occupying different positions between expressed and non-expressed genes, as explored further below. Our results suggest that the arrangement of nucleosomes at *hox* promoters is established gradually during zebrafish embryogenesis.

Several groups have reported a nucleosome-depleted region (NDR) flanked by -1 and +1 nucleosomes upstream of the TSS in many metazoan genes (including *hox* genes) regardless of their expression state (Ercan et al., 2011; Gilchrist et al., 2010; Kharchenko et al., 2008; Mavrich et al., 2008b; Mito et al., 2005; Ozsolak et al., 2007; Sasaki et al., 2009; Schones et al., 2008; Valouev et al., 2008). In many of these reports, the size of the NDR corresponds to approximately one nucleosome. At 2hpf, 4hpf, and 6hpf, nucleosomes around the TSS are too disordered to observe an NDR structure, but we observe an NDR at 9hpf, where the +1 and -1 nucleosome peaks sit ~290bp apart (arrow in

Fig. 2-1D). This is equivalent to an NDR of ~130bp, slightly shorter than one nucleosome length. There is also reduced nucleosome density around +400bp at 9hpf (Fig. 2-1D), but the significance of this observation is unclear. Hence, our data indicate that an NDR slightly shorter than one nucleosome is present at 9hpf.

Expressed and non-expressed promoters display distinct nucleosome profiles

We note that *hox* gene expression is initiated by the 6hpf and 9hpf time points, raising the possibility that nucleosome arrangements may be distinct at promoters of transcribed genes relative to promoters of genes which are not transcribed at these stages. To examine this possibility, we first used microarray analysis to identify all *hox* genes that become expressed during the stages analyzed here and find that six *hox* genes are transcribed by 9hpf (Table 2-1). We next examined the nucleosome arrangement surrounding the TSS of the 31 non-expressed genes compared to the six genes expressed at 9hpf. At 2hpf, promoters of non-expressed genes do not reveal readily apparent nucleosomes (Fig. 2-2C). However, nucleosomes become progressively more apparent at non-expressed promoters as embryogenesis progresses (Fig. 2-2F, I) and by 9hpf several well-positioned and well-occupied nucleosomes are detected (Fig. 2-2L). We note that while there are clear differences in amplitude, nucleosome positioning remains relatively constant across the stages analyzed (Fig. 2-2N). Since 31 of 37 promoters belong to the non-expressed group, it is

Figure 2-2

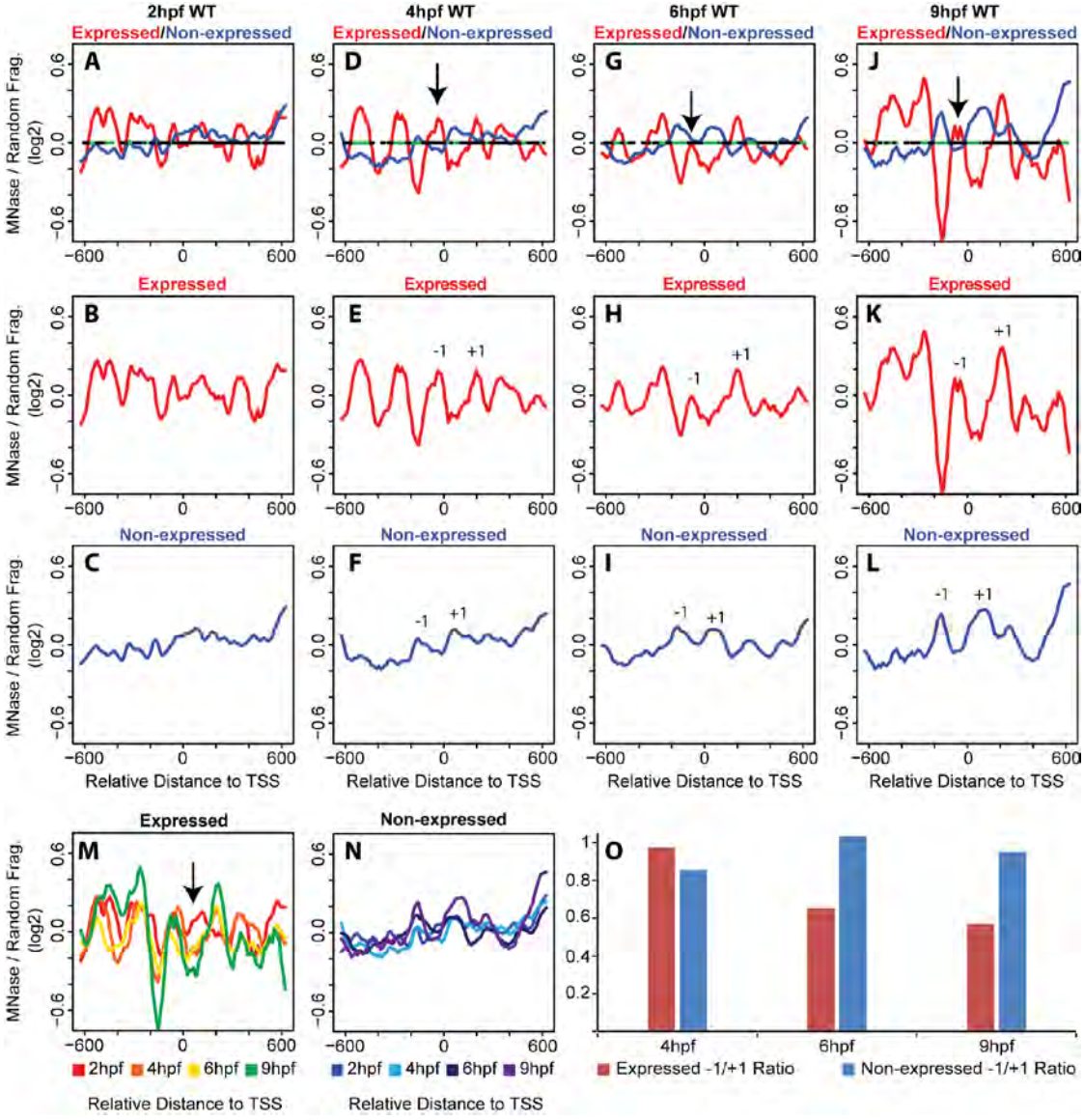
2hpf WT
4hpf WT
6hpf WT
9hpf WT
Expressed/Non-expressed
A
D
G
J
Expressed
B
E
H
K
Non-expressed
C
F
I
L
-1
+1
MNase / Random Frag. (log2)
0.6
0.0
-0.6
-600
0
600
Relative Distance to TSS
M
N
O
2hpf 4hpf 6hpf 9hpf
1
0.8
0.6
0.4
0.2
4hpf
6hpf
9hpf
Expressed -1/+1 Ratio
Non-expressed -1/+1 Ratio

Figure 2-2. Nucleosome organization differs between expressed and non-expressed promoters.

(A-L) Average nucleosome density was calculated as in figure 1 for expressed (red line in panels A, B, D, E, G, H, J, K) and non-expressed (blue lines in panels A, C, D, F, G, I, J, L) promoters at 2hpf (A-C), 4hpf (D-F), 6hpf (G-I) and 9hpf (J-L). Nucleosome densities at expressed and non-expressed promoters were compared using a Wilcoxon Ranked Sum test and statistically significant differences ($p<0.05$) are illustrated in green on the horizontal line in panels A, D, G, J. Arrows in D, G, and J indicate the -1 nucleosome. (M, N) Overlay of profiles for expressed (M) and non-expressed (N) promoters at all time points. Arrow in M indicates region where 2hpf time point (red line) has greater nucleosome density than later time points. (O) Change in occupancy of the -1 nucleosome was calculated as a ratio of density at the -1 nucleosome to density at the +1 nucleosome for expressed (red bars) and non-expressed (blue bars) promoters at 4hpf, 6hpf and 9hpf.

expected that the nucleosome profile at non-expressed promoters will closely parallel the profile seen when all promoters are averaged together. While this is indeed the case (compare Fig. 2-2C, F, I, L to Fig. 2-1A-D), it is noteworthy that there are also clear differences. For instance, nucleosomes can be seen surrounding the TSS at 4hpf at non-expressed promoters (-1 and +1 in Fig. 2-2F), but such nucleosomes are not observed at 4hpf when all promoters are averaged (Fig. 2-1B). Furthermore, the -1 nucleosome is better occupied in non-expressed promoters at 9hpf (Fig. 2-2L) than when all promoters are averaged (Fig. 2-1D). These observations suggest that although the number of expressed promoters is small, they must have a distinct nucleosome profile from non-expressed promoters. This turns out to be the case, as can be seen in Fig. 2-2B, E, H, K. Indeed, promoters of expressed genes reveal relatively well-defined nucleosomes already at 2hpf (Fig. 2-2B) and these are further refined by 4hpf (Fig. 2-2E), and remain as such at 6hpf (Fig. 2-2H) and 9hpf (Fig. 2-2K). In addition to being detected earlier than nucleosome peaks at non-expressed promoters, peaks at expressed promoters are also narrower and have higher amplitudes, suggesting that nucleosomes are better positioned and more highly occupied at expressed promoters. As noted for non-expressed promoters, nucleosome positioning also remains relatively constant at expressed promoters across the stages analyzed here (Fig. 2-2M). One exception is at 2hpf, when nucleosome density is higher near the TSS than at later stages

(arrow in Fig. 2-2M), perhaps indicating that nucleosomes are evicted or repositioned from the TSS upon initiation of gene activation.

A closer examination reveals additional differences in nucleosome positioning at promoters of expressed versus non-expressed *hox* genes. These differences are observed most readily when the profiles are overlayed as in figures 2-2A, D, G and J. In particular, in the region surrounding the TSS (-300 to +300), non-expressed promoters display peaks at -160 and +70, while expressed promoters display peaks at -270,-50 and +200. Notably, the -1 nucleosome in expressed promoters (arrow in Fig. 2-2D, G, J) appears to be dynamic, as it is reduced at 6hpf and 9hpf (when *hox* genes are expressed) relative to 4hpf (when *hox* genes are not expressed). This is particularly clear when the amplitude of the -1 nucleosome peak is compared to the amplitudes of the adjacent peaks. Expressing the amplitude of the -1 nucleosomes as a ratio to the +1 nucleosomes reveals that the -1 nucleosome in expressed promoters at 6hpf and 9hpf is reduced by 35% and 43%,respectively (Fig. 2-2O), while the -1 nucleosome remains unchanged in the non-expressed promoters. The net result is a reduction in nucleosome density between the -270 and +200 peaks in the expressed promoters at stages when *hox* genes are expressed. While this is consistent with previous reports of NDRs forming at expressed promoters, the region is not devoid of nucleosomes since a peak persists at the TSS at 6hpf and 9hpf. It is possible that this peak represents a less stable nucleosome or that it

reflects the fact that not all cells in the embryo express these *hox* genes, but our experiments cannot distinguish between these possibilities.

In an attempt to determine the significance of the observed differences between expressed and non-expressed promoters, we employed a two-sided Wilcoxon rank sum test. The results of this test are indicated on the horizontal line in figure 2-2A, D, G, J where regions with a statistically significant difference in nucleosome density between expressed and non-expressed promoters are indicated in green. As can be seen, the greatest difference between the two conditions is centered near the TSS at 6hpf and 9hpf, although other regions (most notably the region -200 to -600 in 4hpf embryos) also show significant differences. We conclude that nucleosomes are detectable earlier at promoters of expressed *hox* genes and that these nucleosomes are better positioned and more highly occupied than nucleosomes at promoters of non-expressed *hox* genes. We further conclude that nucleosome occupancy changes as *hox* genes become expressed such that nucleosome density decreases near the TSS, although we do not observe the formation of a region truly depleted of nucleosomes. Hence, *hox* promoters may fall into the class of promoters where a nucleosome positioned upstream of the TSS must be actively removed prior to transcription, thereby providing additional regulation and permitting high transcriptional plasticity.

Disruption of retinoic acid signaling blocks hox transcription, but does not affect nucleosome organization

As mentioned, the retinoic acid (RA) signaling pathway is an activator of *hox* gene expression and plays a role in chromatin rearrangements at the *hox* clusters in both cell lines and mouse embryos (Chambeyron and Bickmore, 2004; Chambeyron et al., 2005; Morey et al., 2007). To test if the RA signaling pathway plays a role in the nucleosome positioning observed in our experiments, we treated embryos with diethylaminobenzaldehyde (DEAB), a compound that blocks the RA synthesis pathway by inhibiting retinaldehyde dehydrogenase (RALDH)(Perz-Edwards et al., 2001). DEAB has also previously been shown to affect hindbrain development, particularly *hox* gene expression, in zebrafish embryos (Maves and Kimmel, 2005). DEAB treatment was begun at the 2-4 cell stage in order to prevent initiation of *hox* transcription and embryos were collected at 9hpf to determine transcript levels and nucleosome organization of the six active *hox* genes. RT-qPCR analysis revealed that transcription of the six *hox* genes was maximally blocked by 10uM DEAB, with higher DEAB concentrations not providing further blockade (Fig. 2-3). Plotting average

Figure 2-3

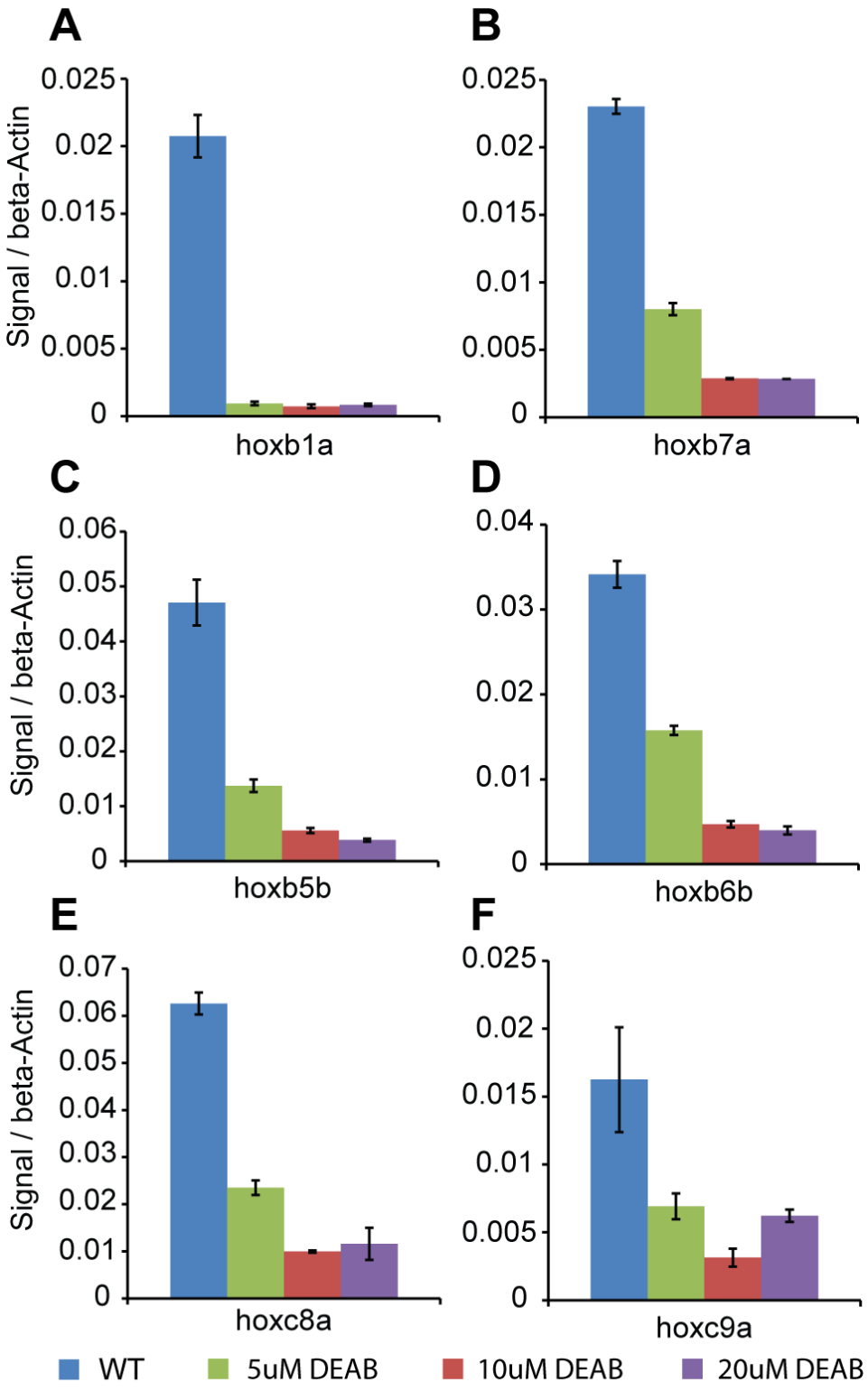
A
B
C
D
E
F
Signal / beta-Actin
0.025
0.02
0.015
0.01
0.005
0
hoxb1a
hoxb7a
0.06
0.05
0.04
0.03
0.02
0.01
hoxb5b
hoxb6b
0.07
hoxc8a
hoxc9a
WT
5uM DEAB
10uM DEAB
20uM DEAB

Figure 2-3. DEAB treatment blocks hox transcription.

(A-F) Zebrafish embryos were left untreated (blue bars) or treated with 5uM (green bars), 10uM (red bars) or 20uM (purple bars) DEAB and harvested at 9hpf. Transcript levels for *hoxb1a* (A), *hoxb7a* (B), *hoxb5b* (C), *hoxb6b* (D), *hoxc8a* (E) and *hoxc9a* (F) were determined by quantitative RT-PCR and normalized to β-actin. Error bars indicate standard deviations of 3 technical replicates.

nucleosome profiles for all 37 *hox* genes from DEAB-treated embryos revealed no change from untreated embryos (Fig. 2-4 A). When *hox* genes are divided into expressed and non-expressed groups, nucleosomes in DEAB-treated embryos are again positioned very similarly to untreated embryos (Fig. 2-4B, compare to Fig. 2-2J). Overlaying nucleosome traces for expressed and non-expressed genes from DEAB and untreated embryos confirms the similarity (Fig. 2-4C, D). Hence, while the six genes expressed at these stages are RA sensitive and blocking RA synthesis disrupts their transcription, no detectable change in nucleosome organization is observed. We conclude that RA-induced transcription is not driving changes in nucleosome organization at the promoter regions of *hox* genes during zebrafish embryogenesis.

Retinoic acid treatment does not promote a nucleosome organization similar to that of endogenously expressed promoters

We next examined if addition of exogenous RA affects nucleosome organization. Embryos were treated with RA starting at the 2-cell stage and collected at 2hpf, 4hpf, 6hpf and 9hpf. We initially examined average nucleosome organization at all 37 *hox* promoters. We find the nucleosome profiles of RA-treated embryos to be similar to the profiles of untreated embryos, although there are some minor differences when overlayed (Fig. 2-5A-D). Using microarray analysis we identified nine *hox* genes whose expression is induced in RA treated embryos (Table 2-1). We next used this information to compare nucleosome organization

Figure 2-4

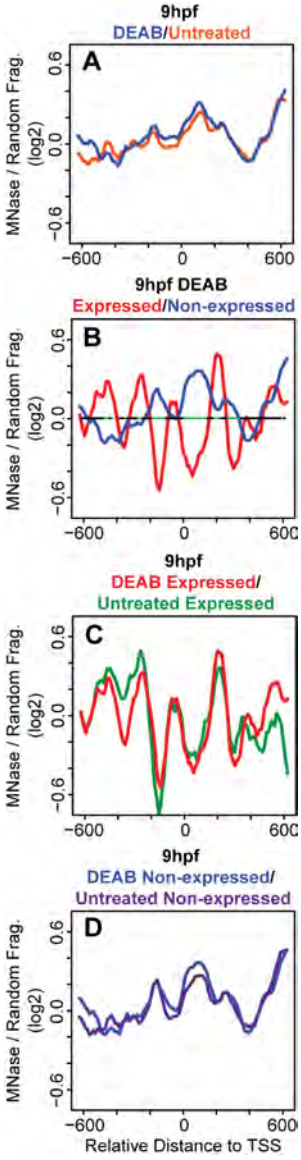
9hpf
DEAB/Untreated
A
MNase / Random Frag. (log2)
0.6
0.0
-0.6
-600
0
600
9hpf DEAB
Expressed/Non-expressed
B
9hpf
DEAB Expressed/
Untreated Expressed
C
9hpf
DEAB Non-expressed/
Untreated Non-expressed
D
Relative Distance to TSS

Figure 2-4. DEAB treatment has little effect on nucleosome positioning at hox promoters.

(A-D) Average nucleosome density was calculated as in figure 1. (A) Overlay of average nucleosome profiles for 37 *hox* promoters from DEAB-treated (blue line) and untreated (orange line) embryos at 9hpf. (B) Overlay of nucleosome profiles for expressed (red line) and non-expressed (blue line) promoters in DEAB-treated embryos at 9hpf. Nucleosome densities at expressed and non-expressed promoters were compared using a Wilcoxon Ranked Sum test and statistically significant differences ($p<0.05$) are illustrated in green on the horizontal line in panel B. (C) Overlay of nucleosome profiles for expressed promoters from DEAB-treated (red line) and untreated (green line) embryos at 9hpf. (D) Overlay of nucleosome profiles for non- expressed promoters from DEAB-treated (blue line) and untreated (purple line) embryos at 9hpf.

Figure 2-5

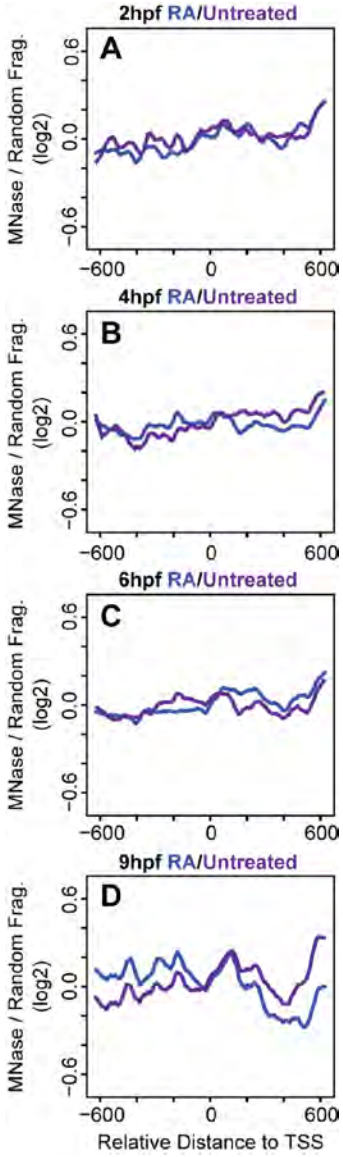
2hpf RA/Untreated
A
4hpf RA/Untreated
B
6hpf RA/Untreated
C
9hpf RA/Untreated
D
MNase / Random Frag. (log2)
0.6
0.0
-0.6
-600
0
600
Relative Distance to TSS

Figure 2-5. Exogenous RA has little effect on nucleosome positioning at *hox* promoters.

(A-D) Average nucleosome density was calculated as in figure 1 for 37 *hox* promoters from RA-treated embryos. Overlay of nucleosome profiles for 37 *hox* promoters from RA-treated (blue line) and untreated (purple line) embryos at 2 hpf (A), 4hpf (B), 6hpf (C) and 9hpf (D).

at RA-induced and uninduced *hox* promoters. Promoters of genes not induced by RA do not display detectable nucleosomes until 9hpf (Fig. 2-6C, F, I, L). As expected, this is similar to the non-expressed promoters in untreated embryos (Fig. 2-2C, F, I, L), although it is somewhat more difficult to detect individual nucleosomes in RA treated embryos and there may be additional nucleosomes forming in the region of -200 to -600 at 9hpf (Fig. 2-6L). RA-induced promoters (Fig. 2-6B, E, H, K) show better positioned and more highly occupied nucleosomes than uninduced promoters (Fig. 2-6C, F, I, L) as can be seen when profiles of the two groups are overlayed (Fig. 2-6A, D, G, J). However, there are essentially no regions with statistically significant differences between RA-induced and uninduced promoters. This finding is in contrast to the changes in nucleosome organization we observed when comparing expressed and unexpressed promoters in untreated embryos (Fig. 2-2A, D, G, J) and suggests that although RA induces transcription of several *hox* genes, it does not drive their nucleosome organization to mimic that of endogenously expressed genes. Indeed, when the nucleosome profiles of RA-induced promoters (from Fig. 2-6B, E, H, K) are overlayed on the profile of endogenously expressed promoters (from Fig. 2-2B, E, H, K) it is clear that the profiles differ (Fig. 2-6M-P). In particular, while nucleosomes are depleted in the region from -100 to -200 in both sets of promoters at 4, 6, and 9hpf, this depletion is less pronounced at RA-induced promoters and depletion in the region from 0 to +100 is not observed at all at RA-induced promoters.

Figure 2-6

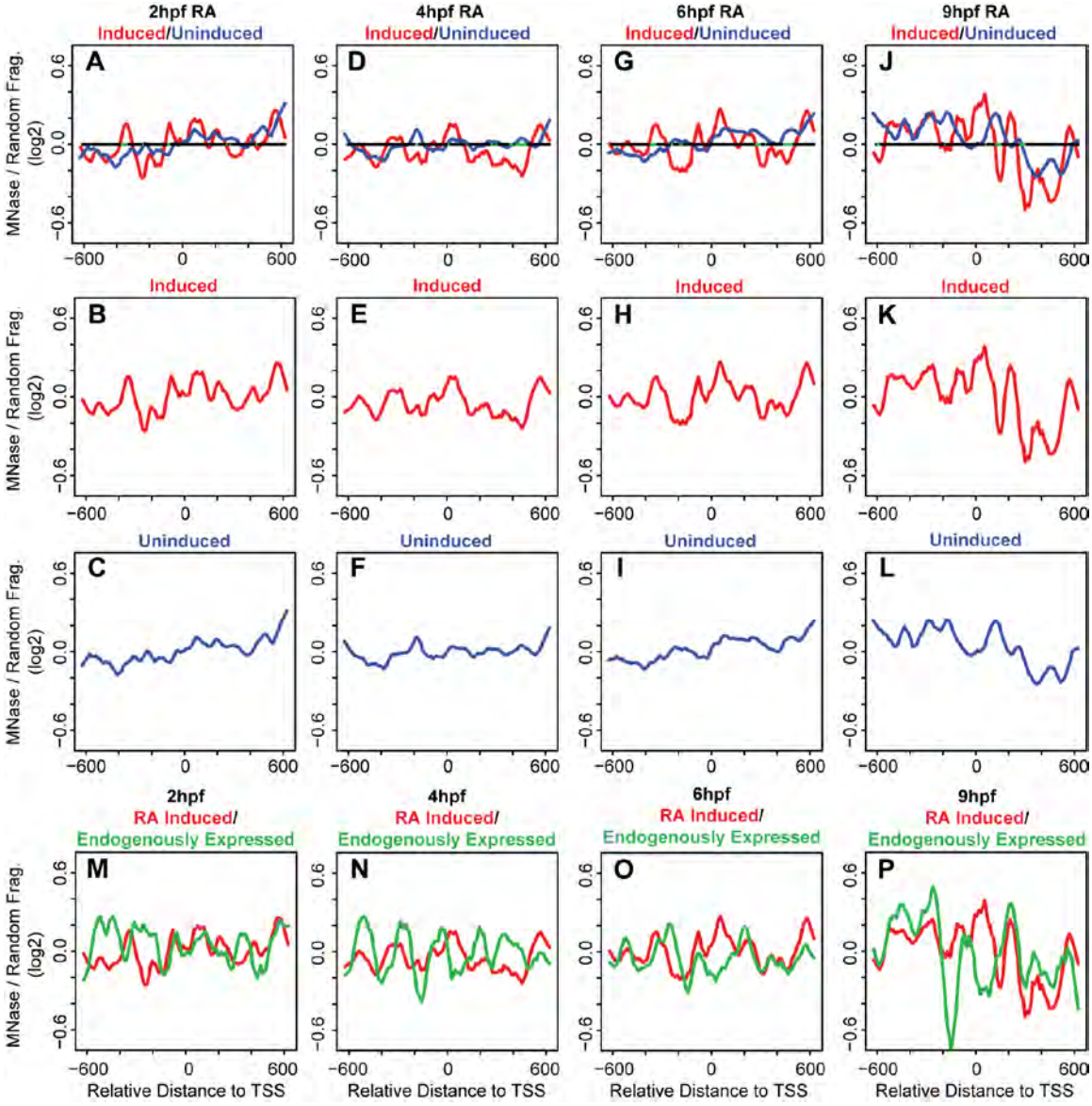
2hpf RA
Induced/Uninduced
4hpf RA
Induced/Uninduced
6hpf RA
Induced/Uninduced
9hpf RA
Induced/Uninduced
A
D
G
J
Induced
B
E
H
K
Uninduced
C
F
I
L
2hpf
RA Induced/
Endogenously Expressed
4hpf
RA Induced/
Endogenously Expressed
6hpf
RA Induced/
Endogenously Expressed
9hpf
RA Induced/
Endogenously Expressed
M
N
O
P
MNase / Random Frag. (log2)
0.6
0.0
-0.6
-600
0
600
Relative Distance to TSS

Figure 2-6. Exogenous RA does not promote a nucleosome profile similar to that of endogenously expressed promoters.

(A-L) Average nucleosome density was calculated as in figure 1 for expressed (red line in panels A, B, D, E, G, H, J, K) and non-expressed (blue lines in panels A, C, D, F, G, I, J, L) promoters at 2hpf (A-C), 4hpf (D-F), 6hpf (G-I) and 9hpf (J-L). Nucleosome densities at induced and uninduced promoters were compared using a Wilcoxon Ranked Sum test and statistically significant differences ($p<0.05$) are indicated in green on the horizontal line in panels A, D, G and J. (M-P) Overlay of nucleosome profiles for expressed promoters in untreated (green line) and RA-treated (red line) embryos at 2hpf (M), 4hpf (N), 6hpf (O) and 9hpf (P).

We note that three *hox* genes are shared between the group of endogenously expressed genes and the group of RA-induced genes (Table 2-1). To better isolate the effects of RA, we created a third group of promoters that are only induced by RA (Table 2-1; RA-only). Overlays of the nucleosome profiles of the six RA-only promoters from RA-treated embryos on the profiles of the same promoters from untreated embryos, reveal the nucleosome profiles to be similar (Fig. 2-7A-D). Hence, while RA induces the expression of these six *hox* genes, it has no effect on nucleosome organization at their promoters. Furthermore, the nucleosome organization at RA-only promoters is clearly distinct from that of endogenously expressed promoters (Fig. 2-7, compare panels A-D to panels E-H). Taken together, the results of our DEAB and RA treatments demonstrate that RA regulates *hox* gene transcription, but does not drive nucleosome organization at *hox* promoters during early zebrafish development.

DISCUSSION

While nucleosomes have been mapped in several different systems, little is known about nucleosome organization in a developing vertebrate embryo. Initial analyses of nucleosome organization focused on yeast and cultured cells that represent relatively uniform populations and that, while responsive to some stimuli, in many cases have relatively limited developmental potential. In contrast, developing embryos are multicellular and contain diverse cell types that represent a range of developmental potentials. Recent studies have analyzed

Figure 2-7

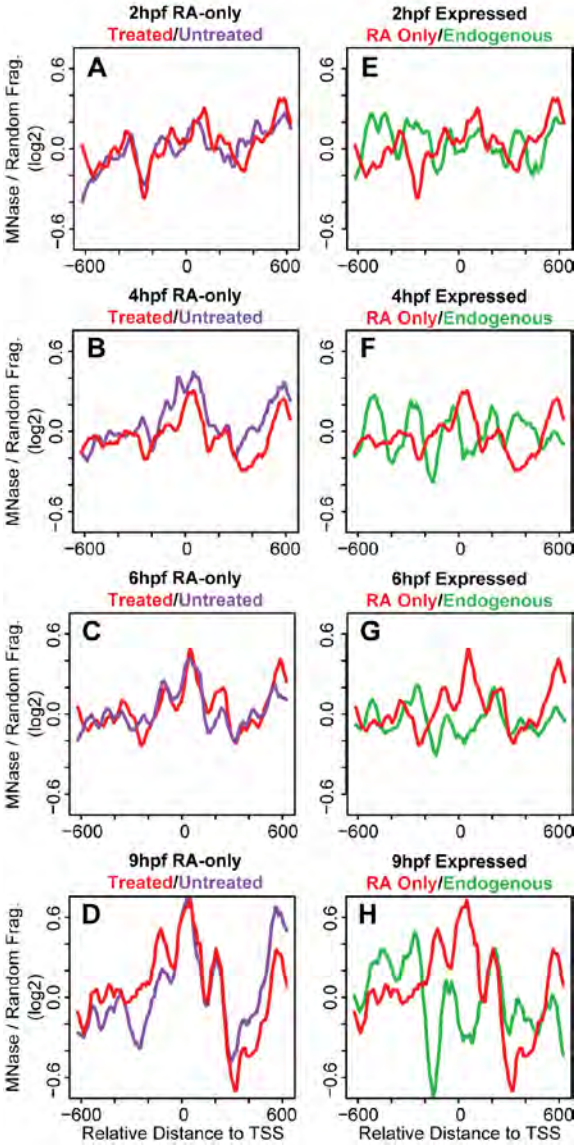
2hpf RA-only
Treated/Untreated
2hpf Expressed
RA Only/Endogenous
4hpf RA-only
Treated/Untreated
4hpf Expressed
RA Only/Endogenous
6hpf RA-only
Treated/Untreated
6hpf Expressed
RA Only/Endogenous
9hpf RA-only
Treated/Untreated
9hpf Expressed
RA Only/Endogenous
A
B
C
D
E
F
G
H
MNase / Random Frag. (log2)
0.6
0.0
−0.6
−600
0
600
Relative Distance to TSS

Figure 2-7. Exogenous RA does not effect nucleosome positioning at induced promoters.

(A-H) Average nucleosome density was calculated as in figure 1 for RA-only genes in RA-treated embryos (red line in panels A-D), for RA-only genes in untreated embryos (purple line in panels A-D), and for endogenously expressed genes in untreated embryos (E-H; data in E-H is identical to Fig.2B, E, H, K, reproduced here to allow direct comparison).

nucleosome arrangements in *C. elegans* (Valouev et al., 2008; Xi et al., 2011) and *D. melanogaster* (Mavrich et al., 2008b) embryos using mixtures of embryonic stages. However, this strategy limits the ability to detect changes in chromatin structure at specific developmental stages. Here we use staged zebrafish embryos to analyze the nucleosome arrangement at *hox* promoters during vertebrate embryogenesis. We find that nucleosomes are poorly organized at early stages, but become better organized by 6hpf and 9hpf. These latter stages correspond to the time when *hox* genes first become expressed in the embryo. Comparing expressed and non-expressed genes, we observe several differences in nucleosome organization at the promoter regions. First, we observe increased nucleosome occupancy at expressed promoters when compared to non-expressed promoters. Interestingly, the increased amplitude is observed in most of the nucleosomes in the promoter region, with exception of the -1 nucleosome. We find that occupancy of the -1 nucleosome decreases at 6hpf and 9hpf at expressed promoters. Second, we detect changes in the spacing between the -1 and +1 nucleosomes of expressed and non-expressed promoters. The larger spacing is most evident at 6hpf and 9hpf in the expressed promoters and coincides with a likely NDR. Due to this change in spacing, nucleosomes also appear out of phase between the expressed and non-expressed promoters. Finally, though *hox* transcription is dependent on RA signaling, we find that blocking RA signaling does not cause changes in nucleosome organization at the expressed promoters, suggesting that

nucleosome arrangement is independent of RA-induced transcription. The fact that nucleosome organization is dynamic, but genomic sequence is invariant, during embryogenesis, also suggests that trans-factors play a role in dynamically positioning nucleosomes at the promoters of *hox* genes in the developing embryo.

The role of transcription in nucleosome organization

Transcription has been shown previously to correlate with specific nucleosome profiles at some TSSs in metazoans (Mito et al., 2005; Ozsolak et al., 2007; Schones et al., 2008). Indeed, in our bulk nucleosome plots at 9hpf, when *hox* transcription is initiated, nucleosomes appear to be better positioned as compared to bulk nucleosome positions at 2hpf-6hpf (Fig. 2-1A-D). Grouping the *hox* genes into expressed and non-expressed promoters revealed that nucleosomes at expressed promoters are better positioned and have increased occupancy when compared to nucleosomes at non-expressed promoters (Fig. 2-2A, D, G, and J). While these data suggest that transcription may have a direct effect on the nucleosome arrangement at *hox* promoters, we find that blocking RA signaling represses *hox* transcription (Fig. 2-3) with no changes in the nucleosome profile (Fig. 2-4). We note that our DEAB protocol was designed to prevent initiation of *hox* transcription and that we may have observed a different effect if *hox* gene transcription had been allowed to initiate prior to being inactivated. Hence, our data suggest that the nucleosome profile at *hox* promoters is independent of RA-induced *hox* transcription. We see further

support for this conclusion when embryos are treated with RA. Though exogenous RA induces *hox* transcription, RA-induced genes do not recapitulate the nucleosome positions observed at endogenously expressed promoters (Fig. 2-6) and display little change from nucleosome positions observed in untreated embryos (Fig. 2-7), again suggesting that the nucleosome profile at *hox* promoters is independent of *hox* transcription.

Our findings raise questions as to if RA signaling plays a role in regulating chromatin structure at *hox* promoters if it does not affect nucleosome organization. Given the complexity of eukaryotic chromatin structure, it is possible that RA affects chromatin structure at a level distinct from the nucleosome. For instance, previous studies detected chromatin changes at the *HoxB* and *HoxD* clusters using fluorescent in situ hybridization (Chambeyron and Bickmore, 2004; Chambeyron et al., 2005; Morey et al., 2007). *Hox* loci were observed to decondense during mouse embryogenesis in correlation with *hox* gene transcription and this process was recapitulated by RA-treatment of ES cells. It is therefore possible that RA affects chromatin at the level of the 30nm fiber without affecting the positioning of individual nucleosomes. It is also possible that RA affects *hox* expression by promoting histone modifications that are supportive of transcription. Indeed, RA receptors are known to recruit histone-modifying enzymes (Perissi et al., 2010). Lastly, RA may simply recruit components of the transcription machinery, again via RA receptors, to *hox* promoters. The fact that RA induces *hox* transcription without affecting

nucleosome organization could also be taken to indicate that many nucleosome arrangements are permissive for transcription. However, it is important to note that the exogenously applied RA is likely in significant excess relative to endogenous levels and this may permit over-riding of a nucleosome arrangement that would not otherwise support transcription. In summary, we propose that an RA-independent mechanism promotes a nucleosome arrangement that is permissive for transcription, but that RA is required for actual transcription. A transcription-independent mechanism for nucleosome organization is also supported by our observation that an NDR forms at non-expressed promoters by 9hpf. Since genes in this group will become expressed at later stages of embryogenesis, it is possible that this NDR forms in preparation for subsequent transcriptional activation.

A likely role for trans-factors in nucleosome organization during vertebrate embryogenesis

Nucleosome positioning has been shown to result from the combination of intrinsic characteristics of DNA sequence, such as base pair composition (cis-elements), and from factors that interact with DNA, such as transcription factors and ATP-dependent chromatin modifiers (trans-factors). However, the relative contribution of each mechanism remains unclear. A recent study addressed how cis-elements and trans-factors influence nucleosome positioning in yeast. By using YACs to transfer large DNA fragments between divergent yeast strains,

analysis of nucleosome organization in the native strain was compared to nucleosome organization on the YAC in the new host strain (Hughes et al., 2012). This analysis revealed that inter-nucleosome spacing and positioning of the +1 nucleosome was altered upon transfer to the new host strain. Since sequence remains constant between the YAC and native yeast strain, these findings suggest that trans-factors play a more important role in nucleosome positioning than cis-elements. Similarly, we find that nucleosome organization changes during embryogenesis, but since the underlying sequence is invariant during development, trans-factors also likely play a role in nucleosome positioning during embryogenesis. We note that the changes in nucleosome organization that we observe correlate with important transitions during embryonic development. In particular, 2hpf and 4hpf embryos display relatively disordered nucleosomes at promoter regions (Fig 2-1A, B); while at 6hpf and 9hpf nucleosomes are readily identified (Fig 2-1C, D). This change takes place around 3-4hpf, coinciding with zygotic genome activation (ZGA). Our data do not reveal whether there is a causative relationship between this transition and the observed nucleosome rearrangement. However, better nucleosome positioning is observed after ZGA, it is plausible that trans-factors (such as transcription factors and ATP-dependent chromatin remodelers) become expressed at the ZGA and subsequently regulate nucleosome arrangements at *hox* promoters.

NDR formation at hox promoters during embryogenesis

Nucleosome depleted regions (NDRs) were initially identified at promoters in yeast, but have subsequently been identified in other cell types. In most cases, NDRs are readily observed in bulk analyses of promoters regardless of whether the promoters are active or not. Indeed, previous analyses of bulk *hox* promoters in human cell lines identified an NDR upstream of the TSS (Kharchenko et al., 2008). Accordingly, when we average nucleosome positions for all 37 zebrafish *hox* genes, we observe an NDR as soon as -1 and +1 nucleosomes are resolved at the TSS (9hpf, Fig. 2-1D). The NDR observed in the bulk plot at 9hpf is ~130bp, while the NDRs observed at expressed promoters at 6hpf and 9hpf are ~100bp and ~110bp respectively and the NDR observed at non-expressed promoters at 9hpf is ~85bp at 9hpf, suggesting an average NDR size of ~100bp. This is relatively similar to NDRs observed in other genome-wide nucleosome mapping studies, including fish, where NDR lengths vary somewhat, but are ~150bp.

Though the NDRs observed in our study are similar to other bulk studies, they are smaller than the NDR previously observed at human *hox* promoters, which was reported to be ~500bp (Kharchenko et al., 2008). We suspect the difference in NDR lengths between the two studies is due to differences between zebrafish embryos and human cell lines. First, the embryo is made up of a heterogeneous population of cell types, while cell lines represent a homogeneous population. The heterogeneity of cell types in the embryo might

lead to variable nucleosome occupancy. For instance, cells in the embryo that do not express a given *hox* gene might have a nucleosome positioned upstream of the TSS, thereby reducing the size of the NDR observed when signals from all cells in the embryo are averaged. Indeed, a previous study found nucleosomes to be differentially positioned at the serum albumin enhancer in a tissue specific manner in mouse (McPherson et al., 1993). Such variable nucleosome occupancy presumably does not occur in cell lines since they represent a homogeneous population of cells that would all have similar nucleosome positions. Interestingly, if some cells in the embryo lacked the -1 nucleosome, then the NDR of these promoters would expand to 310bp and 320bp at 6hpf and 9hpf respectively, making it more similar to the NDR observed at *hox* promoters in human cell lines. Second, the difference in NDR length may be due to differences between fish and humans. For instance, divergence of regulatory sequences in the promoters as well as divergence in the trans-factors responsible for nucleosome positioning may lead to different sized NDRs. Support for this possibility comes from the analysis of NDRs in evolutionary divergent yeast species, which were found to have different sized NDRs at orthologous promoters (Hughes et al., 2012).

Our data do not address how NDRs form, but we consider several possibilities. First, NDRs could form in a competitive process. Evidence exists for competition between nucleosomes and trans-factors for binding to specific sequences (Anderson and Widom, 2000; Bai et al., 2011). Once a trans-factor is

bound, positioning of nucleosomes would be restricted to other available sites in a process similar to that suggested by the “barrier model”. The barrier model is driven by trans-factors interacting with DNA and providing a barrier that blocks free nucleosome diffusion, creating well-ordered and positioned nucleosomes (Fu et al., 2008; Mavrich et al., 2008a). Hence, binding of trans-factors at expressed *hox* promoters would create more uniform nucleosome positions as well as increased amplitude of nucleosome peaks, while the lack of trans-factor binding at non-expressed genes would lead to lower occupancy and less well-positioned nucleosomes. Such competition has been observed at the CLN2 promoter in yeast where binding sites for three sequence specific transcription factors are needed for NDR formation. In the absence of these binding sites, the CLN2 promoter has increased nucleosome occupancy (Bai et al., 2011). Meis and Pbx proteins, which bind elements in many *hox* promoters and are involved in the regulation of *hox* transcription, have been suggested to act as pioneer transcription factors capable of binding nucleosome-occupied DNA (Berkes et al., 2004) and may impact nucleosome binding at *hox* promoters. Since RA-receptors may be bound to DNA even in the absence of RA-signaling (Koide et al., 2001; Mahony et al., 2011), RARs may play a similar role by binding RA response elements. However, our analyses have failed to identify an enrichment of binding sites in the NDR regions of *hox* promoters. Using MEME (http://meme.nbcr.net/meme/), allowing for naïve motif discovery, as well as constricting identification of 4-10bp motifs, did not identify binding sites for any

known sequence specific transcription factors. Furthermore, biasing MEME with a degenerate Pbx-Meis binding site, 5'-A/TGAT/GGAC/T/AA/GG/T-3' (Chang et al., 1997), also failed to identify Pbx-Meis binding sites at the NDRs of *hox* promoters. The failure to identify transcription factor binding motifs potentially indicates that these sites are more cryptic than previously thought, or through many different factors with dissimilar binding sites within the NDRs of these promoters. Second, NDR formation could be an active process mediated throughout embryogenesis by ATP-dependent remodelers. ATP-dependent SWI2/SNF2 complexes, which slide nucleosomes through DNA sequence, have been previously shown to regulate *hox* genes (Li et al., 2010; Xiao et al., 2001). Many of these factors do not bind DNA directly and would therefore need to be recruited to *hox* promoters by DNA binding factors such as the Meis and Pbx factors mentioned above.

Nucleosome occupancy and histone modifications are temporally coincident

The accessibility of genomic DNA is regulated not only by nucleosome positioning, but also by post-translational modifications made to the N-termini of histone tails, that in turn affect chromatin structure. For instance, histone H3 lysine 4 tri-methylation (H3K4me3) by trithorax group proteins and histone H3 lysine 27 tri-methylation (H3K27me3) by polycomb group proteins, associate with active and inactive promoters, respectively (Schuettengruber et al., 2007). A recent study mapped H3K4me3 and H3K27me3 marks throughout the zebrafish

genome at 2.5hpf (pre-ZGA), as well as at 4.5hpf (post-ZGA), and detected chromatin marks only post-ZGA (Vastenhouw et al., 2010). Notably, this coincides with the time point where we first observe well-defined nucleosomes. This temporal coincidence of emerging well-positioned nucleosomes and detectable histone modifications suggests that histones may become modified as soon as they are deposited at a promoter. While the significance of this observation is unclear, it is noteworthy that *hox* promoters are bivalently marked with both H3K4me3 and H3K27me3 at this stage (Vastenhouw et al., 2010). Bivalency is thought to act as a developmental control, poising developmentally important genes for rapid activation at the appropriate stage of embryogenesis (Bernstein et al., 2006). Indeed, the inability to deposit H3K27me3 marks leads to misregulated *hox* gene expression and homeotic transformations in *Drosophila* (Pengelly et al., 2013). Hence, it is possible that recently deposited nucleosomes at *hox* promoters must be rapidly modified in order to ensure proper regulation of *hox* genes.

CHAPTER III: Targeted mutations in zebrafish *hoxb1a* and *hoxb1b* reveal new functions in hindbrain development

CONTRIBUTIONS

Steven Weicksel: Conceived and designed experiments, performed experiments, analyzed data, and prepared manuscript.

Ankit Gupta: Zinc-finger nuclease design

Scot Wolfe: Zinc-finger nuclease design, Zinc-finger/TALE nuclease targeting

Denise Zannino: Confocal microscopy

Charles Sagerström: Conceived and designed experiments, analyzed data, and prepared manuscript.

INTRODUCTION

Hox genes encode a conserved family of homeodomain containing transcription factors essential for metazoan development (Amores et al., 1998; Burglin and Ruvkun, 1993; Lewis, 1978; McGinnis and Krumlauf, 1992). As a result of duplication events, vertebrate genomes contain four clusters of *Hox* genes with the exception of teleost fish species that have seven. In many cases genes that occupy the same position in different clusters (known as paralogs) have similar expression patterns and functions leading to a redundancy of *Hox* gene function in vertebrates. During early development *Hox* genes function to specify tissue identities along the anterior-posterior (AP) axis of the animal. The linear arrangement of *Hox* genes leads to a distinguishing characteristic of expression termed colinearity, where the position of the gene within a cluster coincides with the timing and position along the AP axis that the gene is expressed (Duboule and Dolle, 1989; Kmita and Duboule, 2003; Lewis, 1978). The retinoic acid (RA) signaling pathway activates *Hox* gene expression and has been shown to be important in collinear regulation. RA binds a heterodimeric complex of RA receptors (RARs) and RXRs that are targeted to cis-regulatory sites known as a RA response element (RARE) in RA sensitive genes. The addition of RA drives the decondensation of *Hox* clusters from compact chromosomal chromatin structure in cells and embryos (Chambeyron and Bickmore, 2004; Chambeyron et al., 2005; Morey et al., 2007). Decondensation of *Hox* chromatin further correlates with the progressive activation of *Hox* transcription. This highly

conserved series of *Hox* gene activation and regulation leads to an overlapping pattern of *Hox* domains along the AP axis often referred to as the "*Hox* code" (Krumlauf, 1994).

During early embryogenesis the presumptive vertebrate hindbrain is transiently segmented into 7-8 contiguous structures termed rhombomeres. This segmentation gives rise to distinct cell populations from which the segment specific motor neuron and reticulospinal interneurons differentiate. For motor neurons this includes the trigeminal neurons in r2 and r3, the facial motor neurons (FMNs) in r4, the abducens neurons in r5 and r6, and the vagal neurons in the caudal hindbrain. These neuronal pools form the motor neuron nuclei of the V-X cranial motor nerves that innervate the face, head, and neck of the animal and exit the hindbrain at the level of r2, r4, and r6. Reticulospinal neurons also form in a rhombomere determinate manner and are involved with breathing, circulation, and coordination of locomotion between the spinal cord and the brain. The segmental formation of the reticulospinal interneurons are perhaps most exemplified in zebrafish by Mauthner neurons (MN). The MNs consist of two large cell bodies that form in r4 and extend axons contralaterally to the posterior of the animal.

Segmentation of the hindbrain starts with the formation of r4 followed by r1/r2, r3, r7, and r5/r6. In accordance with this, the first *Hox* genes transcribed in the mouse, *Hoxa1* and *Hoxb1,* are expressed in r4. A series of loss-of-function studies have determined that *Hoxa1* and its downstream target *Hoxb1* have

separate functions. In particular, mouse *Hoxa1* targeted deletions have segmentation defects while *Hoxb1* mutants appear to have neuronal defects related to r4 specification. The segmentation defects observed in *Hoxa1* mutants include an enlarged r3, a reduced r4, and a reduced or completely lost r5 (Carpenter et al., 1993; Chisaka et al., 1992; Lufkin et al., 1991; Rossel and Capecchi, 1999)(Appendix B-7). Similar segmentation defects are also found in mice with mutations made to the retinoic acid response element (RARE) found in the downstream enhancer of *Hoxa1* (Rossel and Capecchi, 1999). These segmentation defects are specific to the function of *Hoxa1* as mouse *Hoxb1*$^{-/-}$ embryos show no defects in hindbrain segmentation (Goddard et al., 1996; Studer et al., 1996). While hindbrain segments form normally in *Hoxb1*$^{-/-}$ mutants, r4 derived FMNs fail to migrate into r5 (Gavalas et al., 1998; Rossel and Capecchi, 1999; Studer et al., 1996)(Appendix B-8). While arrested in r4, FMNs migrate laterally away from the midline of the neural tube, assuming clustered positions similar to r3 trigeminal neurons. Though arrested in r4, these neurons still extend axons out through r4 into the second pharyngeal arch similar to the projection of WT FMN axons. This indicates that the axons from these neurons arrested in r4 still respond properly to the axon guidance cues in the hindbrain.

Prior to this study there have been no published mutants for the orthologous *Hoxa1* and *Hoxb1* genes in zebrafish, *hoxb1b* and *hoxb1a* (respectively). However, loss-of-function studies have been performed using antisense morpholino oligos (MO) to block translation of *hoxb1b* and *hoxb1a* and

thus knocking down Hoxb1b and Hoxb1a protein levels. Embryos injected with *hoxb1bMO* have hindbrain segmentation defects with an expanded r3, a reduced r4, and a reduced r5, while in *hoxb1aMO* injected embryos, segmentation of the hindbrain is unaffected (McClintock et al., 2002)(Appendix B-7). Furthermore, *hoxb1aMO* embryos have r4 restricted FMNs that resemble stalled FMNs observed in mouse *Hoxb1*$^{-/-}$ embryos that also extend axons out of r4 into the second pharyngeal arch (Appendix B-8). These data together indicate that the zebrafish *hoxb1b* and *hoxb1a* genes have roles similar to that of the mouse *Hoxa1* and *Hoxb1* in vertebrate hindbrain development.

There are however, differences between the segmentation defects observed in the mouse targeted deletions and the zebrafish MO loss-of-function experiments. First *Hoxa1*$^{-/-}$ and *Hoxa1*$^{-/-}$*:Hoxb1*$^{-/-}$ segmentation defects appear more severe than those observed in *hoxb1bMO* and *hoxb1bMO: hoxb1aMO* injected zebrafish embryos. Specifically, the r5 domain in *Hoxa1*$^{-/-}$ mouse embryos is lost, while in zebrafish *hoxb1bMO* injected embryos r5 is reduced. *Hoxa1*$^{-/-}$*:Hoxb1*$^{-/-}$ mice also appear to have a greater segmentation defect with the loss of both r4 and r5 while *hoxb1bMO: hoxb1aMO* injected zebrafish embryos only have a 50% reduction in r4. Secondly, unlike the *Hoxa1*$^{-/-}$ mice, *hoxb1bMO* injected embryos have a reduced r6. Thirdly, the *hoxb1aMO* alone shows no effect on the reticulospinal neurons in r4 though gain-of-function experiments indicate that Hoxb1a can posteriorize r2 to an r4 identity, and drive ectopic reticulospinal neuron formation in r2 (McClintock et al., 2001). Instead

hoxb1bMO and *hoxb1aMO* used concurrently only have a partially penetrant phenotype, with an incomplete loss of the Mauthner neurons, a reticulospinal neuron found in teleost and some amphibian, in r4. These differences indicate that the differences observed between the *Hoxa1* and *Hoxb1* mutants and the *hoxb1bMO* and *hoxb1aMO* are either due differences in the functions of the genes in mouse and zebrafish, or that the MO phenotypes do not recapitulate a true loss-of-function model.

Here we present the first *hoxb1a* and *hoxb1b* loss-of-function mutations using Zinc-Finger and TALE nucleases in zebrafish *D. rerio*. Similar to previous studies, we find that Hoxb1b is important in hindbrain segmentation and Hoxb1a has a role in FMN migration. Our data also indicate that Hoxb1b segments the hindbrain differently than in mouse and that Hoxb1a has an important role in the maturation of reticulospinal neurons in r4. We also provide evidence for a role of the RA signaling pathway in *hoxb1a* activation and the role of Hoxb1b in positioning nucleosomes around the promoter of *hoxb1a* during embryogenesis.

METHODS

Fish care

Ekkwill (EK) embryos were collected through natural matings and staged using morphological criteria for two, four, six, and nine hours post fertilization (hpf) as defined by Kimmel et al (Kimmel et al., 1995).

Generation of zinc-finger and Tale nucleases

Zinc-finger nucleases (ZFN) designed for build 1 and 2 (Table 3-1) were designed from a single finger modular library (Meng et al., 2008). ZFNs for build three were designed from a similar library that selected for two-finger modules to increase nuclease binding (Gupta et al., 2011). Nuclease assemblies for all three builds was completed using previously published protocols (Meng et al., 2008). TALENs were constructed using the Golden Gate TALEN assembly kit (addgene: TALEN Kit #1000000024) following previously published protocols (Cermak et al., 2011). pCS2 plasmids containing completed ZFN and TALENs were linearized plasmids were linearized and in vitro transcription was performed with the T7 mMachine ultra kit (Ambion: AMB1345). mRNA was then injected as a titration into WT crawfish embryos at the one cell stage.

Screening for mutants

Similar methods were used to screen for ZFN and TALEN activity and is illustrated in Appendix B-1. Briefly, genomic DNA (gDNA) from 50 phenotypic WT 24hpf embryos was pooled and purified. A 200bp PCR fragment carrying a BtgI restriction site in exon one from *hoxb1a* and a 300bp PCR fragment carrying a BslI restriction site in exon one from *hoxb1b* was amplified from TALEN and ZFN injected embryos. PCR fragments were then digested to identify the loss of the restriction site and lesion formation, indicating an active nuclease.

PCR Primers:

hoxb1a: FWD 5’ TTT CTC AGG TTG TCC CTC CG

RVS 5’ TTA TAG CTG TCA CTA GCG TGT CC

hoxb1b: FWD 5’ CAC CGC ACG AAA CTC ATG GC

RVS 5’ AAT GAG GAG GTC TGG TTT GCT TGC

Embryos injected with active TALEN and ZFN builds were then grown to adulthood. These mosaic founders (F0) were then outcrossed to WT and 50 embryos (F1) were pooled and genotyped for germline transmission of the lesion, as indicated above. Founders with germline mutations were outcrossed again and F1 generation was grown to adulthood. F1 generation was genotyped from gDNA isolated through fin clips (Westerfield, 1993) and screened for lesions as stated above. Lesions from F1 carriers were then sequenced and determined through conceptual translation of the transcript (using ApE v2.0.45 software: http://biologylabs.utah.edu/jorgensen/wayned/ape/) if a frameshift occurred. Carriers with frameshift mutations were grouped based on the allelic sequence and the injection background (i.e. the founder it came from).

Genotyping

Sequencing revealed a BtgI restriction site was introduced in UM195 and UM196 and was used to genotype these *hoxb1b* alleles. UM197 can be genotyped with the original primers as additional bands form or a UM197 specific FWD primer can be combined with the previous RVS primer:

UM197 SP FWD 5’ CAC AAA TTC AAT CGT GTT TCA ATC GTG

No new restriction sites or allele specific primers were found/designed for *hoxb1a* alleles. Instead the same protocol for lesion identification was used.

In situ probes and antibody labeling

In situ protocols were followed as previous published (Vlachakis et al., 2000). In situ probes for the following genes were used: *hoxb1a* (Prince et al., 1998b), *krox20* (Oxtoby and Jowett, 1993), *pax2* (Krauss et al., 1991), *hoxb3a* (Piotrowski and Nusslein-Volhard, 2000), and *hoxd4a* (Maves and Kimmel, 2005). Antibody labeling with Islet1-2 and 3A10 was performed as previously published (Vlachakis et al., 2001).

Micrococcal nuclease digestions and Nucleosome identification

Micrococcal nuclease (MNase) digestions, isolation of mono-nucleosome fragments, and amplification of purified DNA was performed on 4 and 9 hour post fertilization embryos as previously published (Weicksel et al., 2013). Nucleosomes were mapped to the *hoxb1a* promoter using a nucleosome scanning protocol (Sekinger et al., 2005). Briefly, 16 primer pairs were designed by eye (listed in tiled approximately every 50bp, across the *hoxb1a* proximal promoter region starting at ~450bp upstream of the transcription start site (TSS) to ~230bp downstream of the TSS (illustrated in 3-5A).

Primers:

Primer 1_FWD	CAGATTTCCTTCCTAAACACACA

Primer 1_RVS	ATTAAAGAGGACAATCTAGCTCACA
Primer 2_FWD	GGTAAACGCGAACATTACTCC
Primer 2_RVS	GGAAGATAGCACATTCGTAATTAAA
Primer 3_FWD	CCTATGCTCCAGTCCATTACG
Primer 3_RVS	GGTTAAAAGATGCAAGGGGA
Primer 4_FWD	GGTGCGATTAAAATTAGAAACTAATGG
Primer 4_RVS	AATGAGAGAAAAAGAAATAAAGAAAGAGCGC
Primer 5_FWD	AAAGATGCAAGGGGATGAAG
Primer 5_RVS	TATGTCAAACCCTGCGTGAAAGG
Primer 6_FWD	AAGCGCTCTTTCTTTATTTCTTTTTCTCTC
Primer 6_RVS	AAAGCCACTTCAATCAAACCAGCC
Primer 7_FWD	TTTCACGCAGGGTTTGAC
Primer 7_RVs	AAGTTTGTCAGCGCACGGC
Primer 8_FWD	TTTGATTGAAGTGGCTTTGTCATGC
Primer 8_RVS	TGAGACGTCACGGCGCC
Primer 9_FWD	TGACAAACTTCTGGAGGTCCCC
Primer 9_RVS	TTACCTCTGGAGTATTTGCTCGTGC
Primer 9_FWD	CCAGCAGCTGAGGTAAAGATG
Primer 9_RVS	CTTCCGCATGACATACTATTGC
Primer 10_FWD	AAGCACGAGCAAATACTCCAGAGG
Primer 10_RVS	AATTAATGGCGGAGGGACAACC
Primer 11_FWD	ATTGCGAGCTTACAGGACAGGAGG

Primer 11_RVS	TTCGTCCCACGGTTACAAATTGTG
Primer 12_FWD	TTCTCAGGTTGTCCCTCCGCC
Primer 12_RVS	AAGTGGTGGTATCCAGCCTTGG
Primer 12_FWD	ATTTGTAACCGTGGGACGAA
Primer 12_RVS	CTGGACACGCTAGTGACAGC
Primer 13_FWD	TTGGACCAGGCGTTCCCG
Primer 13_RVS	TTCTGGTGCTGATGTTGTGCTGC
Primer 14_FWD	TCCACACTGGACACGCTAGT
Primer 14_RVS	TTCTGGTGCTGATGTTGTGC
Primer 15_FWD	AATCAGCCACCAACAGCAGC
Primer 15_RVS	TTTGATTTTGGTGCTGGTGATGC
Primer 16_FWD	AACATCAGCACCAGAACGGC
Primer 16_RVS	ATAACTTGTTGTCCCAGTTCCACC

qPCR was performed with three biological replicates of MNase and sonicated control gDNA fragments were amplified using Qiagen QuantiFast SYBR Green PCR Kit (Qiagen: 204054) in the Abi 7900HT Sequence detection system in a 384 well format and analyzed using SDS software v2.3. Samples were expressed as a $\log_2$ ratio of the MNase sample to the sonicated control. Standard error and two-tail T-tests were performed using Excel with significance cut-offs set to p=.05.

RESULTS

Generation of *hoxb1a* and *hoxb1b* mutants

To investigate the roles of *hoxb1a* and *hoxb1b* in zebrafish hindbrain development, we set out to generate *hoxb1a* and *hoxb1b* loss of function mutants using zinc finger nucleases (ZFNs) and TALE nucleases (TALENs). ZFNs and TALENs consist of the Fok1 endonuclease tethered to a sequence-specific DNA-binding domain (zinc finger or TALE) that targets the nuclease to a desired genomic location. High target specificity is achieved by severing the Fok1 protein and fusing its N- and C-termini to separate DNA-binding domains. Such N- and C-terminal fusion proteins are inactive by themselves, but activity is restored when one N-terminal and one C-terminal Fok1 fusion protein binds to adjacent genomic sequences. The fact that two fusion proteins must bind adjacent sequences reduces, but does not eliminate, the likelihood of off-target effects. Once targeted, the Fok1 nuclease introduces double strand DNA breaks that are repaired primarily through the non-homologous end joining (NHEJ) repair pathway. NEHJ is relatively error prone and will introduce mutations at a low rate. While many of the resulting mutations do not affect protein function, we were particularly interested in identifying the small number of mutations that lead to shifts in the reading frame and introduce stop codons.

We initially employed ZFNs to target both *hoxb1a* and *hoxb1b* based on several criteria. First, nucleases were targeted to a site in the first exon of each gene in order to increase the likelihood that a frame shift would terminate

translation upstream of known functional domains, particularly the homeodomain. Second, the spacing between the target sequences for each ZFN (consisting of one Fok1 N-terminal fusion and one Fok1 C-terminal fusion) was set to either 5bp or 6bp based on previous reports indicating that these represent optimal spacing (Meng et al., 2008). Third, we targeted regions containing a restriction site that could be used to screen for mutations that disrupt the restriction site. Based on these criteria, we designed several ZFNs to each gene using three separate ZFN "builds" (Table 3-1). The first and second builds were based on a modular library of single zinc finger proteins (ZFPs) (Meng et al., 2008). For build 1, we generated one ZFN targeting *hoxb1a* (Zb1a-1) and one targeting *hoxb1b* (Zb1b-1). The N- and C-terminal fusions for each ZFN contained three ZFPs assembled from the modular library. Build 2 (Zb1a-2 and Zb1b-2) employed the same modular library and targeted the same genomic sites as build 1, but contained four ZFPs each. The rationale behind expanding to four ZFPs was to increase specificity for the target sequence while decreasing the instances of off-target effects. For build 3, we designed two ZFNs to each gene (Zb1a-3, Zb1a-4, Zb1b-3 and Zb1b-4). Zb1b-3 and Zb1b-4 targeted the same genomic sequence as Zb1b-1 and Zb1b-2, although Zb1b-4 was offset 3bp relative to Zb1b-3, while Zb1a-3 and Zb1a-4 targeted sites 60bp and 125bp, respectively, upstream of the site targeted by Zb1a-1 and Zb1a-2. The ZFNs designed in build 3 also used four ZFPs each, but were assembled from an updated version of the ZFP library that includes ZFP dimers (Gupta et al., 2011).

Table 3-1

Gene	Target Coordinate	Upstream ZFP Target	Downstream ZFP Target	Gap	Build
Zb1a-1	Chr3:24060660	CTTATCAGC	GATGCGAAG	6bp	1
Zb1a-2	Chr3:24060660	GATGCGAAGGCC	CATCTTATCAGC	6bp	2
Zb1a-3	Chr3:24060602	GCCGGTGCGTAC	GCCATAGTGTGG	6bp	3
Zb1a-4	Chr3:24060535	GGATGGGATGTA	AGGGTTGATAAA	5bp	3
Zb1b-1	Chr12:28712770	GTGGACATG	CCTTCCACC	5bp	1
Zb1b-2	Chr12:28712770	GTGGACATGGGT	AGCCCTTCCACC	5bp	2
Zb1b-3	Chr12:28712770	GTGGACATGGGT	CAGCCCTTCCAC	6pb	3
Zb1b-4	Chr12:28712773	GACATGGGTAAA	CCCTTCCACCTC	6bp	3
Gene	Target Coordinate	Upstream TALE	Downstream TALE	Gap	# of TALs
Tb1a-1	Chr3:24060209	TTCCAGAATGAACTC	ATTTGTAACCGTGGGA	16bp	15/16
Tb1a-2	Chr3:24060227	TCTTGGAGTACACAAT	AACGCCTACTCGCCCA	16bp	16/16
Tb1a-3	Chr3:24060213	TCCAGAATGAACTCTTTC	GTAACCGTGGGACGA	16bp	18/15

Gene	embryos injected	Activity	Enzyme
Zb1a-1	2916	NO	FatI
Zb1a-2	541	NO	FatI
Zb1a-3	72	NO	BslI
Zb1a-4	56	NO	BslI
Zb1b-1	274	NO	BslI
Zb1b-2	424	NO	BslI
Zb1b-3	109	YES	BslI
Zb1b-4	149	YES	BslI
Gene	embryos injected	Activity	Enzyme
Tb1a-1	50	NO	RsaI
Tb1a-2	50	YES	BtgI
Tb1a-3	50	NO	RsaI

Table 3-1. ZFN and TALEN build information.

Information for ZFN and TALEN constructs and injection totals. Colored rows indicate the ZFN and TALEN constructs used for generating *hoxb1b* and *hoxb1a* targeted mutations.

Such ZFP dimers are selected for their ability to bind DNA efficiently as dimers (as opposed to being selected as monomers), since some ZFP monomers do not bind DNA efficiently in the context of larger assemblies. All the ZFNs generated in build 3 (except the C-terminal Fok1 fusion for Zb1b-3) included one ZFP dimer each. In vitro transcribed mRNA encoding each ZFN pair was injected into early one-cell stage embryos and genomic DNA was prepared from whole embryos collected 24 hours post fertilization (hpf)(scheme illustrated in Fig. 3-1). ZFN activity was measured by amplifying the targeted region, followed by digestion to identify loss of the diagnostic restriction site. Notably, the ZFNs are likely to act after the first several cell divisions (due to the rapid cell cycle of zebrafish embryos, as well as to the need for the ZFN mRNA to be translated) and it is therefore expected that mutations will be induced in only a subset of cells – rendering the embryos genetically mosaic. Accordingly, embryos injected with Zb1b-3 and Zb1b-4 revealed a partial loss of the diagnostic restriction site, suggesting that these ZFNs are active (Table 3-1, Fig. 3-2A), but all other ZFNs appear to be inactive. Based on the band in the diagnostic digest, Zb1b-3 appears to be more active than Zb1b-4 (Fig. 3-2A).

Since ZFNs from all three builds failed to introduce mutations at the *hoxb1a* locus, we turned to TALENs as an alternative method to disrupt the *hoxb1a* gene. To increase the likelihood of success, we generated three different *hoxb1a* TALENs that differ slightly in the length of their target sequences (Table 3-1) using the Golden Gate TALEN assembly (Cermak et al., 2011). As

Figure 3-1

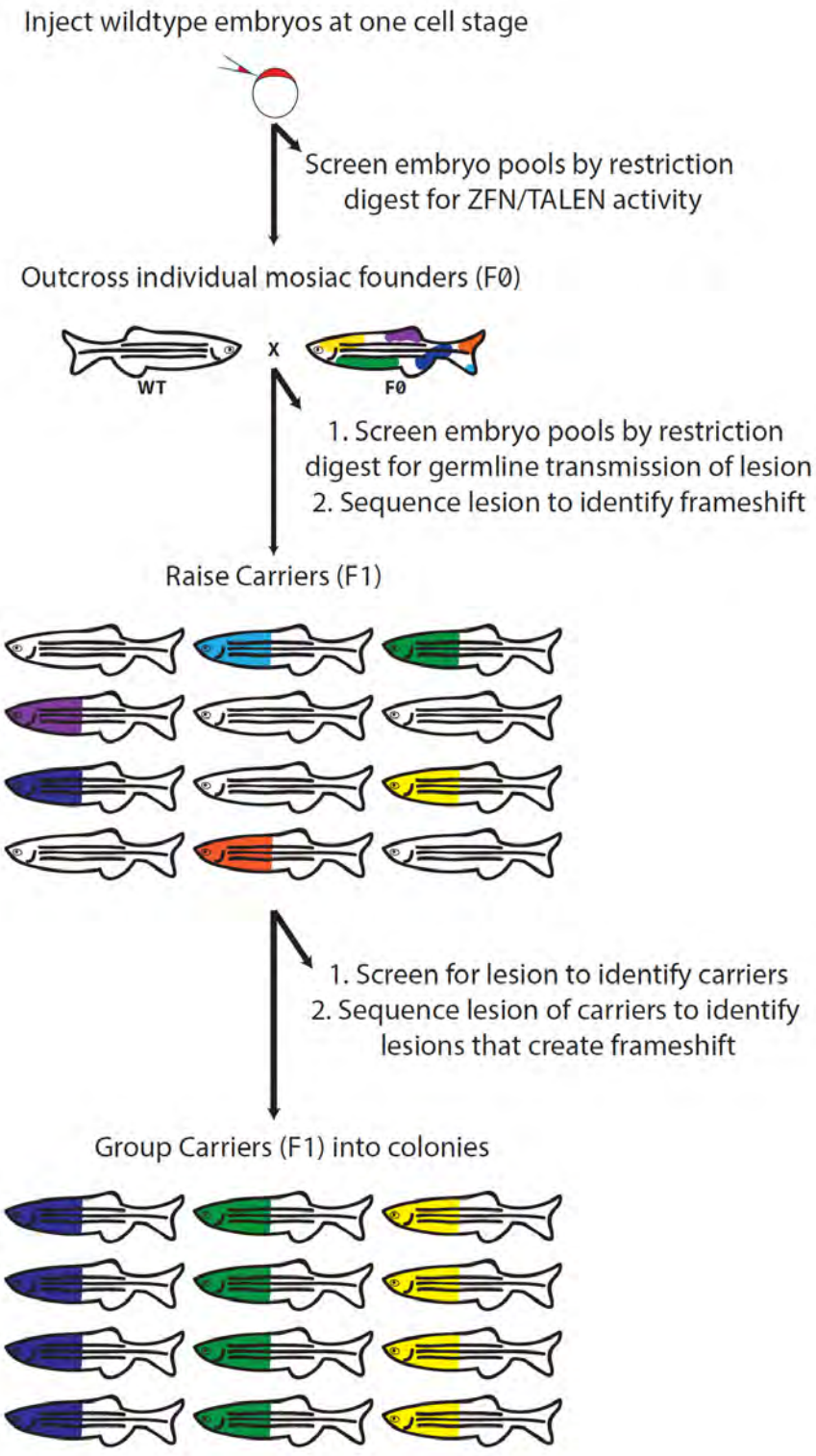
Inject wildtype embryos at one cell stage
Screen embryo pools by restriction digest for ZFN/TALEN activity
Outcross individual mosiac founders (F0)
WT
X
F0
1. Screen embryo pools by restriction digest for germline transmission of lesion
2. Sequence lesion to identify frameshift
Raise Carriers (F1)
1. Screen for lesion to identify carriers
2. Sequence lesion of carriers to identify lesions that create frameshift
Group Carriers (F1) into colonies

Figure 3-1. Schematic of ZFN/TALEN screening and carrier identification

Embryos are injected at the one cell stage and screened as a pool. Nucleases with activity were re-injected and grown to maturity and represent the mosaic F0 founder population. Founders are outcrossed to WT and these embryos are pooled and screened for a lesion. Lesion identification in the F1 carriers indicates lesions in the germline of the F0 founders. F1 embryos are raised and screened by fin clipping. Lesions of the F1 carriers were then sequenced to determine if a frameshift in the reading frame occurred. Carriers with a frameshift were characterized in these experiments.

Figure 3-2

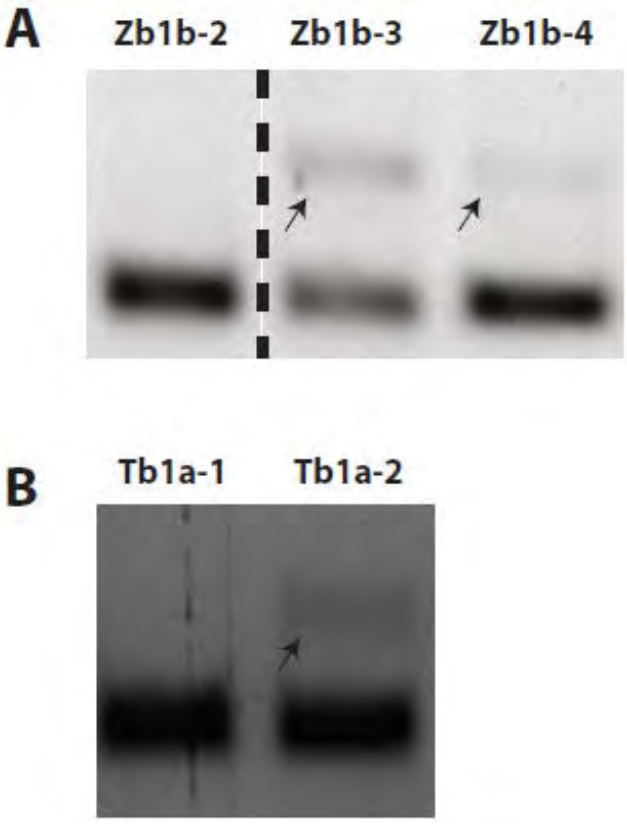

Figure 3-2. ZFN and TALEN activity digest.

(A and B) Digest of PCR product amplifying (A) *hoxb1b* ZFN sites for Zb1b-2, Zb1b-3, and Zb1b-4. (B) *hoxb1a* TALEN sites Tb1a-1 and Tb1a-2. Arrows indicate loss of restriction site indicating nuclease activity in injected embryos.

for the ZFNs, the TALENs were designed to target the first exon of *hoxb1a* and to encompass a diagnostic restriction site. However, the TALENs were directed at sites 450bp (Tb1a-1) or 430bp (Tb1a-2 and Tb1a-3) upstream from the region targeted by the ZFNs. Using the same mRNA microinjection strategy as outlined for the ZFNs, we find that one of the three TALENs (Tb1a-2) introduced mutations – as evidenced by loss of the diagnostic restriction site (Fig. 3-2B). Having identified functional ZFNs and TALENs, we next re-injected one active nuclease targeting each gene (Zb1b-3 and Tb1a-2) and raised the injected embryos to establish an adult F0 founder population. As noted above, fish in this F0 population will be mosaic and each individual fish may carry more than one mutant allele for the same gene. Genotyping of embryos from out-crosses of F0 fish identified 20 *hoxb1a* (out of 24 tested) and 15 *hoxb1b* (out of 35 tested) F0 founders that transmit mutations (defined as disruptions of the diagnostic restriction site) via their germ lines, suggesting mutagenesis rates of 83% and 43% for *hoxb1a* and *hoxb1b*, respectively. Sequencing of the mutant alleles from each F0 founder revealed that two of the 20 *hoxb1a* (A2 and A20) and three of the 15 *hoxb1b* (B2, B11 and B15) F0 founders carry mutations that introduce frame shifts (Table 3-2), while the remaining F0 founders transmitted mutations that disrupt the diagnostic restriction site, but that do not create frame shifts (Appendix B-1). The five F0 fish that carry mutations causing frame shifts were then outcrossed to wild type fish and the resulting offspring raised to generate the F1 generation. Genotyping of F1 fish allowed us to determine the

Table 3-2

Founder	Nuclease	Transmission Frequency	Sequence of Mutations	UM#
A2	Tb1a-2	14%	BtgI TTTGTAAC GTGGGACGAACGCCTACT TTTGTACACAATTTGTACAATTTGGACGAACGCCTACT TTTGTAC GGACGAACGCCTACT TTTGTACTCCATTTGTA CTACT	UM189 UM190 UM191 UM192
A20	Tb1a-2	9%	TT TGGGACGAACGCCTACT TTTGTAATTT GGACGAACGCCTACT	UM193 UM194
B2	Zb1b-3	45%	BslI GCCCTTCC GTGGACATGGG	UM195
B11	Zb1b-3	43%	GCCCTTCCACATTCC GTGGACATGGG	UM196
B15	Zb1b-3	41%	TGTTTCAATCGTGAAACACAAATTCACAAATTCAATCGTGGACATGGG	UM197

Table 3-2. Lesion sequences of *hoxb1a* and *hoxb1b* mutations

Sequenced lesions identified in carriers. Multiple alleles were found in *hoxb1a* carriers while in *hoxb1b* carriers one allele predominated.

transmission rate of mutations from mosaic F0 fish. We find that the *hoxb1b* F0 founders transmit their mutations at a frequency of ~40% (45% for B2, 43% for B11 and 41% for B15), while the *hoxb1a* F0 fish transmit their mutations at ~10% (14% for A2 and 9% for A20). The mutant alleles were then re-sequenced from F1 carriers to determine how many different mutations were transmitted from each F0 fish. We find that the three *hoxb1b* founders each transmitted only one mutant allele, while the two *hoxb1a* founders transmitted multiple mutant alleles each (four alleles from A2 and two alleles from A20). Thus, we have generated six *hoxb1a* (*UM189, 190, 191, 192, 193, 194)* and three *hoxb1b (UM195, 196, 197)* mutant lines (Table 3-2).

Closer analysis of the mutant sequences revealed that Zb1b-3 and Tb1a-2 generated both insertions and deletions (Fig. 3-3). In particular, the Zb1b-3 ZFN introduced deletions ranging from 1bp-10bp, as well as a 36bp insertion in the *hoxb1b* gene, while the Tb1a-2 TALEN introduced deletions ranging from 1bp-8bp, as well as an 11bp insertion, in the *hoxb1a* gene. We note that large insertions and deletions that interfere with the PCR reaction (e.g. by deleting a primer site) would not be detected by our experiments, suggesting that the sizes observed here may be somewhat biased. As expected, conceptual translation of each mutant allele revealed a shift in the reading frame (Appendix B-2). As a result, *hoxb1a* mutant alleles go out of frame after residue 15 (UM191 and UM193), residue 16 (UM190, UM192 and UM194) or residue 17 (UM189) (Fig. 1A) and *hoxb1b* mutants after residue 70 (UM197), residue 73 (UM195) or

Figure 3-3

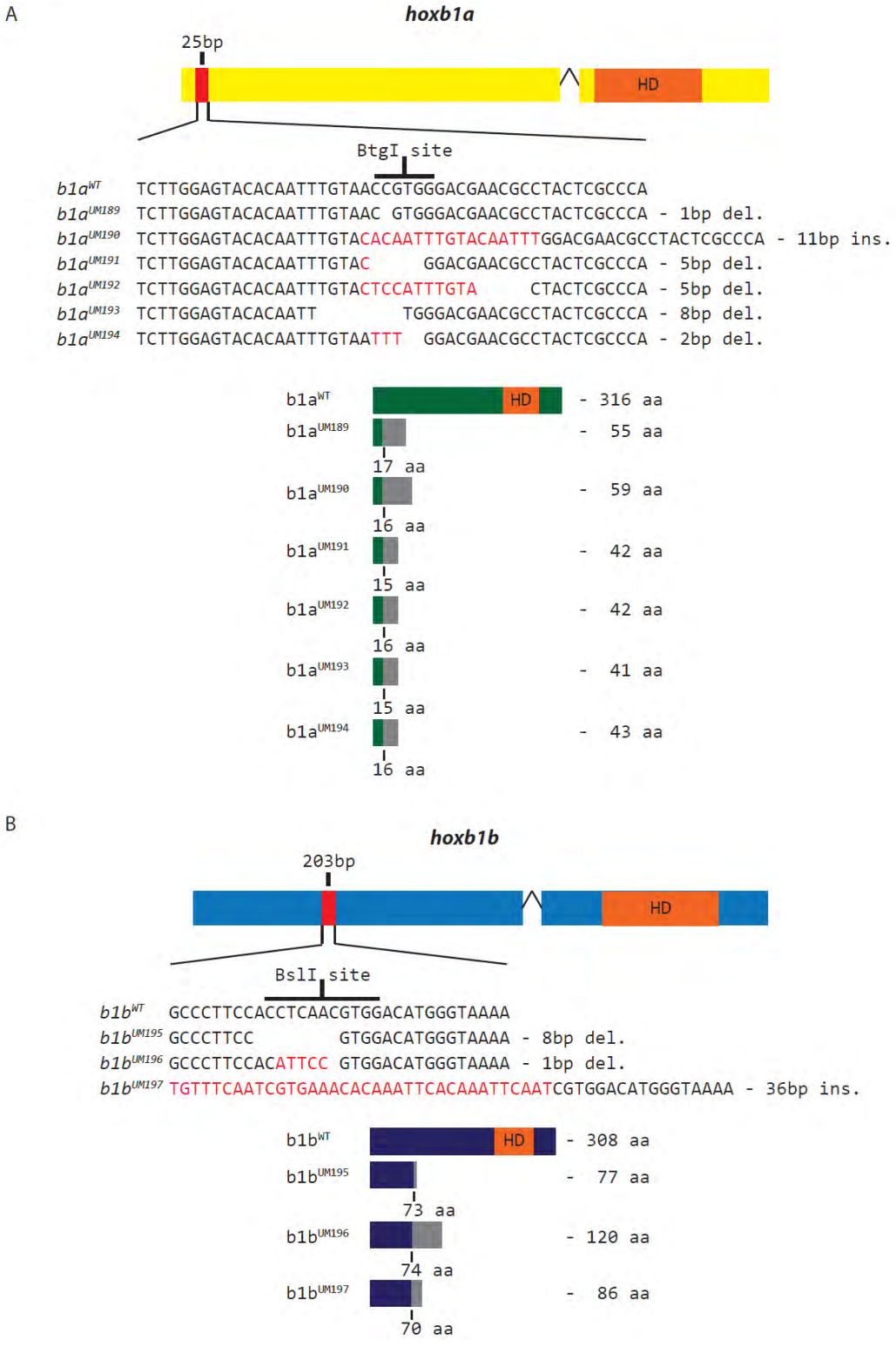
A
hoxb1a
25bp
HD
BtgI site
b1a^WT TCTTGGAGTACACAATTTGTAACCGTGGGACGAACGCCTACTCGCCCA
b1a^UM189 TCTTGGAGTACACAATTTGTAAC GTGGGACGAACGCCTACTCGCCCA - 1bp del.
b1a^UM190 TCTTGGAGTACACAATTTGTACACAATTTGTACAATTTGGACGAACGCCTACTCGCCCA - 11bp ins.
b1a^UM191 TCTTGGAGTACACAATTTGTAC GGACGAACGCCTACTCGCCCA - 5bp del.
b1a^UM192 TCTTGGAGTACACAATTTGTACTCCATTTGTA CTACTCGCCCA - 5bp del.
b1a^UM193 TCTTGGAGTACACAATT TGGGACGAACGCCTACTCGCCCA - 8bp del.
b1a^UM194 TCTTGGAGTACACAATTTGTAATTT GGACGAACGCCTACTCGCCCA - 2bp del.
b1a^WT HD - 316 aa
b1a^UM189 - 55 aa
17 aa
b1a^UM190 - 59 aa
16 aa
b1a^UM191 - 42 aa
15 aa
b1a^UM192 - 42 aa
16 aa
b1a^UM193 - 41 aa
15 aa
b1a^UM194 - 43 aa
16 aa
B
hoxb1b
203bp
HD
BslI site
b1b^WT GCCCTTCCACCTCAACGTGGACATGGGTAAAA
b1b^UM195 GCCCTTCC GTGGACATGGGTAAAA - 8bp del.
b1b^UM196 GCCCTTCCACATTCC GTGGACATGGGTAAAA - 1bp del.
b1b^UM197 TGTTTCAATCGTGAAACACAAATTCACAAATTCAATCGTGGACATGGGTAAAA - 36bp ins.
b1b^WT HD - 308 aa
b1b^UM195 - 77 aa
73 aa
b1b^UM196 - 120 aa
74 aa
b1b^UM197 - 86 aa
70 aa

Figure 3-3. Schematic of *hoxb1a* and *hoxb1b* mutations

Diagram of nuclease targeting for both *hoxb1a* (A) and *hoxb1b* (B) indicated by red bar. Intronic sequence is depicted by wedge and homeodomains (HD) are represented by orange block. Alignments of lesions depict deletions with a space and insertions in red. Finally, representative diagrams of predicted peptides in green for Hoxb1a and purple for Hoxb1b, grey indicates peptides after the frameshift in the coding region.

residue 74 (UM196) (Fig. 3-3B). While the out of frame sequences code for varying numbers of missense residues, all terminate in a premature stop codon and none of the mutant alleles is predicted to encode a homeodomain (Appendix B-3).

We also raised embryos from *hoxb1a*^{UM191} x *hoxb1a*^{UM192} and *hoxb1b*^{UM197} x *hoxb1b*^{UM197} crosses and genotyped adults by PCR followed by diagnostic digest from genomic DNA purified from fin clips. From this we determined that *hoxb1a*$^{-/-}$ embryos did not survive to adulthood, while *hoxb1b*$^{-/-}$ embryos did. Though how the *hoxb1a*$^{-/-}$ died is unclear, *Hoxb1*$^{-/-}$ mice are also not viable. The survival of *hoxb1b*$^{-/-}$ embryos however, was somewhat surprising since *Hoxa1*$^{-/-}$ mouse pups die shortly after birth (Lufkin et al., 1991; Studer et al., 1996).

<u>*hoxb1b* is required for zebrafish hindbrain segmentation</u>

Formation of the vertebrate hindbrain requires segmentation of the neural tube into rhombomere domains, as well as the specification of distinct cell fates and the differentiation of characteristic types of neurons in each rhombomere. Paralog group 1 *hox* genes, such as *hoxb1a* and *hoxb1b*, are among the earliest genes expressed in the hindbrain primordium and *hox* function has been implicated in multiple aspects of hindbrain development. We therefore made use of the *hoxb1a* and *hoxb1b* mutant lines to examine the role of *hoxb1a* and *hoxb1b* in development of the zebrafish hindbrain.

We first examined the expression of several rhombomere-restricted genes – *pax2* (expressed at the midbrain-hindbrain boundary, MHB), *krox20* (expressed in r3 and r5), *hoxb1a* (expressed in r4), *hoxb3a* (expressed in r5 and r6) and *hoxd4a* (expressed in r7 and r8). For this purpose, heterozygous *hoxb1b*^{UM197} F1 fish were in-crossed and the resulting F2 embryos were assayed by in situ hybridization followed by genotyping. We find that homozygous *hoxb1b*^{UM197} mutant embryos express *krox20* in r3 and r5, as well as *hoxb1a* in r4 (Fig. 3-4C). However, the size of r3 is increased and the size of r4 is decreased in *hoxb1b*^{UM197} mutants relative to wild type (or heterozygous) embryos (Fig. 3-4A). To exclude the possibility that the Zb1b-3 ZFN might have introduced off-target mutations that could contribute to this phenotype, we also examined in-crosses of the *hoxb1b*^{UM196} and *hoxb1b*^{UM195} lines, as well as pair-wise inter-crosses among all three lines. We find that mutant embryos derived from all such crosses exhibit the same phenotype (Appendix B-4; Appendix B-5), confirming that the phenotype is due to disruption of the *hoxb1b* gene. Further analysis of *hoxb1b*^{UM197} mutant embryos revealed expression of *pax2*, *hoxb3a* and *hoxd4a* in the expected domains (Fig. 3-4C, G, K). In addition to the enlargement of r3 and the reduction of r4 noted above, this analysis also revealed an apparent reduction of r6 – as evidenced by a smaller gap between r5 *krox20* staining and r7 *hoxd4a* staining (brackets in Fig. 3-4E, G), as well as by a reduction in the size of the *hoxb3a* expression domain (brackets in Fig. 3-4I, K) in mutant embryos relative to wild type embryos. We next quantified these apparent changes in

Figure 3-4

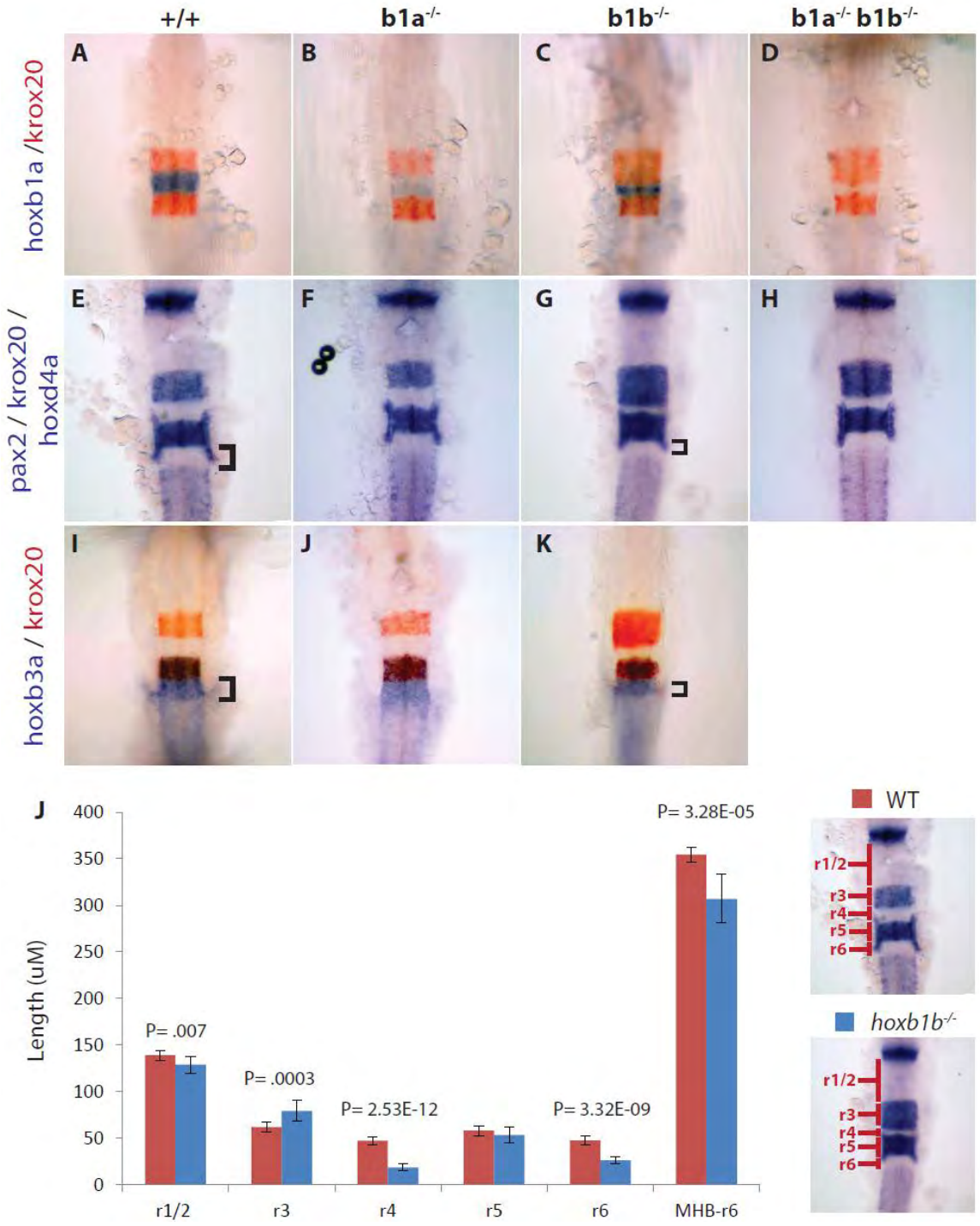
+/+
b1a-/-
b1b-/-
b1a-/- b1b-/-
A
B
C
D
hoxb1a /krox20
E
F
G
H
pax2 / krox20 / hoxd4a
I
J
K
hoxb3a / krox20
J
Length (uM)
400
350
300
250
200
150
100
50
0
P= .007
P= .0003
P= 2.53E-12
P= 3.32E-09
P= 3.28E-05
r1/2
r3
r4
r5
r6
MHB-r6
WT
hoxb1b-/-
r1/2
r3
r4
r5
r6

Figure 3-4. *hoxb1b*$^{-/-}$ embryos have disrupted hindbrain segmentation.

In situ hybridization with molecular markers to visualize hindbrain segmentation phenotypes (A-D) *hoxb1a* (blue, r4) and *krox20* (red, r3/r5), (E-H) *pax2* (blue, midbrain-hindbrain boundary), *krox20* (blue, r3/r5), and *hoxd4a* (blue, r6) (I-K) *hoxb3a* (blue, r5/r6) and *krox20* (red, r3/r5). (J) Graphical representation of hindbrain measurements. P-values indicate significance computed using two-tail t-test and error bars represent standard error. N=10

rhombomere size by direct measurements (Fig. 3-4J). We find that r3 is significantly enlarged (79.4um in *hoxb1b* mutants versus 62.0um in wild type; p = 0.0003) and r4 significantly reduced (18.5um in mutant versus 47.4um in wild type; p = 2.53E-12) in mutant embryos. Notably, we cannot distinguish whether this effect is due to some cells switching from an r4 to an r3 fate, or if r3 cells have a growth advantage in the absence of *hoxb1b* function. We also find that r6 (26.5um in mutant versus 47.6um in wild type; p=3.32E-09) and r1/r2 (129um in mutant versus 139um in wild type; p=.0067) are somewhat reduced, but r5 is unaffected, in *hoxb1b* mutants. Accordingly, measuring the length of the entire hindbrain reveals it to be significantly shorter in *hoxb1b* mutant embryos (306um in mutant versus 354um in wild type; p=3.00E-05 Fig. 2J), presumably as a result of the reduced length of several rhombomeres.

In situ hybridization analysis of *hoxb1a* mutant embryos revealed normal expression of *pax2, krox20, hoxb3a* and *hoxd4a* in the hindbrain (Fig. 3-4B, F, J). However, expression of *hoxb1a* is markedly reduced or absent in r4 (Fig. 3-4B). Since *hoxb1a* regulates its own expression (McClintock et al., 2001), the loss of *hoxb1a* transcript in *hoxb1a* mutants may be due to disruption of this autoregulatory loop. Notably, even though *hoxb1a* expression is reduced, the size of the r4 domain is normal. Indeed, all rhombomeres appear to be of normal size in *hoxb1a* mutant embryos. As observed for the *hoxb1b* lines, mutant embryos from inter-crosses among all available *hoxb1a* mutant lines display the same phenotype, suggesting that it is the result of mutations in *hoxb1a* rather

than due to off-target mutations introduced by the Tb1a-2 TALEN (Appendix B-6). We conclude that *hoxb1b*, but not *hoxb1a*, is required for formation of appropriately sized rhombomere segments.

hoxb1a is important for r4 derived neurons

A key event in hindbrain development is the differentiation of unique complements of neurons in each rhombomere (Figure 1-3). In particular, motor neurons of the Vth cranial nerve (trigeminal) differentiate in r2 and r3, motor neurons of the VIth cranial nerve (abducens) form in r5 and r6 and motor neurons of the Xth cranial nerve (vagal) form in the caudal most region of the hindbrain. In addition, motor neurons of the VIIth cranial nerve (facial) form in r4, but subsequently migrate to r6 and r7. In order to determine if neuronal differentiation is affected in *hoxb1a* and *hoxb1b* mutants, we detected cranial motor neurons by immunostaining using an antibody against the Islet1 and Islet2 transcription factors that are expressed in motor neurons. Immunostaining of wild type embryos detected the stereotypical arrangement of cranial motor neurons (Fig. 3-5A). Notably, this includes an almost complete lack of facial motor neurons (FMNs) in r4 as a result of these neurons having migrated caudally by this stage. In contrast, immunostaining of *hoxb1a* mutant embryos revealed a large number of motor neurons in r4 and reduced numbers in r6 and r7 (Fig. 3-5B), consistent with FMNs being unable to migrate and instead remain in r4. FMNs also remain in r4 of *hoxb1b* mutant embryos, but the phenotype is

Figure 3-5

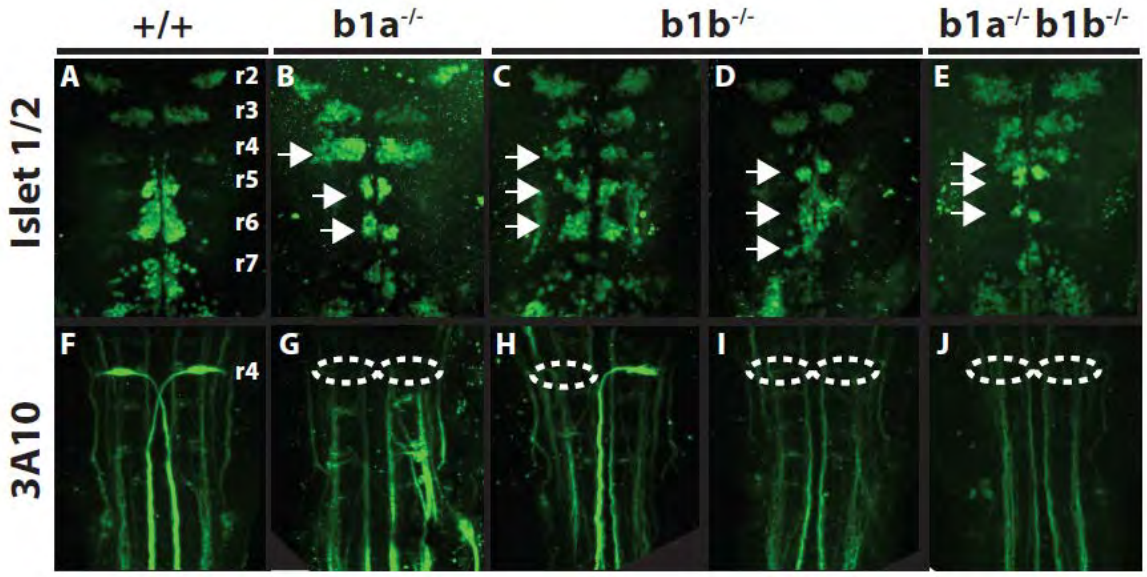

Figure 3-5. *hoxb1a*$^{-/-}$ and *hoxb1b*$^{-/-}$ embryos have disrupted formation and differentiation in the hindbrain.

(A-E) Islet 1/2 antibody labeling of motor neurons of the zebrafish hindbrain, arrows indicate facial motor neurons in r4 and abducens neurons in r5/r6. (F-J) 3A10 antibody labeling of Mauthner neurons in r4 of the zebrafish hindbrain. Dotted circles indicate positions where Mauthner neurons normally form.

less severe and more variable than what is observed in *hoxb1a* mutants. The most severely affected *hoxb1b* mutants reveal a partial retention of FMNs in r4 (Fig. 3-5C), while more mildly affected embryos show nearly normal FMN migration (Fig. 3-5D). In addition to impaired FMN migration from r4, motor neurons in r5-r7 also appear to be less well organized in *hoxb1b* mutants, with cells being less tightly grouped and numerous cells found located outside the main clusters.

Similar to the cranial motor neurons, reticulospinal interneurons also display rhombomere-specific differentiation. Specifically, the bilaterally arranged Mauthner neurons form in r4 and project their axons across the midline down into the spinal cord (Fig. 3-5F). Using immunostaining, we observe a complete loss of Mauthner neurons in *hoxb1a* mutant embryos (Fig. 3-5G). As observed for the cranial motor neurons, *hoxb1b* mutant embryos show a variable phenotype such that some embryos retain one Mauthner neuron, while other embryos lack both Mauthner neurons (Fig. 3-5H, I). We conclude that *hoxb1a* function is absolutely required for FMN migration and Mauthner neuron formation, but that *hoxb1b* is only partially required for these processes.

hoxb1a and *hoxb1b* have separate functions in zebrafish hindbrain development

Since *hoxb1a* and *hoxb1b* are both required for normal r4 formation, we examined their functional relationship by analyzing *hoxb1a/hoxb1b* double mutant embryos. Using in situ hybridization, we find that

hoxb1a$^{UM193/UM194}$*;hoxb1b*$^{UM197/UM197}$ double mutant embryos have hindbrain segmentation defects with an expansion of r3 and a reduction of r4 and r6 (Fig. 3-4 D, H). These changes in rhombomere size are indistinguishable from those observed in *hoxb1b* mutant embryos (compare Fig. 3-4 G to 3-4 H), further demonstrating that *hoxb1a* does not play a role in zebrafish hindbrain segmentation. In contrast, *hoxb1a*$^{UM193/UM194}$*;hoxb1b*$^{UM197/UM197}$ double mutant embryos lack *hoxb1a* expression, while both *hoxb1a* and *hoxb1b* single mutant embryos show variable *hoxb1a* expression (compare Figs. 3-4B-D), indicating that both genes play a role in *hoxb1a* transcription.

Next we examined neuronal differentiation in *hoxb1a*$^{UM193/UM194}$*;hoxb1b*$^{UM197/UM197}$ double mutant embryos. We find that cranial motor neurons form in r4 of double mutant embryos, but do not migrate caudally (Fig. 3-5E). This phenotype is more severe than that observed in *hoxb1b* single mutants – that exhibit variable neuronal migration out of r4 (Fig. 3-5C, D) – and is similar to the phenotype of *hoxb1a* single mutants (Fig. 3-5B). However, we note that the population of motor neurons in r4 is smaller in *hoxb1a/hoxb1b* double mutants than in *hoxb1a* single mutants (compare Fig. 3-5B to 3-5E). This is consistent with the fact that r4 itself is smaller in *hoxb1a/hoxb1b* double mutants, suggesting that fewer neurons are formed in the reduced r4. Hence, it appears that *hoxb1a* function is absolutely required for migration of r4 cranial motor neurons. Additionally, motor neurons in r5-r7 appear better organized in *hoxb1a/hoxb1b* double mutants than in *hoxb1b* single mutants. In particular,

fewer cells are located outside the main motor neuron clusters of double mutants compared to *hoxb1b* single mutants (compare fig. 3-5E to 3-5C, D). Since *hoxb1a* single mutants also exhibit well-organized motor neuron clusters, this observation suggests that the disorganized neurons in *hoxb1b* mutants likely represent motor neurons that are migrating from r4. It also appears that the motor neuron population in r6 may be slightly smaller in *hoxb1a/hoxb1b* double mutants than in *hoxb1a* single mutants, consistent with r6 being smaller in double mutants. Lastly, an examination of Mauthner neuron differentiation revealed that *hoxb1a*$^{UM193/UM194}$*;hoxb1b*$^{UM197/UM197}$ double mutants completely lack Mauthner neurons in r4 (Fig. 3-5J). This is in contrast to *hoxb1b* single mutants that show variable loss of Mauthner neurons, but identical to the *hoxb1a* single mutant phenotype, suggesting that *hoxb1a* is absolutely required for Mauthner neuron formation.

We conclude that *hoxb1a* and *hoxb1b* have different functions in hindbrain development. Specifically, *hoxb1b*, but not *hoxb1a*, is required for hindbrain segmentation while both genes are required for *hoxb1a* expression. Furthermore, *hoxb1a* is absolutely required for proper neuronal differentiation in r4. While our genetic analysis also indicates a role for *hoxb1b* in neuronal differentiation, this is most likely due to residual *hoxb1a* expression in *hoxb1b* mutants.

hoxb1b and retinoic acid cooperate to activate *hoxb1a* expression

Although the size of r4 is reduced in *hoxb1b* mutant embryos, we note that *hoxb1a* expression persists, suggesting that *hoxb1a* transcription can be activated independently of *hoxb1b*. Since retinoic acid (RA) is known to activate *hox* gene transcription in many settings, we next investigated if RA signaling plays a role in activation of *hoxb1a* transcription. To this end, embryos from *hoxb1b*^{UM197} in-crosses were treated with 10uM diethylaminobenzaldehyde (DEAB; a small molecule inhibitor of the RALDH enzyme involved in RA synthesis), or with 100nM exogenous retinoic acid from 1hpf to 19hpf. We find that wild type embryos treated with DEAB lose *krox20* expression in r5, but not in r3, and also retain *hoxb1a* expression in r4 (Fig. 3-6C). In contrast, DEAB-treated *hoxb1b* mutant embryos lack *hoxb1a* expression in r4 (Fig. 3-6D). Since *hoxb1a* expression is abolished upon simultaneous removal of *hoxb1b* and RA, but not when either factor is removed by itself, we conclude that RA and *hoxb1b* cooperate to activate *hoxb1a* expression. RA treatment of wild type embryos leads to a reduction in r5 *krox20* expression, an expansion in r4 *hoxb1a* expression and a loss of r3 *krox20* expression, as well as expression of *hoxb1a* in tissues lateral to the hindbrain (Fig. 3-6E), confirming that RA can induce *hoxb1a* expression. RA-treated *hoxb1b* mutant embryos also exhibit ectopic *hoxb1a* expression laterally and reduced *krox20* expression in r5 (Fig. 3-6F). Furthermore, the expansion of r4 *hoxb1a* expression is less pronounced embryos and *krox20* expression in r3 remains detectable in RA-treated *hoxb1b* mutant

Figure 3-6

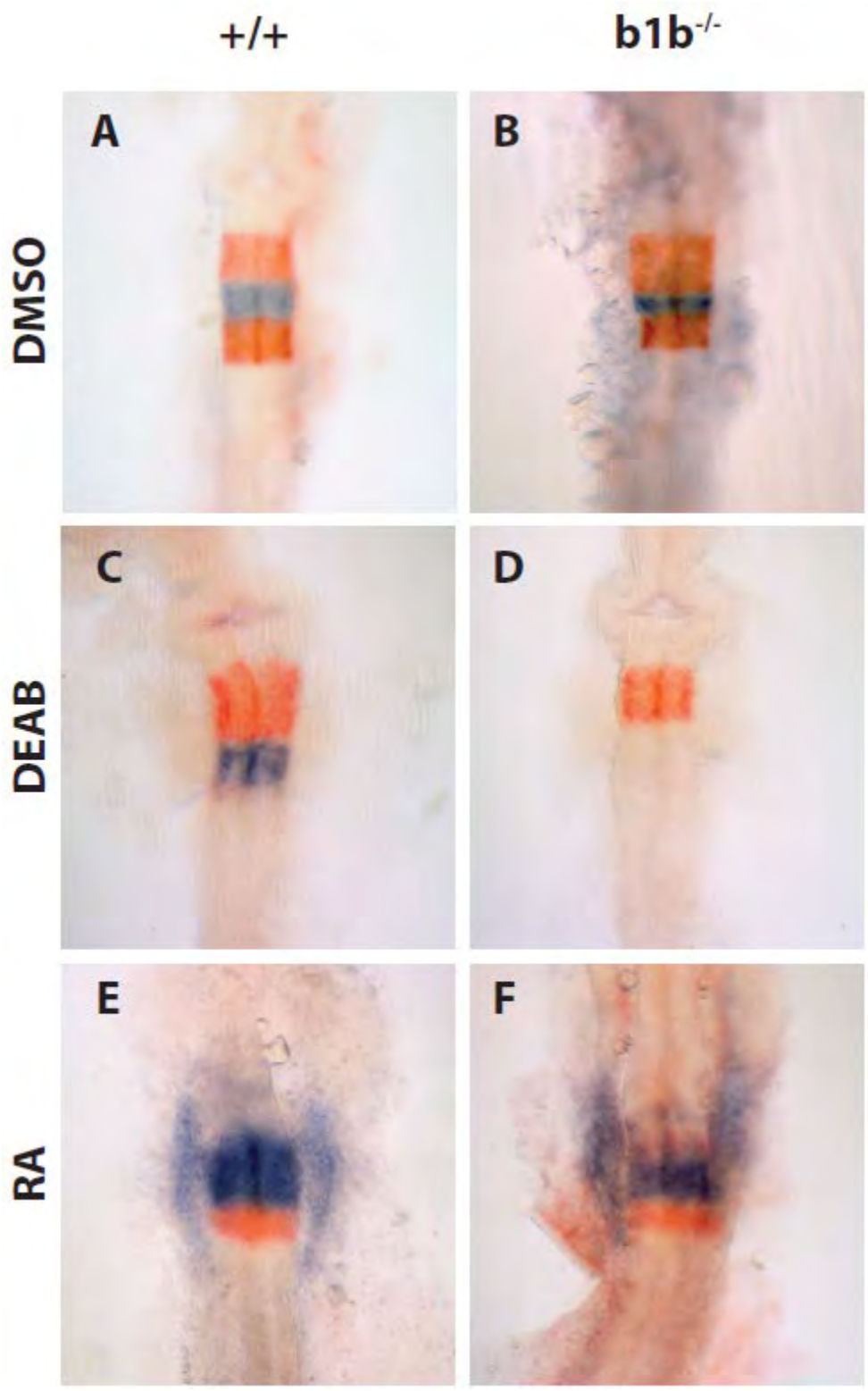

Figure 3-6. A role for RA in *hoxb1a* transcription.

hoxb1b$^{-/-}$ embryos were treated with either 10uM of DEAB or 100nM of RA at 1hpf until collected at 19hpf. Rhombomere boundaries were determined by in situ hybridization for *hoxb1a* (blue, r4) and *krox20* (red-r3/r5).

(Fig. 3-6F), suggesting that *hoxb1b* is required for exogenous RA to expand the *hoxb1a* r4 domain.

hoxb1b effects nucleosome positioning around the promoter of *hoxb1a*

We recently showed that nucleosome positioning around the promoter regions of zebrafish *hox* genes is a progressive processes that occurs over several stages of embryogenesis (Weicksel et al., 2013). Containing ~150bp of DNA wrapped around a histone core, the nucleosome has been shown to be an important chromatin feature in processes such as gene regulation, transcription, and replication (Almer et al., 1986; Fedor and Kornberg, 1989; Kornberg and Lorch, 1999; Lee et al., 2007; Widom, 1998). In our study we observed changes in nucleosome positioning after activation of the zygotic genome (ZGA) indicating that factors transcribed after ZGA were involved in nucleosome positioning at *hox* promoters. Since Hoxb1b plays an active role during early embryonic stages we wanted to see if Hoxb1b plays a role in nucleosome positioning at target promoters. For this study we chose to look at the effects Hoxb1b has on nucleosomes of the *hoxb1a* locus. The promoter of *hoxb1a* is well characterized with known Hoxb1b binding sites mapped upstream of the TSS. We took advantage of the fact that *hoxb1b*$^{-/-}$ embryos were viable and mapped nucleosomes at the *hoxb1a* promoter of WT and *hoxb1b*$^{-/-}$ embryos using a nucleosome scanning (NS) (Sekinger et al., 2005). Briefly, chromatin was isolated from embryos at 4hpf and 9hpf, time points that represent periods where

Hoxb1b would not be and would be bound (respectively) at the *hoxb1a* promoter, and digested by micrococcal nuclease (MNase). Mono-nucleosome sized fragments are purified and amplified by quantitative polymerase chain reaction (qPCR) using tiled primers spaced ~50bp apart, spanning from ~450bp upstream to ~230bp downstream of the *hoxb1a* TSS (Fig. 3-7A). Amplified product of each primer pair from the MNase digested sample is then compared to the product of a sonicated genomic control and expressed as a Log_2 ratio of MNase digested product to the sonicated control.

We first compared the nucleosome profiles of WT embryos at 4 and 9hpf. In an overlay, well positioned nucleosomes are observed in both time points at approximately 360bp, 180bp, and 35bp upstream of the TSS (-3, -2, and -1 nucleosomes respectively) (Fig. 3-7B). However, changes were observed both upstream and downstream of the TSS between the two samples. Downstream from the TSS we observed differences in the nucleosome density, in particular from ~60-180bp where 4hpf WT embryos have greater nucleosome density when compared to 9hpf. We also observed a loss of nucleosome density at the -1 nucleosome of the 4hpf to 9hpf. Finally, the -2 nucleosome of the 4hpf WT embryos also appeared to be wider than the -2 nucleosome observed in the 9hpf WT sample. Using a two-tailed T-test we calculated the significance of the changes observed between the 4hpf and 9hpf time points at each primer set. Based on this analysis we find that the changes at the -2 position, 120bp upstream of the TSS, and positions 60bp and 120bp downstream of the TSS are

Figure 3-7

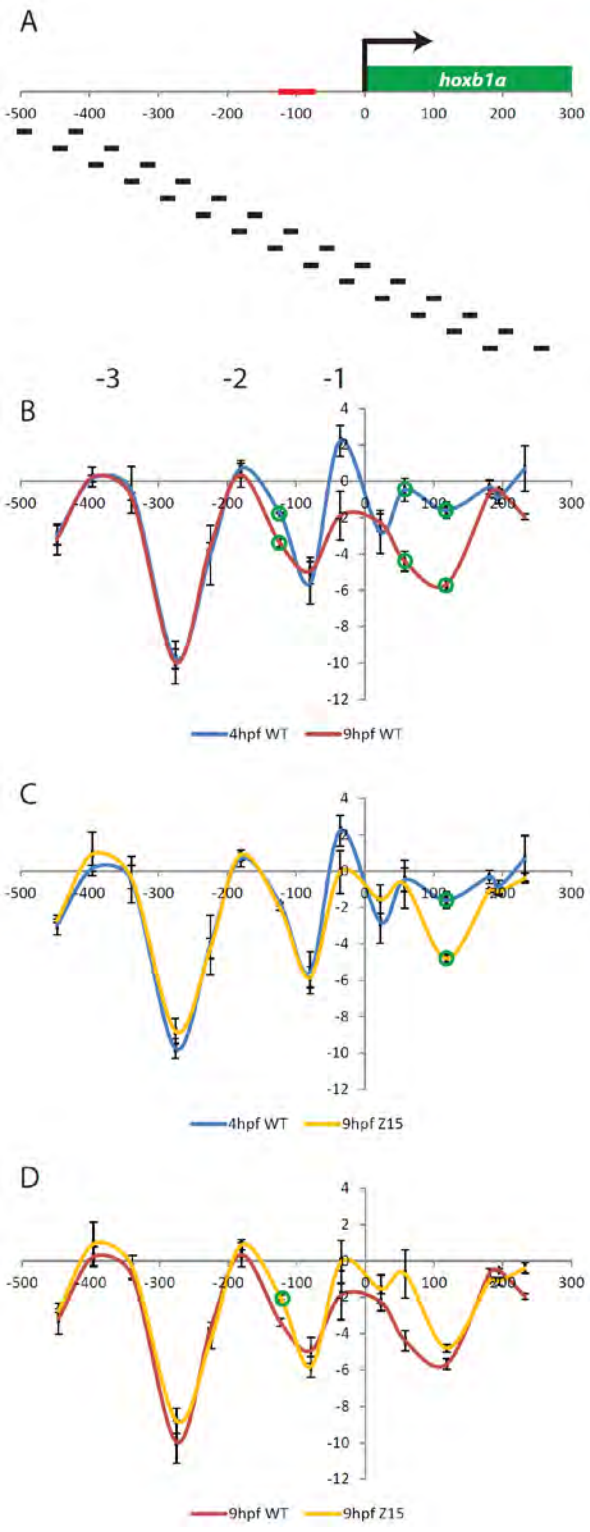
A
hoxb1a
-500 -400 -300 -200 -100 0 100 200 300
-3 -2 -1
B
4hpf WT
9hpf WT
C
4hpf WT
9hpf Z15
D
9hpf WT
9hpf Z15

Figure 3-7. Nucleosome positions are effected at the hoxb1a promoter in hoxb1b-/- embryos.

(A) Schematic of primer design across the hoxb1a promoter, red indicates approximate location of Pbx/Meis/Hox binding sites. (B-D) Nucleosome mapping at the hoxb1a promoter of WT and hoxb1b-/- embryos using nucleosome scanning. -3, -2, and -1 nucleosomes are labeled in (B). Significance is indicated by green circle; $p<.05$. Error bars represent standard error of three biological replicates.

statistically significant (p=0.0016, 0.0094, and 0.0016 respectively, Fig. 3-7B marked by green circles). To determine if nucleosomes were positioned differently in *hoxb1b*$^{-/-}$ embryos, we next compared the nucleosome profiles from 4hpf WT embryos and 9hpf *hoxb1b*$^{-/-}$ mutants. Using NS to map nucleosomes we find that 4hpf WT and 9hpf *hoxb1b*$^{-/-}$ mutant nucleosome profiles are very similar. There are well positioned nucleosomes approximately 360bp, 180bp, and 35bp upstream of the TSS (-3, -2, and -1 nucleosomes respectively) as well as a peak at 60bp downstream of the TSS (Fig. 3-7C). A two-tailed T-test reveals one point of significance at the -2 nucleosome, 120bp upstream of the TSS (Fig. 3-7B green circle). Like the 9hpf WT sample the -1 nucleosome of 9hpf *hoxb1b*$^{-/-}$ embryos also has decreased nucleosome density when compared to the -1 nucleosome of 4hpf WT embryos, though it is still greater density than that of the -1 nucleosome of 9hpf WT embryos (Fig. 3-7 compare B and C,D). We also directly compared the nucleosome positions of the 9hpf WT and *hoxb1b*$^{-/-}$ embryos. We find that there appears to be increased nucleosome density in the *hoxb1b*$^{-/-}$ sample, in particular at -1 nucleosome and 60-180bp in the coding region (Fig. 3-7D). We find statistically one significant point at the wider -2 nucleosome, 120bp upstream of the TSS, a point also observed in the 4hpf WT sample (Fig. 3-7 green circle at 124bp in B and D). Together, these data indicate that in the absence of Hoxb1b, nucleosome positions around the *hoxb1a* promoter are effected.

DISCUSSION

While loss-of-function phenotypes for mouse *Hoxa1* and *Hoxb1* as well as for zebrafish orthologs *hoxb1b* and *hoxb1a* have previously been reported, differences between the zebrafish and mouse phenotypes suggest that the zebrafish phenotypes induced by anti-sense morpholinos (MOs) may not be true nulls(Appendix B-7 and B-8). To clarify these differences we created targeted germline mutations for zebrafish *hoxb1b* and *hoxb1a* with ZFN and TALEN systems, respectively. Our findings indicate that *Hoxa1* and *hoxb1b* share roles in hindbrain segmentation and that *Hoxb1* and *hoxb1a* have similar roles in FMN migration. Comparing the phenotypes of our germline mutants to those of MO loss-of-function indicates that the MO phenotypes are not true nulls in all respects, but also reveal that *hoxb1b* and *hoxb1a* have species specific functions. In addition, we report that *hoxb1a* transcription is partially independent of Hoxb1b function and that Hoxb1b plays a role in nucleosome positioning at the *hoxb1a* promoter.

hoxb1b and *Hoxa1* have universal as well as species specific roles in hindbrain segmentation

Comparison of the reported hindbrain phenotypes of mouse *Hoxa1* (produced by targeted germline disruption) and zebrafish *hoxb1b* (produced by anti-sense MO) loss-of-function studies reveal several similarities. In particular, r3 is expanded and r5 is reduced (Chisaka et al., 1992; Lufkin et al., 1991; McClintock et al.,

2002) in both species, indicating that *Hoxa1* and *hoxb1b* share universal roles in the formation of these rhombomeres. However, differences in the segmentation defects observed in the *Hoxa1* and *hoxb1b* loss-of-function studies do exist, suggesting that the *hoxb1bMO* phenotype may not represent a true null. In particular, the r5 segmentation defect in mouse *Hoxa1*$^{-/-}$ mutants is more severe, with some embryos losing r5 entirely (Chisaka et al., 1992). In contrast, *hoxb1bMO* injected zebrafish embryos display a reduced r5 (McClintock et al., 2002). In *hoxb1bMO* injected embryos r6 is also reduced, a phenotype not observed in *Hoxa1*$^{-/-}$ mice. Comparison of the phenotypes from these previous studies with those from the *hoxb1b* germline mutants presented here, reveal that these difference are species specific. Like *Hoxa1*$^{-/-}$ embryos and *hoxb1bMO* injected embryos, *hoxb1b*$^{-/-}$ embryos have an expanded r3 and a reduced r4 (Fig 3-4 J and compare C,G,K to A,E,I). We also observe a fully formed r5 and a reduced r6. These data suggest that the zebrafish *hoxb1b*$^{-/-}$ phenotype is similar to the observed *hoxb1bMO* phenotype and that the loss of r5 in *Hoxa1*$^{-/-}$ mice is species specific. These data also indicate that *hoxb1b* has a species specific role in r6 segmentation in zebrafish. Taken together, these data indicate that *Hoxa1* and *hoxb1b* share universal roles in the segmentation of r3 and r4 in mouse and zebrafish, respectively, while having species specific roles in the segmentation of r5 in mouse and r6 in zebrafish.

hoxb1a is important for reticulospinal neuron formation

Previous reports indicate that mouse *Hoxb1* and zebrafish *hoxb1a* share functions important to the migration of facial motor neurons (FMNs) out of r4 during vertebrate hindbrain development (Goddard et al., 1996; McClintock et al., 2002; Studer et al., 1996). In these loss-of-function studies, FMNs fail to migrate out of r4, indicating a loss of r4 function in the absence of *Hoxb1* (produced by targeted gene disruption) and *hoxb1a* (produced by anti-sense MO). The role of *hoxb1a* in r4 function was tested further in zebrafish by assaying the formation of the Mauthner neurons (MNs) in r4. Embryos injected with *hoxb1aMO* were found to have normal MNs formation, however, co-injection of *hoxb1bMO* and *hoxb1aMO* disrupted MN formation. The lack of a MN phenotype in embryos injected with *hoxb1aMO* alone, may indicate that the *hoxb1aMO* is not acting as a true null. Using germline mutants for *hoxb1a,* we observe similar FMN phenotypes to previous mouse *Hoxb1* and zebrafish *hoxb1aMO* loss-of-function studies. In *hoxb1a*$^{-/-}$ embryos FMNs fail to migrate out of r4 (Fig. 3-5B). Next we inspected MN formation and found loss of both MNs in *hoxb1a*$^{-/-}$ embryos (Fig. 3-5G). The differences observed in the MN phenotypes between the MO and germline mutation of *hoxb1a* suggests that the *hoxb1aMO* is not a true null and that potentially some *hoxb1a* function still remains in the *hoxb1aMO* embryos. Taken together the data indicate that *hoxb1a* plays an important role in the formation of MN in zebrafish, as well as the specification of the r4 domain.

A role for RA signaling in *hoxb1a* activation, independent of Hoxb1b

The activation of *hoxb1a* has been reported to be dependent on Hoxb1b along with cofactors Pbx and Meis/Prep (McClintock et al., 2001; Vlachakis et al., 2001). Given these data we were surprised to identify *hoxb1a* transcript, by in situ, in r4 of *hoxb1b*$^{-/-}$ embryos (Fig. 3-4C and Appendix B-4). RA is a known activator of *hox* gene transcription and because of this next we tested involvement of the RA signaling pathway in *hoxb1a* activation. Through the addition of exogenous RA, *hoxb1a* was activated in *hoxb1b*$^{-/-}$ embryos, resulting in an r4 that appears to nearly be the same size as a WT-untreated r4 (Fig. 3-6 compare r4 of A and F). Conversely, the addition of DEAB, a chemical inhibitor of RA synthesis, completely blocks transcription of *hoxb1a* in *hoxb1b*$^{-/-}$ embryos (Fig. 3-6D). Together these results present a novel activation pathway for *hoxb1a* in zebrafish and indicate that *hoxb1a* is RA sensitive gene, though it is unclear if it is a direct or indirect target of RA.

Hoxb1b influences nucleosome positioning around the promoter of *hoxb1a*

We recently demonstrated that nucleosome positions around the promoters of *hox* genes were likely influenced by trans-factors binding DNA (Weicksel et al., 2013). To test this theory, nucleosome positions were mapped in *hoxb1b*$^{-/-}$ embryos at the promoter of *hoxb1a*, a known target of Hoxb1b. We find statistically significant changes in the nucleosome positioning between WT 4hpf embryos (when Hoxb1b is not bound and the promoter is repressed), and WT

9hpf embryos (when Hoxb1b is bound to the promoter and the promoter is active) at two positions in the *hoxb1a* promoter (Fig. 3-7B). The first position is found 120bp upstream of the TSS at the -2 nucleosome, while the second position is found between 60-180bp downstream of the TSS. We also find that only one of these positions, downstream of the TSS, are shared when nucleosome positions of the WT 4hpf embryo were compared to that of the *hoxb1b*$^{-/-}$ 9hpf embryo (Fig. 3-7C). These data indicate that there are changes that are directly due to Hoxb1b binding (changes upstream of the TSS) and changes that are independent of Hoxb1b binding (changes downstream of the TSS). Together these data indicate that there are changes in nucleosome positioning at the *hoxb1a* promoter due to Hoxb1b directly competing with nucleosomes and other that are independent of Hoxb1b. Given the shared function of Hox proteins, as a sequence specific transcription factors that activate transcription, these observations potentially indicate a general role for Hox proteins in the positioning of nucleosomes at Hox targets.

CHAPTER IV: Discussion

Despite the wealth of information detailing the molecular players that regulate *Hox* genes, there is little information about how these factors regulation nucleosome positions prior to *Hox* gene activation. Retinoic acid (RA) has been shown to activate global changes in chromatin structure, decondensing *Hox* loci in mouse tissues and embryonic cell lines correlating with temporal-colinear activation of *Hox* genes (Chambeyron and Bickmore, 2004; Chambeyron et al., 2005; Morey et al., 2007). However, little is known about the mechanisms that further regulate chromatin locally at *Hox* promoters, in particular, nucleosome positions. Nucleosome mapping studies have shown that clearance of nucleosomes from the promoter appears to be important, potentially allowing RNA polymerase and other DNA binding factors to interact with regulatory sequences upstream of the transcription start site (TSS) (Badis et al., 2008; Gilchrist et al., 2010; Gilchrist et al., 2008; Schones et al., 2008; Shim et al., 1998; Weiner et al., 2010). In accordance with these observations, genome-wide nucleosome mapping studies from many species have identified well positioned nucleosomes at poised promoters flanking the TSS with a nucleosome depleted region (NDR) in between (Ercan et al., 2011; Mavrich et al., 2008a; Mavrich et al., 2008b; Ozsolak et al., 2007; Sasaki et al., 2009; Schones et al., 2008; Valouev et al., 2008; Yuan et al., 2005). NDR formation has also been observed at *Hox* promoters in human cell lines (Kharchenko et al., 2008), indicating that nucleosome positions are also important at *Hox* promoters. However, these previous nucleosome mapping studies have been performed using differentiated

cell lines or embryos of mixed stages, leaving many questions as to how nucleosome positions are determined during embryogenesis. To address these questions, we mapped nucleosomes at *hox* promoters during early development. We found that nucleosome positioning at the *hox* promoters is a progressive process. Nucleosomes become better positioned as development progressed and these observations correlate with zygotic genome activation (ZGA). We also found that these observed changes in nucleosome positioning were independent of transcription. Treating embryos with diethylaminobenzaldehyde (DEAB) that represses *hox* transcription, or RA that activates *hox* transcription, had no effect on nucleosome positions. Given that the changes observed in nucleosome positioning occurred on invariant DNA sequence, these data led us to conclude that trans-factors likely played a role in positioning nucleosomes at zebrafish *hox* promoters during development.

These results, however, did not adress what mechanisms potentially drove the changes that we observed. *hoxb1b* is the first *hox* gene activated in zebrafish development and directly activates *hoxb1a* by binding *hox* binding sites in the *hoxb1a* promoter. Once activated Hoxb1a maintains expression through an autoregulatory-loop, binding similar *hox* sites as Hoxb1b in the *hoxb1a* promoter. Given the early expression of both *hoxb1b* and *hoxb1a*, shortly after ZGA, we believed these would make good candidates to explore their role in nucleosome positioning at the *hoxb1a* promoter. To this end, we introduced targeted mutations to *hoxb1a* and *hoxb1b* to compare nucleosome positions of

WT and mutant embryos. Mapping of nucleosomes at the *hoxb1a* promoter revealed Hoxb1b dependent and independent changes in nucleosome positioning. The *hoxb1a* and *hoxb1b* mutants also revealed novel phenotypes not observed in previous *hoxb1a* and *hoxb1b* loss-of-function studies generated by anti-sense morpholinos (MO). In addition to these novel phenotypes, we also uncovered a novel RA dependent pathway for *hoxb1a* activation.

The regulation of nucleosome positions at *Hox* promoters during zebrafish development

Together the data presented here, along with previous studies, presents a general model by which chromatin structure is regulated at *hox* genes during zebrafish development (Fig. 4-1). Prior to zygotic genome activation, *hox* cluster chromatin loops out from heterochromatin in a process initiated by RA (Chambeyron and Bickmore, 2004; Chambeyron et al., 2005; Morey et al., 2007). Decondensation of the looped *hox* chromatin to euchromatin is not well understood in the context of *hox* activation. However, presumably the decondensation of looped chromatin at *hox* promoters involves maternal factors from the trx-G of proteins, including SWI/SNF complexes. Once decondensed, different nucleosome profiles can be observed between the genes expressed early in development and those that are expressed later. At promoters of genes expressed later in development (presumably 5' genes in the *hox* clusters) nucleosomes appear disorganized (Fig. 2-2C and F), indicating that prior to ZGA,

Figure 4-1

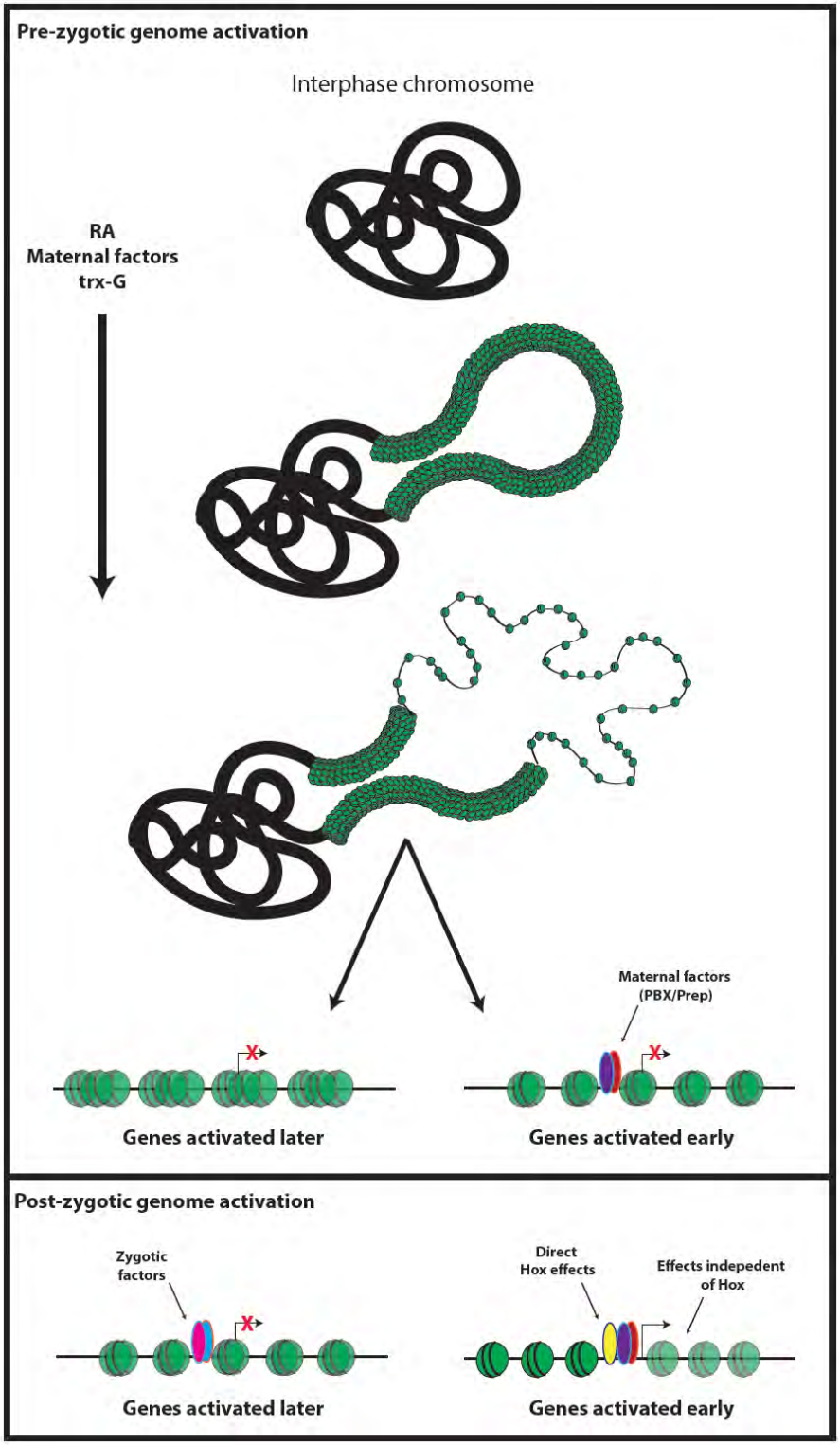
Pre-zygotic genome activation
Interphase chromosome
RA
Maternal factors
trx-G
Maternal factors
(PBX/Prep)
Genes activated later
Genes activated early
Post-zygotic genome activation
Zygotic
factors
Direct
Hox effects
Effects indepedent
of Hox
Genes activated later
Genes activated early

Figure 4-1. Model for nucleosome positioning at *hox* promoters during embryogenesis.

Prior to ZGA, RA activates *hox* chromatin looping that is further condensed by maternal factors. Once decondensed, *hox* regulatory proteins from maternal transcripts bind regulatory elements at early expressing *hox* promoters. Promoters that have maternal factors present have better positioned nucleosome than promoters that do not. Post-ZGA zygotic factors bind *hox* promoters and positioning nucleosomes.

the embryo lacks the factors that position nucleosomes at these promoters. At promoters of *hox* genes activated early in development (such as 3' genes in the *hox* clusters) nucleosomes begin to become loosely positioned, indicating that maternally encoded factors position nucleosomes at these promoters (Fig. 2-2B and E). Pbx/Prep complexes are the most likely candidates. Pbx/Prep complexes bind DNA independent of Hox (Choe et al., 2009), transcripts are maternally supplied (Deflorian et al., 2004; Vaccari et al., 2010), and have been shown to be pioneering transcription factors (Berkes et al., 2004). Pbx/Prep complexes have also recently be shown to bind the *hoxb1a* promoter during blastula stages (Choe et al., 2013). After ZGA, newly synthesized trans-factors, such as Hoxb1b, further modulate nucleosome positions. The binding of trans-factors will induce changes in nucleosome positioning such as competing with nucleosomes for DNA binding sites (Anderson and Widom, 2000; Bai et al., 2011). Effects similar to those we observe upstream of the *hoxb1a* TSS at the -2 nucleosome in the presence of Hoxb1b (Fig. 3-7B). However, not all changes are dependent on Hox binding. The recruitment of general transcription factors as well as active transcription have also been shown to effect nucleosome positions (Schwabish and Struhl, 2004; Shivaswamy et al., 2008). Indeed, Hoxb1b binding to the *hoxb1a* promoter has been shown previously to activate poised RNA-Polymerase (Choe et al., 2009), indicating the potential for nucleosome changes at the promoters of *hox* genes that are Hox independent. Together, this model illustrates a mechanism with many layers of control that

depending on the environmental cues and cellular signals, can fine tune and tightly regulate the expression of *Hox* genes.

Our data added to this model by illustrating that nucleosome positioning at *hox* is a dynamic process. Early in development on nascent chromatin, nucleosome positions are not yet defined. This was a little surprising particularly since histone marks have been shown to be present in these early stages (Hammoud et al., 2009), indicating that regulatory signals are present. However, our data indicates that during early development in the absence of trans-factors, nucleosomes do not strongly occupy positions at *hox* promoters. Together, our observations further implicates trans-factors, over cis-elements (i.e. genomic sequence), as the major determinant of nucleosome positioning at gene promoters.

Project limitations

Our use of nucleosome scanning (NS) and the Hox DNA tiling array led to the successful identification of nucleosomes at *Hox* promoters at different stages of embryogenesis. However, the use of these techniques was not without limitations. In particular, the Hox DNA tiling array provided relatively low resolution of the nucleosome profiles. The Hox tiling array was built to 20bp resolution and once the data was smoothed, resolution was ~90bp or half a nucleosome. Higher resolution would have allowed a more detailed analysis of nucleosome dynamics, including, the identifications of variations in nucleosome

positions under 90bp, changes in nucleosome density, and would have provided a more accurate calculation the nucleosomal unit in zebrafish. The second limitation we encountered was the restriction of sequence space that can be assayed using the Hox tiling array. Chips have a finite amount of space allowing for only certain probe sequence to make up the array. Based on the space restriction, we tiled the seven zebrafish *hox* clusters, in both sense and anti-sense, at 20bp resolution. With only the *hox* genes tiled on the array, we were unable to detect changes in the nucleosome organization at other promoter regions in the genome. Other genes would have been potentially important controls in determining if the gradual positioning of nucleosomes observed at *hox* promoters was *hox* specific or even specific to genes in clusters.

A third limitation was the annotation of the zebrafish genome, in particular the annotation of the transcription start sites. From the initial build of the *hox* tiling array, two more zebrafish genome builds were published, each with changes to *hox* gene TSSs. The TSS annotation was mostly resolved by using TSSs defined from an RNA-seq data set (Pauli et al., 2012). However, some concerns still remain due to a portion of *hox* genes that have multiple transcripts produced from different TSSs. One reason for this concern is that a particular transcript may have significance in a specific developmental stage and not at another. For this study genes with multiple reported transcripts were removed from our analysis, however, it still brings into question if other TSSs, particularly

the TSSs of silent genes, are biologically relevant at the time points assayed here.

The fourth limitation was due to the use of whole embryos for these experiments. As stated previously, the four time points that were assayed throughout this work were chosen to limit the cellular diversity within the samples. Cellular diversity has the potential to cause noise within the sample due to differentially positioned nucleosomes at differentially expressed genes from one cell to another. The 2hpf and 4hpf samples represent time-points in which cell fate decisions have yet to been made, along with the zygotic genome remaining inactive. The 6hpf and 9hpf embryos, however, represented the most diverse samples, with zygotic transcription active as well as embryonic tissues being formed. Despite the inherent diversity, we still observed well positioned nucleosomes in the 6hpf and 9hpf embryos (Fig. 2-1C and D, and Fig. 2-2G and J). In these data we can also identify indicators of noise due to different cellular populations within the embryos. This is apparent in the “shoulders” that broaden nucleosome peaks, as well as double peaks or adjacent nucleosome peaks that occupy distances shorter than a nucleosomal unit of 150bp. With more uniform cell populations, the variation introduced by these factors would be reduced, allowing for clearer analysis and stronger interpretation of the data.

How to address these limitations

As stated above, there are two main limitations of this project, the limitation of the sequence space available to assay on the array and the cellular diversity inherent in working with whole organisms. If this project were to be attempted again, these limitations could be address by using next generation sequencing technologies (Deep-sequencing) and cell sorting of the embryonic tissues.

Deep-sequencing technologies have improved since the inception of this project, making the use of this technique more feasible. In particular, there has been a decrease in the cost in conjunction with an increase in quality and quantity of sequencing reads per run. For this particular project, we would use Solexa paired-end sequencing. This technique has already been used extensively to map micrococcal nuclease (MNase) protected sequences and can even be modified to detected MNase protected sequences shorter than nucleosome sized fragments (Henikoff et al., 2011). The use of pair-end sequencing would increase the resolution to 1bp while also providing quantitative data as to the number MNase protected fragments within a sample. Both of these factors would strengthen statistical analysis of the data, allowing for stronger interpretation of the data. This clearer analysis would aid our study greatly, by allowing us to better identifying small changes observed at the promoters of *hox* genes during development. Deep-sequencing would also not only sequence the *hox* promoters, but the promoters of other genes as well. This

would provide other control promoters to study and compare the *hox* promoters with.

To address our second technical limitation of cell diversity, I propose cell sorting. Chromatin studies have been performed most extensively in yeast, as well as other various cell lines, to avoid the cellular diversity of whole organisms. Similar uniformity found in cell lines can be achieved with an embryo by using fluorescence-activated cell sorting (FACS). Use of FACS has also been shown in other chromatin studies to drastically reduce the background noise of other tissues, providing a clearer understanding of the chromatin states within a specific tissue of a multicellular organism (Bonn et al., 2012). To use FACS for this study, transgenic zebrafish lines with fluorescently labeled tissues would be most ideal. Many fluorescent lines are already available, including transgenic lines that label rhombomeres such the *hoxb1a:gfp* (Choe et al., 2012) and *krox20:gpf* (Grant and Moens, 2010) lines that label r4 and r3/r5, respectively. Due to the nature of *hox* expression, transgenic lines that label the hindbrain would be most ideal. Though our study focused primarily on nucleosome changes at early time points, FACS could potentially be used at later stages allowing for comparisons between promoters from initiation to repression of transcription.

Future experiments: Determining the molecular factors that position nucleosomes at *hox* promoters

The nucleosome mapping data presented here correlates with developmental stages that would suggest that trans-factors play a role in positioning nucleosomes at *hox* promoters. Indeed, we observe changes in the nucleosome positions at the *hoxb1a* promoter of *hoxb1b*$^{-/-}$ mutant embryos when compared to WT. The changes appear to be due to Hoxb1b binding, as well as changes downstream of the *hoxb1a* TSS that appear to be due to active transcription (Fig. 3-7B-D). The data also suggest proteins from maternal transcripts (Pbx and Prep) bind *hox* promoters prior to *hox* activation and that this interaction plays a role in nucleosome positioning (Fig. 2-2B and E and Fig. 3-7). Our general model for the role these factors play in nucleosome positioning at *hox* promoters correlates with developmental processes, however lacks direct evidence. Proceeding forward there are two questions that should be addressed: (1) Are changes in nucleosome positions observed, between WT and *hoxb1b*$^{-/-}$ embryos, downstream of the *hoxb1a* TSS due to the direct effect of *hoxb1b* binding or are these changes independent of Hoxb1b and due to the recruitment of other factors such as trx-G proteins and ATP-dependent chromatin modifiers to the TSS? (2) Do maternally transcribed factors, Pbx and Prep, position nucleosomes at *hox* promoters prior to gene activation? Addressing these questions will provide insight into the molecular factors that drive nucleosome positioning at *hox* promoters.

To determine the direct effects of Hoxb1b binding from the independent effects on nucleosome positioning at the *hoxb1a* promoter, truncated and chimeric forms of Hoxb1b and Pbx (respectively) can be used. To test the direct effect of Hoxb1b on nucleosome positions, mRNA transcripts encoding *hoxb1b* that lacks an activation domain (*delta-hoxb1b*), can be injected into WT and *hoxb1b*$^{-/-}$ embryos. Chromatin would be digested by MNase from injected embryos and nucleosomes at the *hoxb1a* promoter mapped by NS. A similar *delta-hoxb1b* construct has been developed in our lab and binds DNA at the *hoxb1a* promoter while reducing *hoxb1a* transcription. Therefore, changes in the nucleosome positions observed at the *hoxb1a* locus would be due to delta-Hoxb1b binding and not to transcription. The converse experiments would use a chimeric form of Pbx that contains the Hoxb1b activation domain (Pbx-b1b). In a similar strategy as listed above *Pbx-b1b* mRNA would be injected into WT and *hoxb1b*$^{-/-}$ embryos and nucleosomes would be mapped at the *hoxb1a* promoter with NS. In the *Pbx-b1b* experiments any changes in nucleosome positioning would occur in the absence of Hoxb1b binding and thus Hoxb1b independent. Together, the differences in nucleosome positioning between the *delta-hoxb1b* and *Pbx-b1b* constructs will identify the direct effect of Hoxb1b binding at the *hoxb1a* promoter as well as the Hoxb1b independent changes.

The second set of experiments would determine if Pbx/Prep complexes are the maternal factors that associate with *hox* genes prior to *hox* activation (Fig. 2-2B and E). In addition to being maternally transcribed, Pbx/Prep are good

candidates for this function because they have been shown to poise *hoxb1a* for transcription prior to Hoxb1b binding to DNA (Choe et al., 2013). To test that these complexes are important to position nucleosome at the *hoxb1a* promoter, we propose removing Pbx/Prep from the embryo. Pbx and Prep protein levels can be knocked down in WT and *hoxb1b*$^{-/-}$ mutants using previously published antisense MO. Nucleosomes at the *hoxb1a* promoter would be mapped with NS. If Pbx/Prep complexes play a role in nucleosome positioning, nucleosomes in MO injected embryos should be disrupted. If nucleosomes are disrupted at the *hoxb1a* promoter in MO injected embryos it would imply that other promoters regulated by Pbx/Prep may have similar changes. Since Pbx and Prep are ubiquitous factors that function at other promoters in addition to *hox*, a genome-wide nucleosome mapping approach, such as Deep-sequencing, would be appropriate. From this genome-wide data set we could determine if Pbx/Prep function at other promoters as they do at *hox* promoters. To identify direct targets of Pbx/Prep, nucleosome mapping could be coupled with Pbx and Prep ChIP-seq, to map Pbx/Prep binding sites and target promoters. Together, these experiments would address the roles of Pbx and Prep in positioning nucleosomes prior to ZGA.

The roles of *hoxb1a* and *hoxb1b* in zebrafish hindbrain development

Characterization of the *hoxb1a* and *hoxb1b* mutants presented here revealed species specific roles for the Hoxb1a and Hoxb1b not observed in previous

loss-of-function studies. The importance of our findings was that it clarified the roles of Hoxb1b and Hoxb1a in zebrafish development. For instance, Hoxb1b has a role in the segmentation of r3, r4, and r6 in the hindbrain of zebrafish. In mouse, the Hoxb1b ortholog, HoxA1 has a role in the segmentation of r3, r4, and r5. The identification of these separate functions in r6 (for zebrafish Hoxb1b) and r5 (for mouse HoxA1) segmentation has the potential to identify specific differences in Hoxb1b and Hoxa1 that could explain their differential function at a molecular level. Identifying a role for Hoxb1a in MN formation can lead to the identification of other factors within the pathway that drives MN formation. Currently there are no known "loss of MN" phenotypes in zebrafish. Starting with Hoxb1a will provide insight into this pathway. Finally, we identified a Hoxb1b independent pathway for *hoxb1a* that is partially activated by the retinoic acid. This finding has the potential to identify new retinoic acid receptor elements (RAREs) in the *hoxb1a* promoter as well as a novel mode of *hoxb1a* activation.

Remaining questions from *hox* mutants

As stated above, characterization of the *hoxb1a* and *hoxb1b* mutants revealed two novel observations: (1) We determined that Mauthner neurons (MN) needed *hoxb1a* function to form in r4, (2) We uncovered a Hoxb1b independent mechanism of *hoxb1a* transcription. These observations bring up several questions about the function of *hoxb1a* and how it is regulated during development.

MN formation and differentiation is not well understood. However, several mutations have been identified that effect MN maturation, deadly seven/notch1a that effects (Liu et al., 2003), and axon projection, robo3 (Burgess et al., 2009), both these mutations effect MN neuronal circuitry. Determining factors that control MN formation would also be important as they would also be important to r4 development and downstream of Hoxb1a activity. Though *hox* gene function is well defined, their targets and downstream functions are still not well understood. These factors can be identified by screening for transcripts down regulated in *hoxb1a* mutants. These factors can then be ectopically expressed in *hoxb1a*$^{-/-}$ embryos, through mRNA injection, and the rescue of MNs can be identified through antibody labeling. Studying MN formation would also uncover novel factors important to r4 function downstream of Hoxb1a.

Finally the activation of *hoxb1a* independent of Hoxb1b through the RA signaling pathway has not been previously identified in zebrafish. The implication of this finding is that RA either directly activates *hoxb1a*, or that *hoxb1a* is an indirect target and transcription is driven by another factor. To determine this, retinoic acid receptors (RARs) binding to retinoic acid receptor elements (RAREs) within *hoxb1a* cis-regulatory elements would have to be identified. Previous studies have determined, based on sequence homology, that *hoxb1a* lacks RAREs within these regulatory elements. To identify a direct role of RA in *hoxb1a* transcription, ChIP can be performed for RARs in the 3' and

5’ regions around the *hoxb1a* gene locus. Identifying RAREs and RAR binding at the *hoxb1a* locus would identify evidence of a novel pathway activating *hoxb1a*.

CONCLUSION

In conclusion, this work presents new insights into *hox* gene regulation and function in zebrafish development. By using staged embryos we have been able to observe the changes that occur at *hox* promoters prior to ZGA, and identify changes that were important to gene activation post-ZGA. Through the creation of a *hoxb1b*$^{-/-}$ mutant line we further showed that changes in nucleosome positions post-ZGA at the *hoxb1a* promoter were driven by Hoxb1b. This finding supports our proposed role for trans-factors positioning nucleosomes at *hox* promoters post-ZGA. Characterization of the *hoxb1b* and *hoxb1a* targeted deletions phenotypes also provided new insight in to the roles of these genes in zebrafish development. Specifically, the *hoxb1b* mutant identified species specific function in hindbrain segmentation, while *hoxb1a* mutants identified new a role for *hoxb1a* in reticulospinal neuron differentiation in the hindbrain. In addition to these observations we also identified a previously uncharacterized *hoxb1a* pathway that relies partially on RA signaling. Together, these data demonstrate that *hox* function is observed in many aspects of development, in segmentation, in differentiation, and in function, illustrating its fundamental role as developmental molecule.

APPENDIX A

Figure A-1

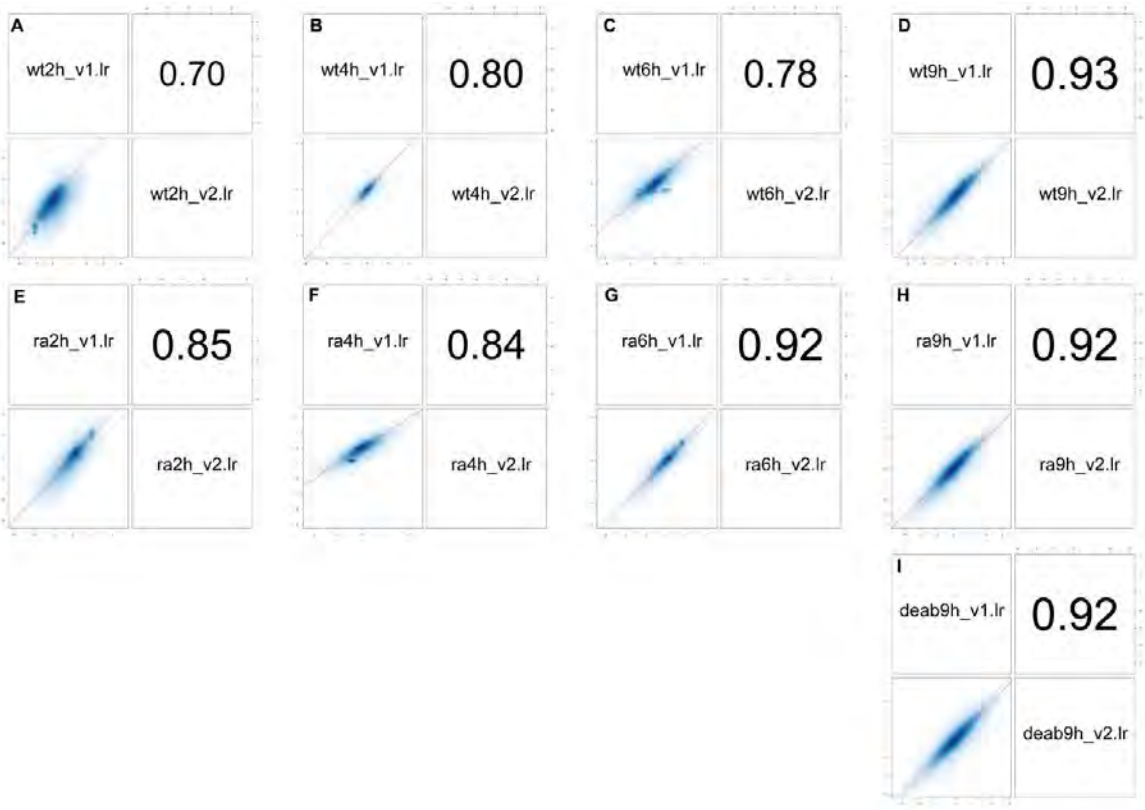
A
wt2h_v1.lr
0.70
wt2h_v2.lr
B
wt4h_v1.lr
0.80
wt4h_v2.lr
C
wt6h_v1.lr
0.78
wt6h_v2.lr
D
wt9h_v1.lr
0.93
wt9h_v2.lr
E
ra2h_v1.lr
0.85
ra2h_v2.lr
F
ra4h_v1.lr
0.84
ra4h_v2.lr
G
ra6h_v1.lr
0.92
ra6h_v2.lr
H
ra9h_v1.lr
0.92
ra9h_v2.lr
I
deab9h_v1.lr
0.92
deab9h_v2.lr

Figure A-1. Comparison of biological replicates used for calculation of nucleosome densities.

Data from two biological replicates were plotted against each other for untreated embryos at 2hpf (A), 4hpf (B), 6hpf (C), 9hpf (D), as well as for RA-treated embryos at 2hpf (E), 4hpf (F), 6hpf (G), 9hpf (H) and for DEAB-treated embryos at 9hpf (I). R^2 values are indicated in the top right quadrant of each panel.

Figure A-2

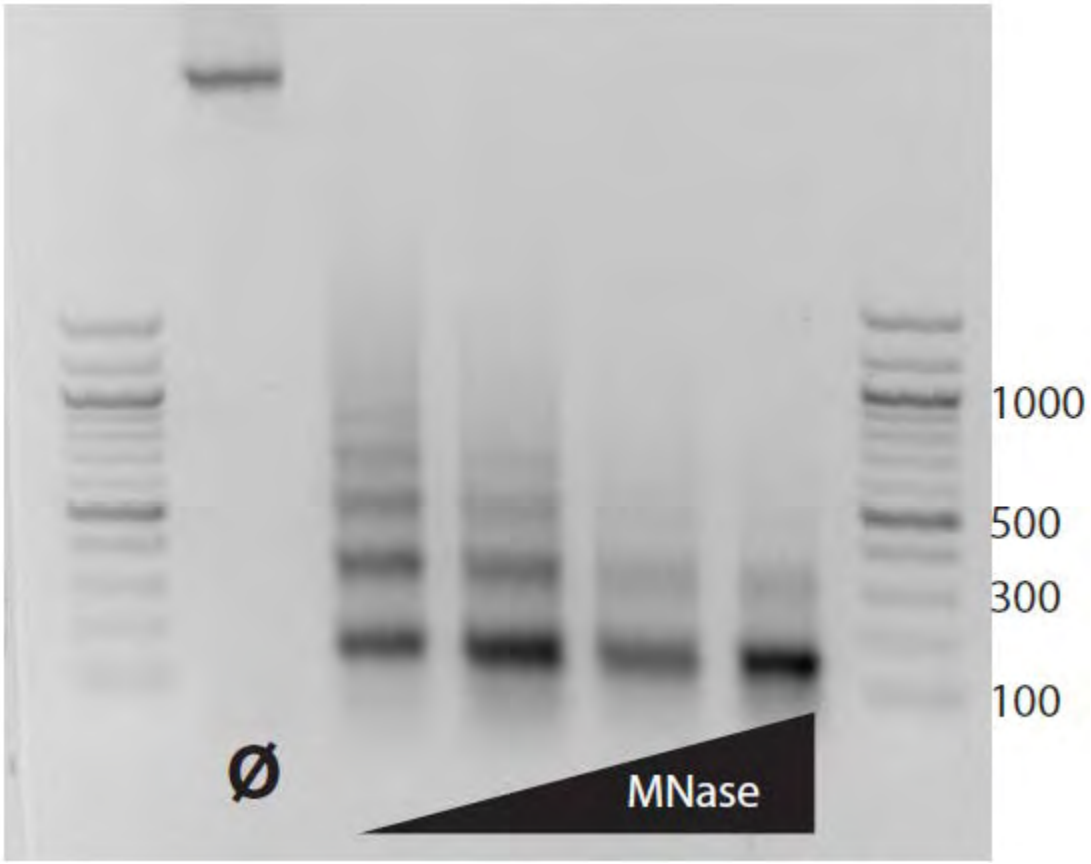

Figure A-2. Representative MNase digestion.

Cross-linked genomic DNA from 4hpf embryo was left untreated (lane 2) or treated for 10 minutes at 37ºC with serially diluted concentrations of micrococcal nuclease (MNase) increasing from 0.5units/ml -8 units/ml (lanes 3-6) and separated by agarose gel electrophoresis**.** Lanes 1 and 7 contain size ladders.

APPENDIX B

Table B-1

Founder	Nuclease	Sequence of Mutations
A12	Tb1a-2	TTTGTAAC**GCCTACAATTTA**GGGACGA BtgI
B1	Zb1b-3	GCCCTT GGACATGGG BslI

Table B-1. Sequences of non-frame shift mutations.

Representative list of lesions identified that did not cause frameshift mutations in the coding of *hoxb1a* and *hoxb1b*.

Figure B-2


********** :
hoxb1a_WT MDSSRMNSFLEYTICNRGTNAYSPKAGYHHLDQAFPGPFHTGHASDSYNADGRLYVGGSNQPPTAAAQHQHQNGIYAHHQ 80
hoxb1a_UM189 MDSSRMNSFLEYTICNVGRTPTRPRLDTTTWTRRSRALSTLDTLVTAITLMDDFT 55
hoxb1a_UM190 MDSSRMNSFLEYTICTQFVQFGRTPTRPRLDTTTWTRRSRALSTLDTLVTAITLMDDFT 59
hoxb1a_UM191 MDSSRMNSFLEYTICTDERLLAQGWIPPLGPGVPGPFPHWTR 42
hoxb1a_UM192 MDSSRMNSFLEYTICTPFVLLAQGWIPPLGPGVPGPFPHWTR 42
hoxb1a_UM193 MDSSRMNSFLEYTIWDERLLAQGWIPPLGPGVPGPFPHWTR 41
hoxb1a_UM194 MDSSRMNSFLEYTICNLDERLLAQGWIPPLGPGVPGPFPHWTR 43
hoxb1a_WT HQNQTGMGLTYGGTGTTSYGTQACANSDYAQHQYFINPEQDGMYYHSSGFSTSNASPHYGSMAGAYCGAQGAVPAAPYQH 160
hoxb1a_UM189 55
hoxb1a_UM190 59
hoxb1a_UM191 42
hoxb1a_UM192 42
hoxb1a_UM193 41
hoxb1a_UM194 43
hoxb1a_WT HGCEGQDHQRAYSQGTYADLSASQGTEKDTDQPPPGKTFDWMKVKRNPPKTGKVAEYGLGPQNTIRTNFTTKQLTELEKE 240
hoxb1a_UM189 55
hoxb1a_UM190 59
hoxb1a_UM191 42
hoxb1a_UM192 42
hoxb1a_UM193 41
hoxb1a_UM194 43
hoxb1a_WT FHFSKYLTRARRVEIAATLELNETQVKIWFQNRRMKQKKREKEGLAPASSTSSKDLEDQSDHSTSTSPEASPSPDS 316
hoxb1a_UM189 55
hoxb1a_UM190 59
hoxb1a_UM191 42
hoxb1a_UM192 42
hoxb1a_UM193 41
hoxb1a_UM194 43

Figure B-1. Hoxb1a peptide alignment.

Peptide alignment of conceptual translation of mutant *hoxb1a* alleles. Red indicates new residues while blue indicates homeodomain. From this one can see that predicted peptides never reach the homeodomain.

Figure B-3

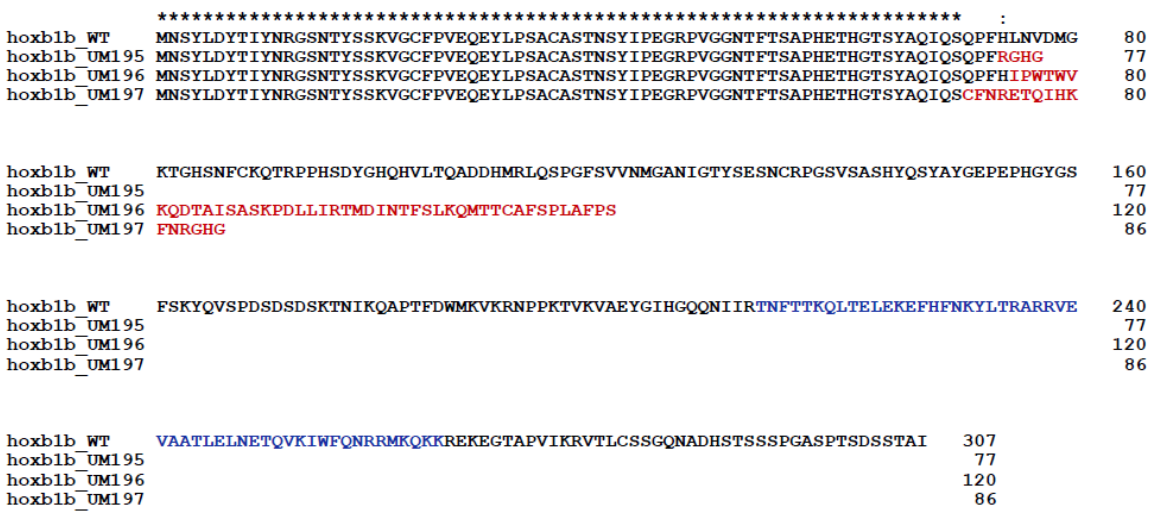
hoxb1b_WT MNSYLDYTIYNRGSNTYSSKVGCFPVEQEYLPSACASTNSYIPEGRPVGGNTFTSAPHETHGTSYAQIQSQPFHLNVDMG 80
hoxb1b_UM195 MNSYLDYTIYNRGSNTYSSKVGCFPVEQEYLPSACASTNSYIPEGRPVGGNTFTSAPHETHGTSYAQIQSQPFRGHG 77
hoxb1b_UM196 MNSYLDYTIYNRGSNTYSSKVGCFPVEQEYLPSACASTNSYIPEGRPVGGNTFTSAPHETHGTSYAQIQSQPFHIPWTWV 80
hoxb1b_UM197 MNSYLDYTIYNRGSNTYSSKVGCFPVEQEYLPSACASTNSYIPEGRPVGGNTFTSAPHETHGTSYAQIQSCFNRETQIHK 80
hoxb1b_WT KTGHSNFCKQTRPPHSDYGHQHVLTQADDHMRLQSPGFSVVNMGANIGTYSESNCRPGSVSASHYQSYAYGEPEPHGYGS 160
hoxb1b_UM195 77
hoxb1b_UM196 KQDTAISASKPDLLIRTMDINTFSLKQMTTCAFSPLAFPS 120
hoxb1b_UM197 FNRGHG 86
hoxb1b_WT FSKYQVSPDSDSDSKTNIKQAPTFDWMKVKRNPPKTVKVAEYGIHGQQNIIRTNFTTKQLTELEKEFHFNKYLTRARRVE 240
hoxb1b_UM195 77
hoxb1b_UM196 120
hoxb1b_UM197 86
hoxb1b_WT VAATLELNETQVKIWFQNRRMKQKKREKEGTAPVIKRVTLCSSGQNADHSTSSSPGASPTSDSSTAI 307
hoxb1b_UM195 77
hoxb1b_UM196 120
hoxb1b_UM197 86

Figure B-2. Hoxb1b peptide alignment.

Peptide alignment of conceptual translation of mutant *hoxb1b* alleles. Red indicates new residues while blue indicates homeodomain. From this one can see that predicted peptides never reach the homeodomain.

Figure B-4

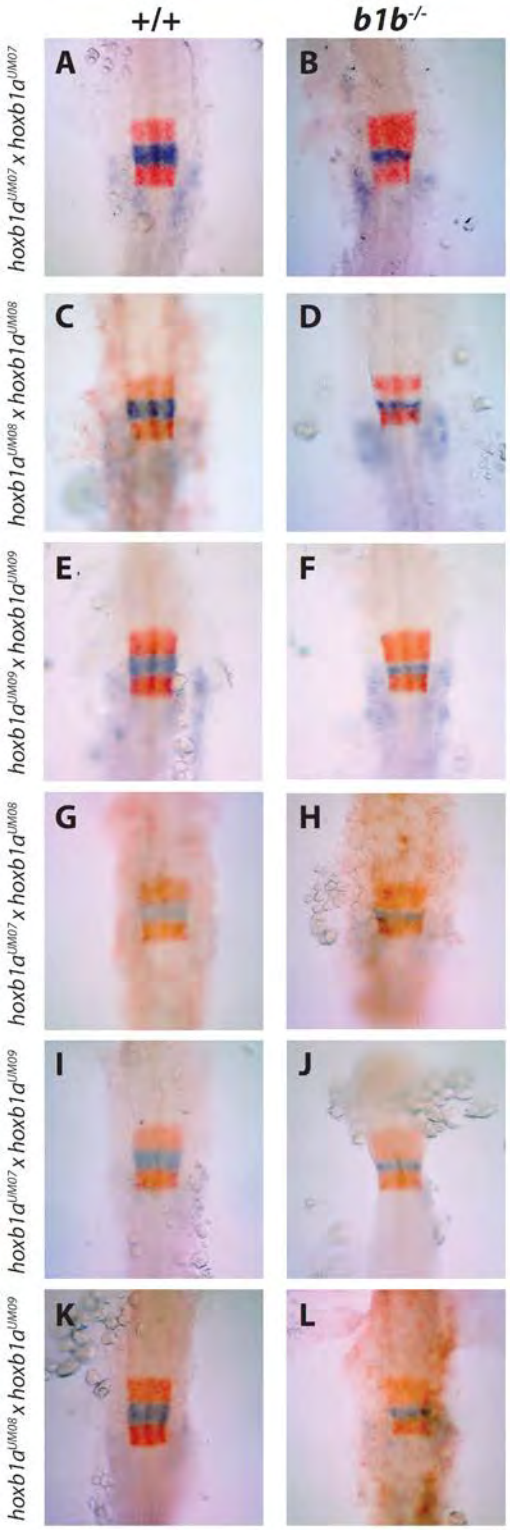
+/+
b1b-/-
A
B
C
D
E
F
G
H
I
J
K
L
hoxb1aUM07 x hoxb1aUM07
hoxb1aUM08 x hoxb1aUM08
hoxb1aUM09 x hoxb1aUM09
hoxb1aUM07 x hoxb1aUM08
hoxb1aUM07 x hoxb1aUM09
hoxb1aUM08 x hoxb1aUM09

Figure B-3. Various crosses of *hoxb1b* mutant lines.

Inter- and in-crosses of *hoxb1b* alleles reveals that consistent hindbrain segmentation phenotype. Molecular markers, *krox-20* is in red staining r3/r5 while *hoxb1a* is in blue staining r4.

Table B-5

Genotype	Phenotype							
	Krox20/hoxb1a				Pax2/Krox20/hoxd4a		Krox20/hoxb3a	
	Wild type	Wild type No hoxb1a	Affected	Affected No hoxb1a	Wild type	Affected	Wild type	Affected
hoxb1a^{UM189} x hoxb1a^{UM190} +/+ ; +/- ; -/+ -/-	39	11						
hoxb1a^{UM191} x hoxb1a^{UM192} +/+ ; +/- ; -/+ -/-	43	12			39 9		38 9	
hoxb1b^{UM195} x hoxb1b^{UM195} +/+ ; +/- ; -/+ -/-	40 3		16					
hoxb1b^{UM196} x hoxb1b^{UM196} +/+ ; +/- ; -/+ -/-	36		10					
hoxb1b^{UM197} x hoxb1b^{UM197} +/+ ; +/- ; -/+ -/-	35		12		38	14	45 1	1 9
hoxb1b^{UM195} x hoxb1b^{UM196} +/+ ; +/- ; -/+ -/-	33 1		1 12					
hoxb1b^{UM195} x hoxb1b^{UM197} +/+ ; +/- ; -/+ -/-	39		4 11					
hoxb1b^{UM196} x hoxb1b^{UM197} +/+ ; +/- ; -/+ -/-	34		11					
hoxb1a;hoxb1b^{UM193} x hoxb1a;hoxb1b^{UM194} *b1a;b1b* +/+ ; +/- ; -/+ *b1b* -/- ; *b1a* +/+ ; +/- ; -/+ *b1a* -/- ; *b1b* +/+ ; +/- ; -/+ *b1a;b1b* -/-	111	2 25	1 38	1 9	105 3 19	31 1		

Table B-5. In situ genotyping results.

In situs phenotypes were scored and then individual embryos were genotyped. All possible genotypic combinations are listed on left. Data indicates that phenotype is linked to genotype.

Figure B-6

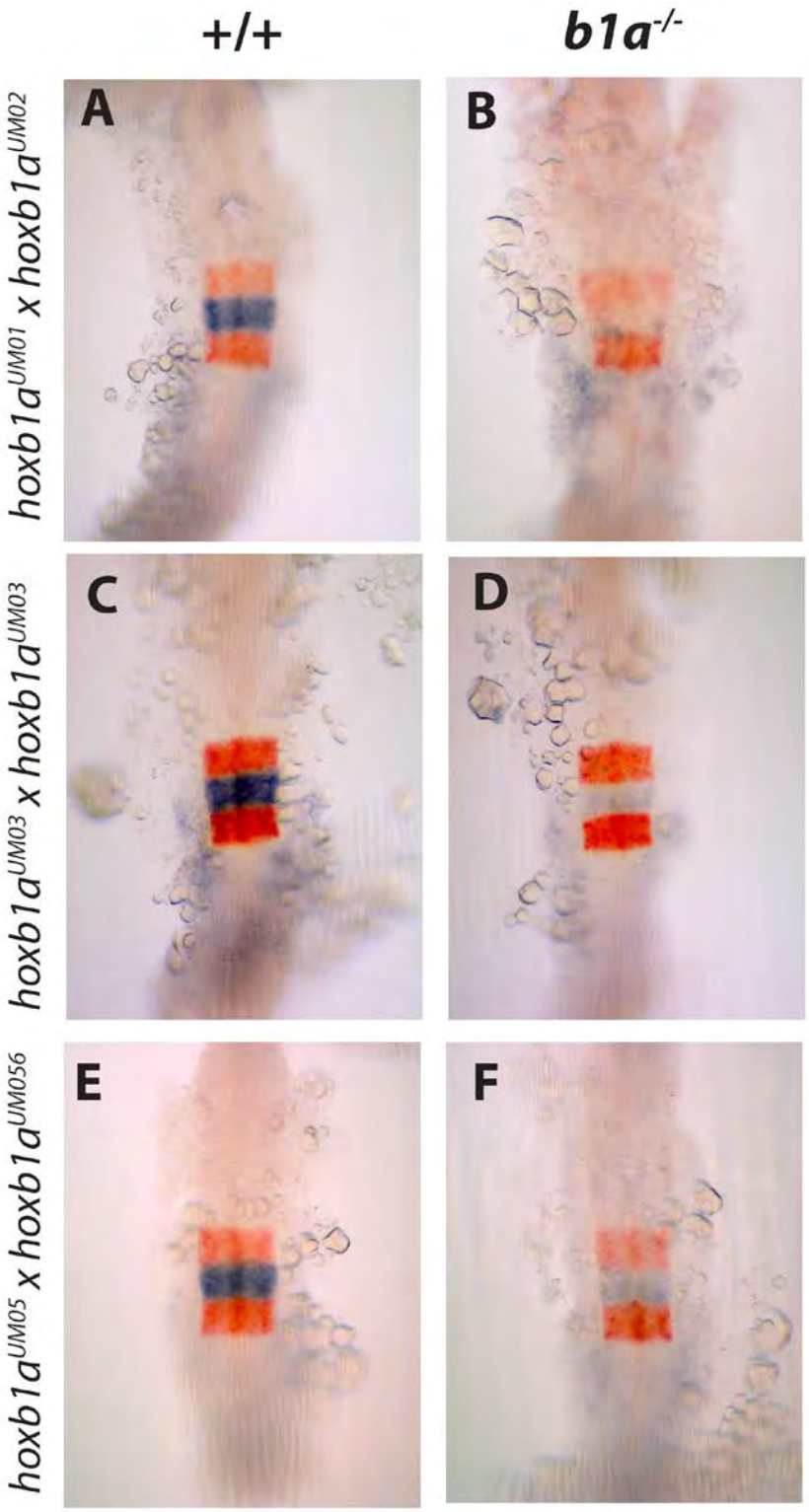
+/+
b1a-/-
hoxb1aUM01 x hoxb1aUM02
hoxb1aUM03 x hoxb1aUM03
hoxb1aUM05 x hoxb1aUM056
A
B
C
D
E
F

Figure B-6. Various crosses of *hoxb1a*$^{-/-}$ embryos.

Inter-crosses of *hoxb1a* alleles reveals that consistent hindbrain segmentation phenotype. Molecular markers, *krox-20* is in red staining r3/r5 while *hoxb1a* is in blue staining r4.

Figure B-7

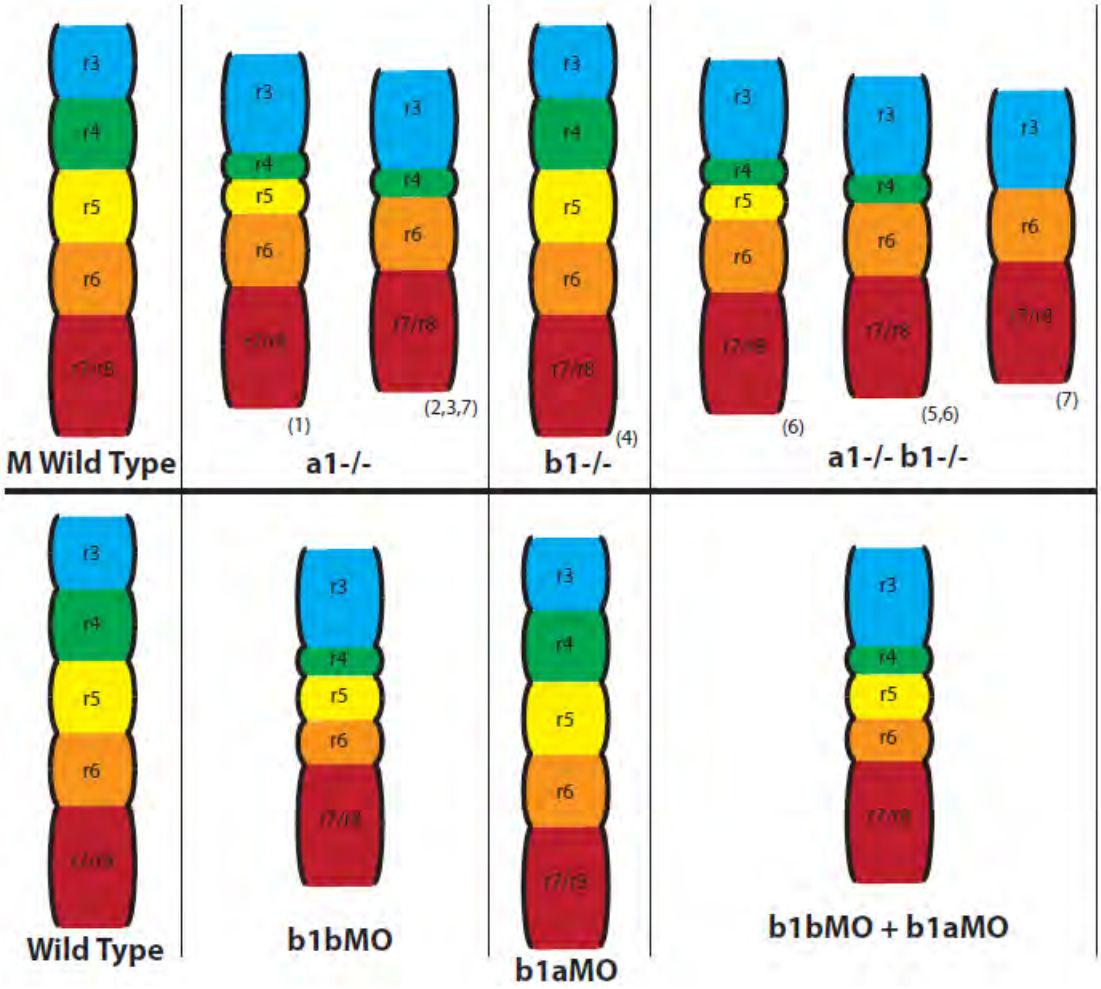
r3
r4
r5
r6
r7/r8
M Wild Type
(1)
(2,3,7)
a1-/-
(4)
b1-/-
(6)
(5,6)
(7)
a1-/- b1-/-
Wild Type
b1bMO
b1aMO
b1bMO + b1aMO

Figure B-7. *Hox* segmentation phenotypes for mouse and zebrafish.

Schematic of reported mouse and zebrafish hindbrain phenotypes. Numbers indicate the mouse studies: Lufkin et al Cell 1991[1] ,Chisaka et al Nature 1992 [2], Carpenter et al Dev 1993 [3], Studer et al Nature 1996 [4], Studer et al Dev 1998 [5], Gavalas et al Dev 1998 [6], Rossel et al Dev 1999 [7]. Zebrafish studies McClintock et al Dev 2002.

Figure B-8

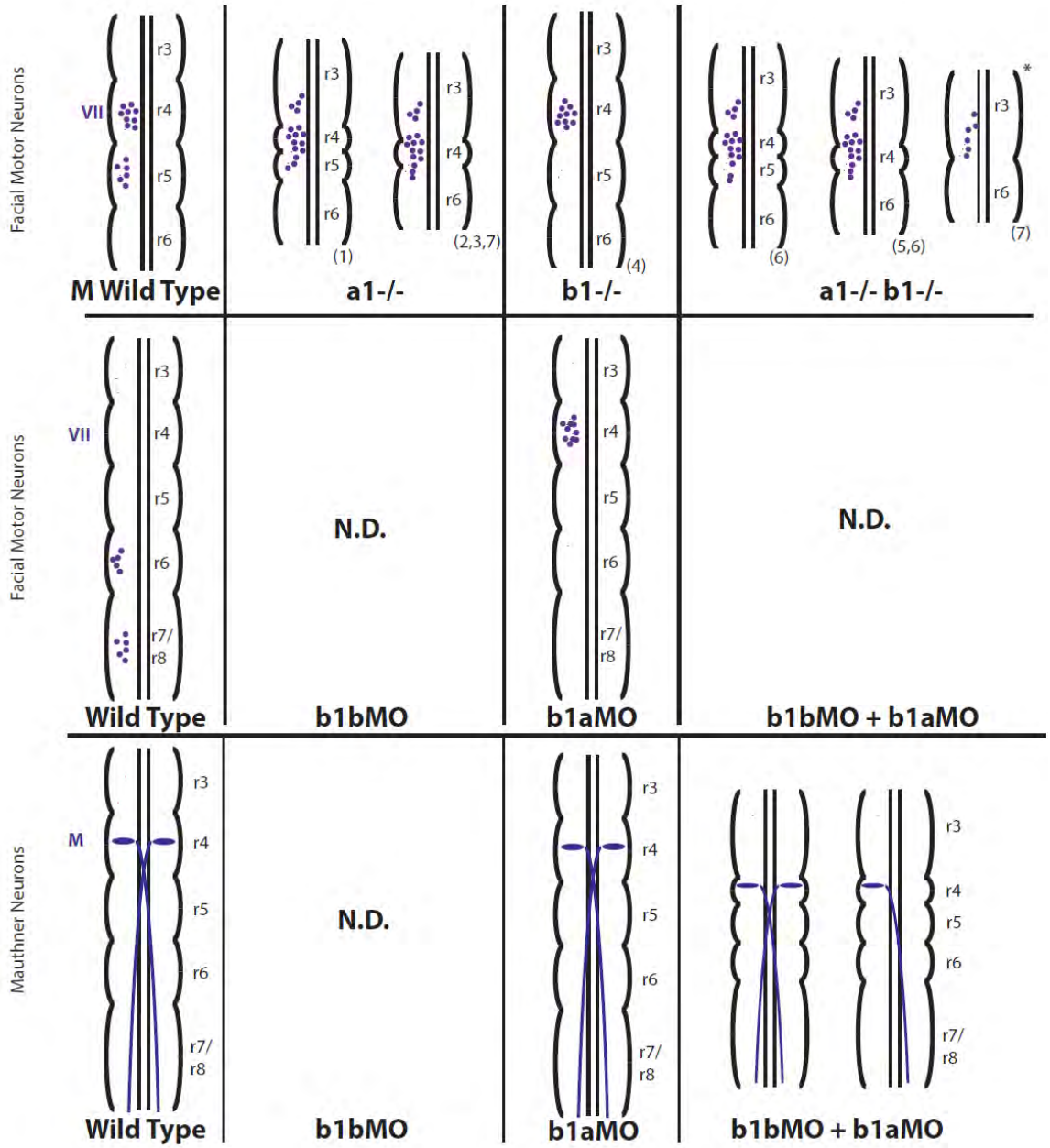
Facial Motor Neurons
VII
r3
r4
r5
r6
M Wild Type
(1)
(2,3,7)
a1-/-
(4)
b1-/-
(6)
(5,6)
(7)
*
a1-/- b1-/-
Facial Motor Neurons
VII
r7/
r8
Wild Type
N.D.
b1bMO
b1aMO
b1bMO + b1aMO
Mauthner Neurons
M
Wild Type
N.D.
b1bMO
b1aMO
b1bMO + b1aMO

Figure B-8. Reported *Hox* neuronal phenotypes.

Schematic of reported mouse and zebrafish facial motor neuron phenotypes and zebrafish Mauthner neuron phenotypes. Numbers indicate the mouse studies: Lufkin et al Cell 1991[1] ,Chisaka et al Nature 1992 [2], Carpenter et al Dev 1993 [3], Studer et al Nature 1996 [4], Studer et al Dev 1998 [5], Gavalas et al Dev 1998 [6], Rossel et al Dev 1999 [7]. Zebrafish studies McClintock et al Dev 2002.

Abu-Abed, S., Dolle, P., Metzger, D., Beckett, B., Chambon, P., Petkovich, M., 2001. The retinoic acid-metabolizing enzyme, CYP26A1, is essential for normal hindbrain patterning, vertebral identity, and development of posterior structures. Genes Dev 15, 226-240.

Ades, S.E., Sauer, R.T., 1995. Specificity of minor-groove and major-groove interactions in a homeodomain-DNA complex. Biochemistry 34, 14601-14608.

Albert, I., Mavrich, T.N., Tomsho, L.P., Qi, J., Zanton, S.J., Schuster, S.C., Pugh, B.F., 2007. Translational and rotational settings of H2A.Z nucleosomes across the Saccharomyces cerevisiae genome. Nature 446, 572-576.

Alexandre, D., Clarke, J.D., Oxtoby, E., Yan, Y.L., Jowett, T., Holder, N., 1996. Ectopic expression of Hoxa-1 in the zebrafish alters the fate of the mandibular arch neural crest and phenocopies a retinoic acid-induced phenotype. Development 122, 735-746.

Almer, A., Rudolph, H., Hinnen, A., Horz, W., 1986. Removal of positioned nucleosomes from the yeast PHO5 promoter upon PHO5 induction releases additional upstream activating DNA elements. Embo J 5, 2689-2696.

Amores, A., Force, A., Yan, Y.L., Joly, L., Amemiya, C., Fritz, A., Ho, R.K., Langeland, J., Prince, V., Wang, Y.L., Westerfield, M., Ekker, M., Postlethwait, J.H., 1998. Zebrafish hox clusters and vertebrate genome evolution. Science 282, 1711-1714.

Anderson, J.D., Widom, J., 2000. Sequence and position-dependence of the equilibrium accessibility of nucleosomal DNA target sites. J Mol Biol 296, 979-987.

Andreu-Vieyra, C., Lai, J., Berman, B.P., Frenkel, B., Jia, L., Jones, P.A., Coetzee, G.A., 2011. Dynamic nucleosome-depleted regions at androgen receptor enhancers in the absence of ligand in prostate cancer cells. Mol Cell Biol 31, 4648-4662.

Ang, H.L., Deltour, L., Hayamizu, T.F., Zgombic-Knight, M., Duester, G., 1996. Retinoic acid synthesis in mouse embryos during gastrulation and craniofacial development linked to class IV alcohol dehydrogenase gene expression. J Biol Chem 271, 9526-9534.

Apfel, C.M., Kamber, M., Klaus, M., Mohr, P., Keidel, S., LeMotte, P.K., 1995. Enhancement of HL-60 differentiation by a new class of retinoids with selective activity on retinoid X receptor. J Biol Chem 270, 30765-30772.

Badis, G., Chan, E.T., van Bakel, H., Pena-Castillo, L., Tillo, D., Tsui, K., Carlson, C.D., Gossett, A.J., Hasinoff, M.J., Warren, C.L., Gebbia, M., Talukder, S., Yang, A., Mnaimneh, S., Terterov, D., Coburn, D., Li Yeo, A., Yeo, Z.X., Clarke, N.D., Lieb, J.D., Ansari, A.Z., Nislow, C., Hughes, T.R., 2008. A library of yeast transcription factor motifs reveals a widespread function for Rsc3 in targeting nucleosome exclusion at promoters. Mol Cell 32, 878-887.

Bai, L., Ondracka, A., Cross, F.R., 2011. Multiple sequence-specific factors generate the nucleosome-depleted region on CLN2 promoter. Mol Cell 42, 465-476.

Bateson, W., 1894. Materials for the study of variation. MacMillan, London.

Begemann, G., Schilling, T.F., Rauch, G.J., Geisler, R., Ingham, P.W., 2001. The zebrafish neckless mutation reveals a requirement for raldh2 in mesodermal signals that pattern the hindbrain. Development 128, 3081-3094.

Berkes, C.A., Bergstrom, D.A., Penn, B.H., Seaver, K.J., Knoepfler, P.S., Tapscott, S.J., 2004. Pbx marks genes for activation by MyoD indicating a role for a homeodomain protein in establishing myogenic potential. Mol Cell 14, 465-477.

Bernstein, B.E., Mikkelsen, T.S., Xie, X., Kamal, M., Huebert, D.J., Cuff, J., Fry, B., Meissner, A., Wernig, M., Plath, K., Jaenisch, R., Wagschal, A., Feil, R., Schreiber, S.L., Lander, E.S., 2006. A bivalent chromatin structure marks key developmental genes in embryonic stem cells. Cell 125, 315-326.

Birgbauer, E., Fraser, S.E., 1994. Violation of cell lineage restriction compartments in the chick hindbrain. Development 120, 1347-1356.

Bonn, S., Zinzen, R.P., Girardot, C., Gustafson, E.H., Perez-Gonzalez, A., Delhomme, N., Ghavi-Helm, Y., Wilczynski, B., Riddell, A., Furlong, E.E., 2012. Tissue-specific analysis of chromatin state identifies temporal signatures of enhancer activity during embryonic development. Nat Genet 44, 148-156.

Burgess, H.A., Johnson, S.L., Granato, M., 2009. Unidirectional startle responses and disrupted left-right co-ordination of motor behaviors in robo3 mutant zebrafish. Genes, brain, and behavior 8, 500-511.

Burglin, T.R., Ruvkun, G., 1993. The Caenorhabditis elegans homeobox gene cluster. Curr Opin Genet Dev 3, 615-620.

Byrd, K.N., Shearn, A., 2003. ASH1, a Drosophila trithorax group protein, is required for methylation of lysine 4 residues on histone H3. Proc Natl Acad Sci U S A 100, 11535-11540.

Cao, R., Wang, L., Wang, H., Xia, L., Erdjument-Bromage, H., Tempst, P., Jones, R.S., Zhang, Y., 2002. Role of histone H3 lysine 27 methylation in Polycomb-group silencing. Science 298, 1039-1043.

Carpenter, E.M., Goddard, J.M., Chisaka, O., Manley, N.R., Capecchi, M.R., 1993. Loss of Hox-A1 (Hox-1.6) function results in the reorganization of the murine hindbrain. Development 118, 1063-1075.

Carrasco, A.E., McGinnis, W., Gehring, W.J., De Robertis, E.M., 1984. Cloning of an X. laevis gene expressed during early embryogenesis coding for a peptide region homologous to Drosophila homeotic genes. Cell 37, 409-414.

Cermak, T., Doyle, E.L., Christian, M., Wang, L., Zhang, Y., Schmidt, C., Baller, J.A., Somia, N.V., Bogdanove, A.J., Voytas, D.F., 2011. Efficient design and assembly of custom TALEN and other TAL effector-based constructs for DNA targeting. Nucleic Acids Res 39, e82.

Chambeyron, S., Bickmore, W.A., 2004. Chromatin decondensation and nuclear reorganization of the HoxB locus upon induction of transcription. Genes Dev 18, 1119-1130.

Chambeyron, S., Da Silva, N.R., Lawson, K.A., Bickmore, W.A., 2005. Nuclear re-organisation of the Hoxb complex during mouse embryonic development. Development 132, 2215-2223.

Chang, C.P., Jacobs, Y., Nakamura, T., Jenkins, N.A., Copeland, N.G., Cleary, M.L., 1997. Meis proteins are major in vivo DNA binding partners for wild-type but not chimeric Pbx proteins. Mol Cell Biol 17, 5679-5687.

Chang, C.P., Shen, W.F., Rozenfeld, S., Lawrence, H.J., Largman, C., Cleary, M.L., 1995. Pbx proteins display hexapeptide-dependent cooperative DNA binding with a subset of Hox proteins. Genes Dev 9, 663-674.

Chauvet, S., Merabet, S., Bilder, D., Scott, M.P., Pradel, J., Graba, Y., 2000. Distinct hox protein sequences determine specificity in different tissues. Proc Natl Acad Sci U S A 97, 4064-4069.

Chisaka, O., Musci, T.S., Capecchi, M.R., 1992. Developmental defects of the ear, cranial nerves and hindbrain resulting from targeted disruption of the mouse homeobox gene Hox-1.6. Nature 355, 516-520.

Choe, S.K., Ladam, F., Sagerstrom, C., 2013. TALE factors poise promoters for activation by Hox proteins. Dev Cell *Submitted*.

Choe, S.K., Lu, P., Nakamura, M., Lee, J., Sagerstrom, C.G., 2009. Meis cofactors control HDAC and CBP accessibility at Hox-regulated promoters during zebrafish embryogenesis. Dev Cell 17, 561-567.

Choe, S.K., Nakamura, M., Ladam, F., Etheridge, L., Sagerstrom, C.G., 2012. A Gal4/UAS system for conditional transgene expression in rhombomere 4 of the zebrafish hindbrain. Dev Dyn 241, 1125-1132.

Choe, S.K., Vlachakis, N., Sagerstrom, C.G., 2002. Meis family proteins are required for hindbrain development in the zebrafish. Development 129, 585-595.

Cooke, J., Moens, C., Roth, L., Durbin, L., Shiomi, K., Brennan, C., Kimmel, C., Wilson, S., Holder, N., 2001. Eph signalling functions downstream of Val to regulate cell sorting and boundary formation in the caudal hindbrain. Development 128, 571-580.

Damante, G., Pellizzari, L., Esposito, G., Fogolari, F., Viglino, P., Fabbro, D., Tell, G., Formisano, S., Di Lauro, R., 1996. A molecular code dictates sequence-specific DNA recognition by homeodomains. EMBO J 15, 4992-5000.

Deflorian, G., Tiso, N., Ferretti, E., Meyer, D., Blasi, F., Bortolussi, M., Argenton, F., 2004. Prep1.1 has essential genetic functions in hindbrain development and cranial neural crest cell differentiation. Development 131, 613-627.

Dennis, J.H., Fan, H.Y., Reynolds, S.M., Yuan, G., Meldrim, J.C., Richter, D.J., Peterson, D.G., Rando, O.J., Noble, W.S., Kingston, R.E., 2007. Independent and complementary methods for large-scale structural analysis of mammalian chromatin. Genome Res 17, 928-939.

Dibner, C., Elias, S., Frank, D., 2001. XMeis3 protein activity is required for proper hindbrain patterning in Xenopus laevis embryos. Development 128, 3415-3426.

Duboule, D., Dolle, P., 1989. The structural and functional organization of the murine HOX gene family resembles that of Drosophila homeotic genes. EMBO J 8, 1497-1505.

Dupe, V., Davenne, M., Brocard, J., Dolle, P., Mark, M., Dierich, A., Chambon, P., Rijli, F.M., 1997. In vivo functional analysis of the Hoxa-1 3' retinoic acid response element (3'RARE). Development 124, 399-410.

Dupe, V., Ghyselinck, N.B., Wendling, O., Chambon, P., Mark, M., 1999. Key roles of retinoic acid receptors alpha and beta in the patterning of the caudal hindbrain, pharyngeal arches and otocyst in the mouse. Development 126, 5051-5059.

Dupe, V., Lumsden, A., 2001. Hindbrain patterning involves graded responses to retinoic acid signalling. Development 128, 2199-2208.

Ebner, A., Cabernard, C., Affolter, M., Merabet, S., 2005. Recognition of distinct target sites by a unique Labial/Extradenticle/Homothorax complex. Development 132, 1591-1600.

Ekker, S.C., Jackson, D.G., von Kessler, D.P., Sun, B.I., Young, K.E., Beachy, P.A., 1994. The degree of variation in DNA sequence recognition among four Drosophila homeotic proteins. EMBO J 13, 3551-3560.

Emoto, Y., Wada, H., Okamoto, H., Kudo, A., Imai, Y., 2005. Retinoic acid-metabolizing enzyme Cyp26a1 is essential for determining territories of hindbrain and spinal cord in zebrafish. Dev Biol 278, 415-427.

Ercan, S., Lubling, Y., Segal, E., Lieb, J.D., 2011. High nucleosome occupancy is encoded at X-linked gene promoters in C. elegans. Genome Res 21, 237-244.

Fedor, M.J., Kornberg, R.D., 1989. Upstream activation sequence-dependent alteration of chromatin structure and transcription activation of the yeast GAL1-GAL10 genes. Mol Cell Biol 9, 1721-1732.

Feng, L., Hernandez, R.E., Waxman, J.S., Yelon, D., Moens, C.B., 2010. Dhrs3a regulates retinoic acid biosynthesis through a feedback inhibition mechanism. Dev Biol 338, 1-14.

Ferretti, E., Marshall, H., Popperl, H., Maconochie, M., Krumlauf, R., Blasi, F., 2000. Segmental expression of Hoxb2 in r4 requires two separate sites that integrate cooperative interactions between Prep1, Pbx and Hox proteins. Development 127, 155-166.

Fischle, W., Wang, Y., Jacobs, S.A., Kim, Y., Allis, C.D., Khorasanizadeh, S., 2003. Molecular basis for the discrimination of repressive methyl-lysine marks in histone H3 by Polycomb and HP1 chromodomains. Genes Dev 17, 1870-1881.

Fraenkel, E., Rould, M.A., Chambers, K.A., Pabo, C.O., 1998. Engrailed homeodomain-DNA complex at 2.2 A resolution: a detailed view of the interface and comparison with other engrailed structures. J Mol Biol 284, 351-361.

Francis, N.J., Kingston, R.E., Woodcock, C.L., 2004. Chromatin compaction by a polycomb group protein complex. Science 306, 1574-1577.

Fraser, S., Keynes, R., Lumsden, A., 1990. Segmentation in the chick embryo hindbrain is defined by cell lineage restrictions. Nature 344, 431-435.

Fritzsch, B., 1998. Of mice and genes: evolution of vertebrate brain development. Brain, behavior and evolution 52, 207-217.

Fu, Y., Sinha, M., Peterson, C.L., Weng, Z., 2008. The insulator binding protein CTCF positions 20 nucleosomes around its binding sites across the human genome. PLoS Genet 4, e1000138.

Fujii, H., Sato, T., Kaneko, S., Gotoh, O., Fujii-Kuriyama, Y., Osawa, K., Kato, S., Hamada, H., 1997. Metabolic inactivation of retinoic acid by a novel P450 differentially expressed in developing mouse embryos. EMBO J 16, 4163-4173.

Gavalas, A., Davenne, M., Lumsden, A., Chambon, P., Rijli, F.M., 1997. Role of Hoxa-2 in axon pathfinding and rostral hindbrain patterning. Development 124, 3693-3702.

Gavalas, A., Studer, M., Lumsden, A., Rijli, F.M., Krumlauf, R., Chambon, P., 1998. Hoxa1 and Hoxb1 synergize in patterning the hindbrain, cranial nerves and second pharyngeal arch. Development 125, 1123-1136.

Germain, P., Gaudon, C., Pogenberg, V., Sanglier, S., Van Dorsselaer, A., Royer, C.A., Lazar, M.A., Bourguet, W., Gronemeyer, H., 2009. Differential action on coregulator interaction defines inverse retinoid agonists and neutral antagonists. Chemistry & biology 16, 479-489.

Gilchrist, D.A., Dos Santos, G., Fargo, D.C., Xie, B., Gao, Y., Li, L., Adelman, K., 2010. Pausing of RNA polymerase II disrupts DNA-specified nucleosome organization to enable precise gene regulation. Cell 143, 540-551.

Gilchrist, D.A., Nechaev, S., Lee, C., Ghosh, S.K., Collins, J.B., Li, L., Gilmour, D.S., Adelman, K., 2008. NELF-mediated stalling of Pol II can enhance gene expression by blocking promoter-proximal nucleosome assembly. Genes Dev 22, 1921-1933.

Glover, J.C., 2001. Correlated patterns of neuron differentiation and Hox gene expression in the hindbrain: a comparative analysis. Brain research bulletin 55, 683-693.

Goddard, J.M., Rossel, M., Manley, N.R., Capecchi, M.R., 1996. Mice with targeted disruption of Hoxb-1 fail to form the motor nucleus of the VIIth nerve. Development 122, 3217-3228.

Grant, P.K., Moens, C.B., 2010. The neuroepithelial basement membrane serves as a boundary and a substrate for neuron migration in the zebrafish hindbrain. Neural development 5, 9.

Gupta, A., Meng, X., Zhu, L.J., Lawson, N.D., Wolfe, S.A., 2011. Zinc finger protein-dependent and -independent contributions to the in vivo off-target activity of zinc finger nucleases. Nucleic Acids Res 39, 381-392.

Guthrie, S., Lumsden, A., 1991. Formation and regeneration of rhombomere boundaries in the developing chick hindbrain. Development 112, 221-229.

Hammoud, S.S., Nix, D.A., Zhang, H., Purwar, J., Carrell, D.T., Cairns, B.R., 2009. Distinctive chromatin in human sperm packages genes for embryo development. Nature 460, 473-478.

Hanneman, E., Trevarrow, B., Metcalfe, W.K., Kimmel, C.B., Westerfield, M., 1988. Segmental pattern of development of the hindbrain and spinal cord of the zebrafish embryo. Development 103, 49-58.

Hargreaves, D.C., Crabtree, G.R., 2011. ATP-dependent chromatin remodeling: genetics, genomics and mechanisms. Cell Res 21, 396-420.

Hazelrigg, T., Kaufman, T.C., 1983. Revertants of Dominant Mutations Associated with the Antennapedia Gene Complex of DROSOPHILA MELANOGASTER: Cytology and Genetics. Genetics 105, 581-600.

Henikoff, J.G., Belsky, J.A., Krassovsky, K., MacAlpine, D.M., Henikoff, S., 2011. Epigenome characterization at single base-pair resolution. Proc Natl Acad Sci U S A 108, 18318-18323.

Hernandez, R.E., Putzke, A.P., Myers, J.P., Margaretha, L., Moens, C.B., 2007. Cyp26 enzymes generate the retinoic acid response pattern necessary for hindbrain development. Development 134, 177-187.

Hernandez, R.E., Rikhof, H.A., Bachmann, R., Moens, C.B., 2004. vhnf1 integrates global RA patterning and local FGF signals to direct posterior hindbrain development in zebrafish. Development 131, 4511-4520.

Higashijima, S., Hotta, Y., Okamoto, H., 2000. Visualization of cranial motor neurons in live transgenic zebrafish expressing green fluorescent protein under the control of the islet-1 promoter/enhancer. The Journal of neuroscience : the official journal of the Society for Neuroscience 20, 206-218.

Hoey, T., Levine, M., 1988. Divergent homeo box proteins recognize similar DNA sequences in Drosophila. Nature 332, 858-861.

Hughes, A.L., Jin, Y., Rando, O.J., Struhl, K., 2012. A functional evolutionary approach to identify determinants of nucleosome positioning: a unifying model for establishing the genome-wide pattern. Mol Cell 48, 5-15.

Hurley, I., Hale, M.E., Prince, V.E., 2005. Duplication events and the evolution of segmental identity. Evolution & development 7, 556-567.

Ingham, P.W., 1985. A clonal analysis of the requirement for the trithorax gene in the diversification of segments in Drosophila. Journal of embryology and experimental morphology 89, 349-365.

Ioshikhes, I., Bolshoy, A., Derenshteyn, K., Borodovsky, M., Trifonov, E.N., 1996. Nucleosome DNA sequence pattern revealed by multiple alignment of experimentally mapped sequences. J Mol Biol 262, 129-139.

Ioshikhes, I.P., Albert, I., Zanton, S.J., Pugh, B.F., 2006. Nucleosome positions predicted through comparative genomics. Nat Genet 38, 1210-1215.

Iyer, V., Struhl, K., 1995. Poly(dA:dT), a ubiquitous promoter element that stimulates transcription via its intrinsic DNA structure. Embo J 14, 2570-2579.

Jacobs, Y., Schnabel, C.A., Cleary, M.L., 1999. Trimeric association of Hox and TALE homeodomain proteins mediates Hoxb2 hindbrain enhancer activity. Mol Cell Biol 19, 5134-5142.

Jin, C., Felsenfeld, G., 2007. Nucleosome stability mediated by histone variants H3.3 and H2A.Z. Genes Dev 21, 1519-1529.

Johnson, S.M., Tan, F.J., McCullough, H.L., Riordan, D.P., Fire, A.Z., 2006. Flexibility and constraint in the nucleosome core landscape of Caenorhabditis elegans chromatin. Genome Res 16, 1505-1516.

Kaplan, N., Moore, I.K., Fondufe-Mittendorf, Y., Gossett, A.J., Tillo, D., Field, Y., LeProust, E.M., Hughes, T.R., Lieb, J.D., Widom, J., Segal, E., 2009. The DNA-encoded nucleosome organization of a eukaryotic genome. Nature 458, 362-366.

Kaufman, T.C., Lewis, R., Wakimoto, B., 1980. Cytogenetic Analysis of Chromosome 3 in DROSOPHILA MELANOGASTER: The Homoeotic Gene Complex in Polytene Chromosome Interval 84a-B. Genetics 94, 115-133.

Kharchenko, P.V., Woo, C.J., Tolstorukov, M.Y., Kingston, R.E., Park, P.J., 2008. Nucleosome positioning in human HOX gene clusters. Genome Res 18, 1554-1561.

Kimmel, C.B., Ballard, W.W., Kimmel, S.R., Ullmann, B., Schilling, T.F., 1995. Stages of embryonic development of the zebrafish. Dev Dyn 203, 253-310.

King, I.F., Emmons, R.B., Francis, N.J., Wild, B., Muller, J., Kingston, R.E., Wu, C.T., 2005. Analysis of a polycomb group protein defines regions that link repressive activity on nucleosomal templates to in vivo function. Mol Cell Biol 25, 6578-6591.

Kissinger, C.R., Liu, B.S., Martin-Blanco, E., Kornberg, T.B., Pabo, C.O., 1990. Crystal structure of an engrailed homeodomain-DNA complex at 2.8 A resolution: a framework for understanding homeodomain-DNA interactions. Cell 63, 579-590.

Klemm, J.D., Rould, M.A., Aurora, R., Herr, W., Pabo, C.O., 1994. Crystal structure of the Oct-1 POU domain bound to an octamer site: DNA recognition with tethered DNA-binding modules. Cell 77, 21-32.

Kmita, M., Duboule, D., 2003. Organizing axes in time and space; 25 years of colinear tinkering. Science 301, 331-333.

Koide, T., Downes, M., Chandraratna, R.A., Blumberg, B., Umesono, K., 2001. Active repression of RAR signaling is required for head formation. Genes Dev 15, 2111-2121.

Kornberg, R.D., Lorch, Y., 1999. Twenty-five years of the nucleosome, fundamental particle of the eukaryote chromosome. Cell 98, 285-294.

Krauss, S., Johansen, T., Korzh, V., Fjose, A., 1991. Expression of the zebrafish paired box gene pax[zf-b] during early neurogenesis. Development 113, 1193-1206.

Krumlauf, R., 1994. Hox genes in vertebrate development. Cell 78, 191-201.

LaRonde-LeBlanc, N.A., Wolberger, C., 2003. Structure of HoxA9 and Pbx1 bound to DNA: Hox hexapeptide and DNA recognition anterior to posterior. Genes Dev 17, 2060-2072.

Lee, C.K., Shibata, Y., Rao, B., Strahl, B.D., Lieb, J.D., 2004. Evidence for nucleosome depletion at active regulatory regions genome-wide. Nat Genet 36, 900-905.

Lee, W., Tillo, D., Bray, N., Morse, R.H., Davis, R.W., Hughes, T.R., Nislow, C., 2007. A high-resolution atlas of nucleosome occupancy in yeast. Nat Genet 39, 1235-1244.

Lemons, D., McGinnis, W., 2006. Genomic evolution of Hox gene clusters. Science 313, 1918-1922.

Lewis, E.B., 1978. A gene complex controlling segmentation in Drosophila. Nature 276, 565-570.

Li, M., Belozerov, V.E., Cai, H.N., 2010. Modulation of chromatin boundary activities by nucleosome-remodeling activities in Drosophila melanogaster. Mol Cell Biol 30, 1067-1076.

Liu, K.S., Gray, M., Otto, S.J., Fetcho, J.R., Beattie, C.E., 2003. Mutations in deadly seven/notch1a reveal developmental plasticity in the escape response circuit. The Journal of neuroscience : the official journal of the Society for Neuroscience 23, 8159-8166.

Lufkin, T., Dierich, A., LeMeur, M., Mark, M., Chambon, P., 1991. Disruption of the Hox-1.6 homeobox gene results in defects in a region corresponding to its rostral domain of expression. Cell 66, 1105-1119.

Mahony, S., Mazzoni, E.O., McCuine, S., Young, R.A., Wichterle, H., Gifford, D.K., 2011. Ligand-dependent dynamics of retinoic acid receptor binding during early neurogenesis. Genome Biol 12, R2.

Manns, M., Fritzsch, B., 1992. Retinoic acid affects the organization of reticulospinal neurons in developing Xenopus. Neuroscience letters 139, 253-256.

Margueron, R., Li, G., Sarma, K., Blais, A., Zavadil, J., Woodcock, C.L., Dynlacht, B.D., Reinberg, D., 2008. Ezh1 and Ezh2 maintain repressive chromatin through different mechanisms. Mol Cell 32, 503-518.

Maves, L., Kimmel, C.B., 2005. Dynamic and sequential patterning of the zebrafish posterior hindbrain by retinoic acid. Dev Biol 285, 593-605.

Mavrich, T.N., Ioshikhes, I.P., Venters, B.J., Jiang, C., Tomsho, L.P., Qi, J., Schuster, S.C., Albert, I., Pugh, B.F., 2008a. A barrier nucleosome model for statistical positioning of nucleosomes throughout the yeast genome. Genome Res 18, 1073-1083.

Mavrich, T.N., Jiang, C., Ioshikhes, I.P., Li, X., Venters, B.J., Zanton, S.J., Tomsho, L.P., Qi, J., Glaser, R.L., Schuster, S.C., Gilmour, D.S., Albert, I., Pugh, B.F., 2008b. Nucleosome organization in the Drosophila genome. Nature 453, 358-362.

McClintock, J.M., Carlson, R., Mann, D.M., Prince, V.E., 2001. Consequences of Hox gene duplication in the vertebrates: an investigation of the zebrafish Hox paralogue group 1 genes. Development 128, 2471-2484.

McClintock, J.M., Kheirbek, M.A., Prince, V.E., 2002. Knockdown of duplicated zebrafish hoxb1 genes reveals distinct roles in hindbrain patterning and a novel mechanism of duplicate gene retention. Development 129, 2339-2354.

McGinnis, W., Hart, C.P., Gehring, W.J., Ruddle, F.H., 1984a. Molecular cloning and chromosome mapping of a mouse DNA sequence homologous to homeotic genes of Drosophila. Cell 38, 675-680.

McGinnis, W., Krumlauf, R., 1992. Homeobox genes and axial patterning. Cell 68, 283-302.

McGinnis, W., Levine, M.S., Hafen, E., Kuroiwa, A., Gehring, W.J., 1984b. A conserved DNA sequence in homoeotic genes of the Drosophila Antennapedia and bithorax complexes. Nature 308, 428-433.

McNulty, C.L., Peres, J.N., Bardine, N., van den Akker, W.M., Durston, A.J., 2005. Knockdown of the complete Hox paralogous group 1 leads to dramatic hindbrain and neural crest defects. Development 132, 2861-2871.

McPherson, C.E., Shim, E.Y., Friedman, D.S., Zaret, K.S., 1993. An active tissue-specific enhancer and bound transcription factors existing in a precisely positioned nucleosomal array. Cell 75, 387-398.

Meng, X., Noyes, M.B., Zhu, L.J., Lawson, N.D., Wolfe, S.A., 2008. Targeted gene inactivation in zebrafish using engineered zinc-finger nucleases. Nat Biotechnol 26, 695-701.

Mic, F.A., Haselbeck, R.J., Cuenca, A.E., Duester, G., 2002. Novel retinoic acid generating activities in the neural tube and heart identified by conditional rescue of Raldh2 null mutant mice. Development 129, 2271-2282.

Milne, T.A., Briggs, S.D., Brock, H.W., Martin, M.E., Gibbs, D., Allis, C.D., Hess, J.L., 2002. MLL targets SET domain methyltransferase activity to Hox gene promoters. Mol Cell 10, 1107-1117.

Mito, Y., Henikoff, J.G., Henikoff, S., 2005. Genome-scale profiling of histone H3.3 replacement patterns. Nat Genet 37, 1090-1097.

Moens, C.B., Cordes, S.P., Giorgianni, M.W., Barsh, G.S., Kimmel, C.B., 1998. Equivalence in the genetic control of hindbrain segmentation in fish and mouse. Development 125, 381-391.

Moens, C.B., Selleri, L., 2006. Hox cofactors in vertebrate development. Dev Biol 291, 193-206.

Moens, C.B., Yan, Y.L., Appel, B., Force, A.G., Kimmel, C.B., 1996. valentino: a zebrafish gene required for normal hindbrain segmentation. Development 122, 3981-3990.

Morey, C., Da Silva, N.R., Perry, P., Bickmore, W.A., 2007. Nuclear reorganisation and chromatin decondensation are conserved, but distinct, mechanisms linked to Hox gene activation. Development 134, 909-919.

Muller, J., Hart, C.M., Francis, N.J., Vargas, M.L., Sengupta, A., Wild, B., Miller, E.L., O'Connor, M.B., Kingston, R.E., Simon, J.A., 2002. Histone methyltransferase activity of a Drosophila Polycomb group repressor complex. Cell 111, 197-208.

Niederreither, K., Abu-Abed, S., Schuhbaur, B., Petkovich, M., Chambon, P., Dolle, P., 2002. Genetic evidence that oxidative derivatives of retinoic acid are not involved in retinoid signaling during mouse development. Nat Genet 31, 84-88.

Niederreither, K., Subbarayan, V., Dolle, P., Chambon, P., 1999. Embryonic retinoic acid synthesis is essential for early mouse post-implantation development. Nat Genet 21, 444-448.

Niederreither, K., Vermot, J., Schuhbaur, B., Chambon, P., Dolle, P., 2000. Retinoic acid synthesis and hindbrain patterning in the mouse embryo. Development 127, 75-85.

Noordermeer, D., Leleu, M., Splinter, E., Rougemont, J., De Laat, W., Duboule, D., 2011. The dynamic architecture of Hox gene clusters. Science 334, 222-225.

Noyes, M.B., Christensen, R.G., Wakabayashi, A., Stormo, G.D., Brodsky, M.H., Wolfe, S.A., 2008. Analysis of homeodomain specificities allows the family-wide prediction of preferred recognition sites. Cell 133, 1277-1289.

Oliveira, E., Casado, M., Raldua, D., Soares, A., Barata, C., Pina, B., 2013. Retinoic acid receptors' expression and function during zebrafish early development. The Journal of steroid biochemistry and molecular biology 138C, 143-151.

Otting, G., Qian, Y.Q., Billeter, M., Muller, M., Affolter, M., Gehring, W.J., Wuthrich, K., 1990. Protein--DNA contacts in the structure of a homeodomain--DNA complex determined by nuclear magnetic resonance spectroscopy in solution. EMBO J 9, 3085-3092.

Oxtoby, E., Jowett, T., 1993. Cloning of the zebrafish krox-20 gene (krx-20) and its expression during hindbrain development. Nucleic Acids Res 21, 1087-1095.

Ozsolak, F., Song, J.S., Liu, X.S., Fisher, D.E., 2007. High-throughput mapping of the chromatin structure of human promoters. Nat Biotechnol 25, 244-248.

Pauli, A., Valen, E., Lin, M.F., Garber, M., Vastenhouw, N.L., Levin, J.Z., Fan, L., Sandelin, A., Rinn, J.L., Regev, A., Schier, A.F., 2012. Systematic identification of long noncoding RNAs expressed during zebrafish embryogenesis. Genome Res 22, 577-591.

Peckham, H.E., Thurman, R.E., Fu, Y., Stamatoyannopoulos, J.A., Noble, W.S., Struhl, K., Weng, Z., 2007. Nucleosome positioning signals in genomic DNA. Genome Res 17, 1170-1177.

Peifer, M., Wieschaus, E., 1990. Mutations in the Drosophila gene extradenticle affect the way specific homeo domain proteins regulate segmental identity. Genes Dev 4, 1209-1223.

Pengelly, A.R., Copur, O., Jackle, H., Herzig, A., Muller, J., 2013. A histone mutant reproduces the phenotype caused by loss of histone-modifying factor Polycomb. Science 339, 698-699.

Perissi, V., Jepsen, K., Glass, C.K., Rosenfeld, M.G., 2010. Deconstructing repression: evolving models of co-repressor action. Nat Rev Genet 11, 109-123.

Perissi, V., Staszewski, L.M., McInerney, E.M., Kurokawa, R., Krones, A., Rose, D.W., Lambert, M.H., Milburn, M.V., Glass, C.K., Rosenfeld, M.G., 1999. Molecular determinants of nuclear receptor-corepressor interaction. Genes Dev 13, 3198-3208.

Perz-Edwards, A., Hardison, N.L., Linney, E., 2001. Retinoic acid-mediated gene expression in transgenic reporter zebrafish. Dev Biol 229, 89-101.

Phelan, M.L., Sadoul, R., Featherstone, M.S., 1994. Functional differences between HOX proteins conferred by two residues in the homeodomain N-terminal arm. Mol Cell Biol 14, 5066-5075.

Piotrowski, T., Nusslein-Volhard, C., 2000. The endoderm plays an important role in patterning the segmented pharyngeal region in zebrafish (Danio rerio). Dev Biol 225, 339-356.

Piper, D.E., Batchelor, A.H., Chang, C.P., Cleary, M.L., Wolberger, C., 1999. Structure of a HoxB1-Pbx1 heterodimer bound to DNA: role of the hexapeptide and a fourth homeodomain helix in complex formation. Cell 96, 587-597.

Popperl, H., Bienz, M., Studer, M., Chan, S.K., Aparicio, S., Brenner, S., Mann, R.S., Krumlauf, R., 1995. Segmental expression of Hoxb-1 is controlled by a highly conserved autoregulatory loop dependent upon exd/pbx. Cell 81, 1031-1042.

Popperl, H., Rikhof, H., Chang, H., Haffter, P., Kimmel, C.B., Moens, C.B., 2000. lazarus is a novel pbx gene that globally mediates hox gene function in zebrafish. Mol Cell 6, 255-267.

Prince, V.E., Moens, C.B., Kimmel, C.B., Ho, R.K., 1998a. Zebrafish hox genes: expression in the hindbrain region of wild-type and mutants of the segmentation gene, valentino. Development 125, 393-406.

Prince, V.E., Price, A.L., Ho, R.K., 1998b. Hox gene expression reveals regionalization along the anteroposterior axis of the zebrafish notochord. Development genes and evolution 208, 517-522.

Qian, Y.Q., Billeter, M., Otting, G., Muller, M., Gehring, W.J., Wuthrich, K., 1989. The structure of the Antennapedia homeodomain determined by NMR spectroscopy in solution: comparison with prokaryotic repressors. Cell 59, 573-580.

Remacle, S., Abbas, L., De Backer, O., Pacico, N., Gavalas, A., Gofflot, F., Picard, J.J., Rezsohazy, R., 2004. Loss of function but no gain of function caused by amino acid substitutions in the hexapeptide of Hoxa1 in vivo. Mol Cell Biol 24, 8567-8575.

Rossant, J., Zirngibl, R., Cado, D., Shago, M., Giguere, V., 1991. Expression of a retinoic acid response element-hsplacZ transgene defines specific domains of transcriptional activity during mouse embryogenesis. Genes Dev 5, 1333-1344.

Rossel, M., Capecchi, M.R., 1999. Mice mutant for both Hoxa1 and Hoxb1 show extensive remodeling of the hindbrain and defects in craniofacial development. Development 126, 5027-5040.

Roy, B., Taneja, R., Chambon, P., 1995. Synergistic activation of retinoic acid (RA)-responsive genes and induction of embryonal carcinoma cell differentiation by an RA receptor alpha (RAR

alpha)-, RAR beta-, or RAR gamma-selective ligand in combination with a retinoid X receptor-specific ligand. Mol Cell Biol 15, 6481-6487.

Russo, J.E., Hauguitz, D., Hilton, J., 1988. Inhibition of mouse cytosolic aldehyde dehydrogenase by 4-(diethylamino)benzaldehyde. Biochemical pharmacology 37, 1639-1642.

Ryoo, H.D., Marty, T., Casares, F., Affolter, M., Mann, R.S., 1999. Regulation of Hox target genes by a DNA bound Homothorax/Hox/Extradenticle complex. Development 126, 5137-5148.

Sandell, L.L., Sanderson, B.W., Moiseyev, G., Johnson, T., Mushegian, A., Young, K., Rey, J.P., Ma, J.X., Staehling-Hampton, K., Trainor, P.A., 2007. RDH10 is essential for synthesis of embryonic retinoic acid and is required for limb, craniofacial, and organ development. Genes Dev 21, 1113-1124.

Sasaki, S., Mello, C.C., Shimada, A., Nakatani, Y., Hashimoto, S., Ogawa, M., Matsushima, K., Gu, S.G., Kasahara, M., Ahsan, B., Sasaki, A., Saito, T., Suzuki, Y., Sugano, S., Kohara, Y., Takeda, H., Fire, A., Morishita, S., 2009. Chromatin-associated periodicity in genetic variation downstream of transcriptional start sites. Science 323, 401-404.

Schier, A.F., Talbot, W.S., 2005. Molecular genetics of axis formation in zebrafish. Annu Rev Genet 39, 561-613.

Schones, D.E., Cui, K., Cuddapah, S., Roh, T.Y., Barski, A., Wang, Z., Wei, G., Zhao, K., 2008. Dynamic regulation of nucleosome positioning in the human genome. Cell 132, 887-898.

Schuettengruber, B., Chourrout, D., Vervoort, M., Leblanc, B., Cavalli, G., 2007. Genome regulation by polycomb and trithorax proteins. Cell 128, 735-745.

Schwabish, M.A., Struhl, K., 2004. Evidence for eviction and rapid deposition of histones upon transcriptional elongation by RNA polymerase II. Mol Cell Biol 24, 10111-10117.

Scott, M.P., Weiner, A.J., 1984. Structural relationships among genes that control development: sequence homology between the Antennapedia, Ultrabithorax, and fushi tarazu loci of Drosophila. Proc Natl Acad Sci U S A 81, 4115-4119.

Segal, E., Fondufe-Mittendorf, Y., Chen, L., Thastrom, A., Field, Y., Moore, I.K., Wang, J.P., Widom, J., 2006. A genomic code for nucleosome positioning. Nature 442, 772-778.

Sekinger, E.A., Moqtaderi, Z., Struhl, K., 2005. Intrinsic histone-DNA interactions and low nucleosome density are important for preferential accessibility of promoter regions in yeast. Mol Cell 18, 735-748.

Serpente, P., Tumpel, S., Ghyselinck, N.B., Niederreither, K., Wiedemann, L.M., Dolle, P., Chambon, P., Krumlauf, R., Gould, A.P., 2005. Direct crossregulation between retinoic acid receptor {beta} and Hox genes during hindbrain segmentation. Development 132, 503-513.

Shahhoseini, M., Taghizadeh, Z., Hatami, M., Baharvand, H., 2013. Retinoic acid dependent histone 3 demethylation of the clustered HOX genes during neural differentiation of human embryonic stem cells. Biochemistry and cell biology = Biochimie et biologie cellulaire 91, 116-122.

Shim, E.Y., Woodcock, C., Zaret, K.S., 1998. Nucleosome positioning by the winged helix transcription factor HNF3. Genes Dev 12, 5-10.

Shimozono, S., Iimura, T., Kitaguchi, T., Higashijima, S., Miyawaki, A., 2013. Visualization of an endogenous retinoic acid gradient across embryonic development. Nature 496, 363-366.

Shivaswamy, S., Bhinge, A., Zhao, Y., Jones, S., Hirst, M., Iyer, V.R., 2008. Dynamic remodeling of individual nucleosomes across a eukaryotic genome in response to transcriptional perturbation. PLoS biology 6, e65.

Simeone, A., Acampora, D., Arcioni, L., Andrews, P.W., Boncinelli, E., Mavilio, F., 1990. Sequential activation of HOX2 homeobox genes by retinoic acid in human embryonal carcinoma cells. Nature 346, 763-766.

Simeone, A., Mavilio, F., Acampora, D., Giampaolo, A., Faiella, A., Zappavigna, V., D'Esposito, M., Pannese, M., Russo, G., Boncinelli, E., et al., 1987. Two human homeobox genes, c1 and c8: structure analysis and expression in embryonic development. Proc Natl Acad Sci U S A 84, 4914-4918.

Sirbu, I.O., Gresh, L., Barra, J., Duester, G., 2005. Shifting boundaries of retinoic acid activity control hindbrain segmental gene expression. Development 132, 2611-2622.

Studer, M., Gavalas, A., Marshall, H., Ariza-McNaughton, L., Rijli, F.M., Chambon, P., Krumlauf, R., 1998. Genetic interactions between Hoxa1 and Hoxb1 reveal new roles in regulation of early hindbrain patterning. Development 125, 1025-1036.

Studer, M., Lumsden, A., Ariza-McNaughton, L., Bradley, A., Krumlauf, R., 1996. Altered segmental identity and abnormal migration of motor neurons in mice lacking Hoxb-1. Nature 384, 630-634.

Suter, B., Schnappauf, G., Thoma, F., 2000. Poly(dA.dT) sequences exist as rigid DNA structures in nucleosome-free yeast promoters in vivo. Nucleic Acids Res 28, 4083-4089.

Taylor, J.S., Raes, J., 2004. Duplication and divergence: the evolution of new genes and old ideas. Annu Rev Genet 38, 615-643.

Thastrom, A., Lowary, P.T., Widlund, H.R., Cao, H., Kubista, M., Widom, J., 1999. Sequence motifs and free energies of selected natural and non-natural nucleosome positioning DNA sequences. J Mol Biol 288, 213-229.

Theil, T., Frain, M., Gilardi-Hebenstreit, P., Flenniken, A., Charnay, P., Wilkinson, D.G., 1998. Segmental expression of the EphA4 (Sek-1) receptor tyrosine kinase in the hindbrain is under direct transcriptional control of Krox-20. Development 125, 443-452.

Tillo, D., Kaplan, N., Moore, I.K., Fondufe-Mittendorf, Y., Gossett, A.J., Field, Y., Lieb, J.D., Widom, J., Segal, E., Hughes, T.R., 2010. High nucleosome occupancy is encoded at human regulatory sequences. PLoS One 5, e9129.

Tirosh, I., Barkai, N., 2008. Two strategies for gene regulation by promoter nucleosomes. Genome Res 18, 1084-1091.

Vaage, S., 1969. The segmentation of the primitive neural tube in chick embryos (Gallus domesticus). A morphological, histochemical and autoradiographical investigation. Ergebnisse der Anatomie und Entwicklungsgeschichte 41, 3-87.

Vaccari, E., Deflorian, G., Bernardi, E., Pauls, S., Tiso, N., Bortolussi, M., Argenton, F., 2010. prep1.2 and aldh1a2 participate to a positive loop required for branchial arches development in zebrafish. Dev Biol 343, 94-103.

Valouev, A., Ichikawa, J., Tonthat, T., Stuart, J., Ranade, S., Peckham, H., Zeng, K., Malek, J.A., Costa, G., McKernan, K., Sidow, A., Fire, A., Johnson, S.M., 2008. A high-resolution, nucleosome position map of C. elegans reveals a lack of universal sequence-dictated positioning. Genome Res 18, 1051-1063.

Vastenhouw, N.L., Zhang, Y., Woods, I.G., Imam, F., Regev, A., Liu, X.S., Rinn, J., Schier, A.F., 2010. Chromatin signature of embryonic pluripotency is established during genome activation. Nature 464, 922-926.

Vlachakis, N., Choe, S.K., Sagerstrom, C.G., 2001. Meis3 synergizes with Pbx4 and Hoxb1b in promoting hindbrain fates in the zebrafish. Development 128, 1299-1312.

Vlachakis, N., Ellstrom, D.R., Sagerstrom, C.G., 2000. A novel pbx family member expressed during early zebrafish embryogenesis forms trimeric complexes with Meis3 and Hoxb1b. Dev Dyn 217, 109-119.

Wang, H., Wang, L., Erdjument-Bromage, H., Vidal, M., Tempst, P., Jones, R.S., Zhang, Y., 2004. Role of histone H2A ubiquitination in Polycomb silencing. Nature 431, 873-878.

Waskiewicz, A.J., Rikhof, H.A., Moens, C.B., 2002. Eliminating zebrafish pbx proteins reveals a hindbrain ground state. Dev Cell 3, 723-733.

Watari, N., Kameda, Y., Takeichi, M., Chisaka, O., 2001. Hoxa3 regulates integration of glossopharyngeal nerve precursor cells. Dev Biol 240, 15-31.

Weicksel, S.E., Xu, J., Sagerstrom, C.G., 2013. Dynamic nucleosome organization at hox promoters during zebrafish embryogenesis. PLoS One 8, e63175.

Weiner, A., Hughes, A., Yassour, M., Rando, O.J., Friedman, N., 2010. High-resolution nucleosome mapping reveals transcription-dependent promoter packaging. Genome Res 20, 90-100.

Wellik, D.M., Capecchi, M.R., 2003. Hox10 and Hox11 genes are required to globally pattern the mammalian skeleton. Science 301, 363-367.

Westerfield, M., 1993. The Zebrafish Book. University of Oregon Press, Eugene, OR.

White, J.A., Guo, Y.D., Baetz, K., Beckett-Jones, B., Bonasoro, J., Hsu, K.E., Dilworth, F.J., Jones, G., Petkovich, M., 1996. Identification of the retinoic acid-inducible all-trans-retinoic acid 4-hydroxylase. J Biol Chem 271, 29922-29927.

White, R.J., Schilling, T.F., 2008. How degrading: Cyp26s in hindbrain development. Dev Dyn 237, 2775-2790.

Widom, J., 1998. Structure, dynamics, and function of chromatin in vitro. Annu Rev Biophys Biomol Struct 27, 285-327.

Wolberger, C., Vershon, A.K., Liu, B., Johnson, A.D., Pabo, C.O., 1991. Crystal structure of a MAT alpha 2 homeodomain-operator complex suggests a general model for homeodomain-DNA interactions. Cell 67, 517-528.

Xi, Y., Yao, J., Chen, R., Li, W., He, X., 2011. Nucleosome fragility reveals novel functional states of chromatin and poises genes for activation. Genome Res 21, 718-724.

Xiao, H., Sandaltzopoulos, R., Wang, H.M., Hamiche, A., Ranallo, R., Lee, K.M., Fu, D., Wu, C., 2001. Dual functions of largest NURF subunit NURF301 in nucleosome sliding and transcription factor interactions. Mol Cell 8, 531-543.

Xu, Q., Alldus, G., Holder, N., Wilkinson, D.G., 1995. Expression of truncated Sek-1 receptor tyrosine kinase disrupts the segmental restriction of gene expression in the Xenopus and zebrafish hindbrain. Development 121, 4005-4016.

Xu, Q., Mellitzer, G., Robinson, V., Wilkinson, D.G., 1999. In vivo cell sorting in complementary segmental domains mediated by Eph receptors and ephrins. Nature 399, 267-271.

Yuan, G.C., Liu, J.S., 2008. Genomic sequence is highly predictive of local nucleosome depletion. PLoS Comput Biol 4, e13.

Yuan, G.C., Liu, Y.J., Dion, M.F., Slack, M.D., Wu, L.F., Altschuler, S.J., Rando, O.J., 2005. Genome-scale identification of nucleosome positions in S. cerevisiae. Science 309, 626-630.

Zhang, M., Hu, P., Krois, C.R., Kane, M.A., Napoli, J.L., 2007. Altered vitamin A homeostasis and increased size and adiposity in the rdh1-null mouse. FASEB J 21, 2886-2896.

Zhao, Y., Potter, S.S., 2001. Functional specificity of the Hoxa13 homeobox. Development 128, 3197-3207.

Zhao, Y., Potter, S.S., 2002. Functional comparison of the Hoxa 4, Hoxa 10, and Hoxa 11 homeoboxes. Dev Biol 244, 21-36.